

Supplementary Information

First high resolution chronostratigraphy for the early North African Acheulean at Casablanca (Morocco)

Rosalia Gallotti^{1-3*}, Giovanni Muttoni⁴, David Lefèvre^{1,2}, Jean-Philippe Degeai^{1,2}, Denis Geraads⁵, Andrea Zerboni⁴, Valérie Andrieu-Ponel⁶, Matteo Maron⁷, Serena Perini⁴, Mohssine El Graoui⁸, Séverine Sanz-Laliberté^{1,2}, Camille Daujeard⁹, Paul Fernandes^{3,8,10}, Mathieu Rué^{1,10}, Lionel Magoga¹¹, Abderrahim Mohib^{8,12}, Jean-Paul Raynal^{3,8,13}

¹Université Paul Valéry Montpellier 3, CNRS, UMR 5140 Archéologie des sociétés méditerranéennes, Campus Saint Charles, 34199 Montpellier, France.

²LabEx Archimède, Université Paul Valéry Montpellier 3, Campus Saint Charles, 34199 Montpellier, France.

³Université Bordeaux, CNRS, UMR 5199 PACEA-PPP, Bâtiment B18 allée Geoffroy Saint-Hilaire CS 50023 F - 33615 Pessac Cedex, France.

⁴Dipartimento di Scienze della Terra "Ardito Desio", Università degli Studi di Milano, Via L. Mangiagalli 34, I-20133, Milano, Italy.

⁵CR2P-UMR 7207, CNRS, MNHN, Sorbonne Université, CP 38, 8 rue Buffon, 75231, Paris cedex 05, France.

⁶Aix Marseille Université, CNRS, IRD, IMBE - Institut Méditerranéen de Biodiversité et d'Ecologie marine et continentale, Technopôle Arbois-Méditerranée, Bât. Villemain, BP 80, F-13545 Aix-en-Provence Cedex 04, France.

⁷Dipartimento di Ingegneria e Geologia, Università "G. d'Annunzio" di Chieti-Pescara, Via dei Vestini 31, 66100, Chieti, Italy.

⁸Institut National des Sciences de l'Archéologie et du Patrimoine, Madinat Al Irfane, Angle rue N°5 et rue N°7, Rabat-Institut, BP 6828, Rabat, Morocco.

⁹HNHP-UMR 7194, CNRS, MNHN, UPVD, Sorbonne Université, Institut de Paléontologie Humaine, 1 rue René Panhard, 75013, Paris, France.

¹⁰Paléotime, 75 avenue Jean Séraphin Achard-Picard, 38250, Villard-de-Lans, France.

¹¹France-Morocco Casablanca project.

¹²Centre d'interprétation du Patrimoine du Gharb, Direction provinciale de la Culture, Quartier administratif, Bd Mohamed V, Kenitra, Morocco.

¹³Department of Human Evolution, Max Planck Institute for Evolutionary Anthropology, Deutscher Platz 6, 04103 Leipzig, Germany.

*Corresponding author: rosalia.gallotti@univ-montp3.fr (Rosalia Gallotti)

1. Litho-chronostratigraphy of Thomas Quarry I

The Casablanca hinterland shows a vast system of longitudinal dune ridges parallel to modern coast, composed of marine and aeolian calcarenites. It records an exceptional succession of palaeoshorelines since the end of the Miocene¹⁻⁴.

In the South-West of Casablanca, four Formations associated with four raised platforms and including several Members have been defined from the late Early to the Late Pleistocene: the Oulad Hamida Formation (late Early Pleistocene-early Middle Pleistocene), the Anfa and the Kef Haroun Formations (Middle Pleistocene), and the Dar Bou Azza Formation (Late Pleistocene) (Fig. 2A)^{1,5,6}.

The sedimentary formations of ThI were succinctly described by Biberson and considered as an extension of the Sidi Abderrahmane formations even if their altitude was higher⁷. The stratigraphic revision carried out in relation to the excavation of the *Grotte à Hominidés* (GH) and Thomas Quarry I-Unit L (ThI-L) archaeological sites showed that these deposits could not be continuous with those of the Sidi Abderahmane quarries, and belonged to an earlier morphostratigraphic unit that we have called the Oulad Hamida Formation (OHF)^{1,2,6,8}.

1.1 Lithostratigraphy. OHF sits on a major unconformity formed at an altitude of ~28 m above sea level (asl) at the expense of the Cretaceous and Palaeozoic substratum, ~10 m above the platform of the Anfa Formation (AF) in the Sidi Abderrahmane quarries.

OHF includes four allostratigraphic units or Members – OH1 to OH4 from bottom to top (Fig. 2B and Supplementary Fig. S1).

OH1 Member: *Bed 1* is composed of a coarse calcirudite at the base and a stratified coarse-grained biocalcarenite. The lower part of *Bed 2* consists of over 2 m succession of fine to coarse locally trough cross-bedded sands and calcareous mudstone, called L1 to L4. These beds form sequences into little inset channels. In the upper part of each micro-sequence, features due to hydration-desiccation alternations (platy structure levels), to exundation (thin laminar calcareous crusts), to drying phenomena (fissural polygonal network emphasized by ferric oxides) and to bioturbation (rootlets marks associated to ferric coatings) occur. These deposits are interpreted as evidence of intermittently flowing braided streams in a nearshore fluviolacustrine hydrosystem⁵.

Bioclastic sands more or less bioturbated, partially decarbonated and cemented form the upper part- L5- of Bed 2. L5 is subdivided in three sub-units: 5a, light brownish grey clay with a roughly polyhedral structure; 5b, whitish to light reddish sandy clayey silt and 5c, reddish sandy silt. They probably represent aeolian deposits which accumulated in damp vegetated depressions with evidence of pedogenesis during warm episodes of subaerial exposure.

In the limestone deposits of Bed 2 (ThI-L site), several levels contain early Acheulean lithic artefacts^{9,10,11}, as well as the remains of large mammals dominated by hippopotamus along with *Kobus*; *Equus cf mauritanicus*; *Elephas* sp. Among the microfauna, there are reptiles; amphibians and rodents, predominantly the *Praomys*; *Paraethomys*; *Meriones* and the *Gerbillus* species.

OH2 Member: Overlying an unconformity above the OH1 Member deposits, OH deposits are coarse biocalcarenites with a curved cross-bedding followed by a finer inclined planar-bedding biocalcarenites formed within intertidal depositional environments (OH2A); vertically there follows massive coarse bioclastic aeolianites about ten or so metres thick (OH2B), the upper part of which is affected by fersalsol pedogenesis.

OH3 Member is associated with a shoreline marked by a basal erosion platform and a cliff carved into OH1 and OH2 deposits, whose base is at an altitude of 37 m NGM. The OH3 deposits are composed from bottom to top of blocs and pebbles from OH1 and OH2 calcarenite and limestone, passing to coarse and/or coquinoid biocalcarenites with inclined planar bedding, overlying at the upper part by aeolian calcarenites.

OH4 Member is associated with a palaeoshoreline marked with cliff and deep cavities cut into OH1 and OH3. In the cavities, OH4 deposits are composed of 1) a calcirudite with a coarse coquinoid matrix and plurimetric collapsed blocks of calcarenites originating partly from OH3 Member which constitutes the cavity ceiling and blocks of calcirudite coming from earlier formations. These deposits are associated with a well-defined notch shaped at the expense of OH1 and OH3 Members at an altitude of about 34 m asl, 2) this chaos of blocks, whose surfaces are smoothed, is drowned out by a fine, planar-bedding calcarenite which is well developed laterally, which is inserted between the blocks and covers them; upwards, these sands become more massive. OH4 marine deposits constitute the lower set of the infilling of the GH large cavity^{12,13}. The upper set of the infilling is composed of continental deposits (GH-Continental Cave Complex). Without any apparent disconformity with OH4, GH-CCC lower units 4-3 deposits are composed of bioclastic and quartzose sands containing lithic objects, macrofauna, microfauna and hominin fossils, hence the cavity's name, probably edified in several episodes. The upper part of the GH-CCC is composed from bottom to top of a multilayer dripstone interbedded with loose red sands (GH-CCC-unit 2) which laterally links up with a speleothem, overlying by massive bedded, rubefied sands rich in microfauna and fragments of gasteropods shells, originating from reworked superficial red soils (GH-CCC-unit 1)^{12,13}.

At the entrance of the cavity, the wide cross-bedding “gray” sands of an aeolianite (OH5) are intercalated between the lower (3-4) and the upper units (1-2) of the GH-CCC.

1.2 Chronostratigraphy. According to the sequence stratigraphy, OH1 to OH4 Member are allostratigraphic units defined by a sedimentary sequence characterized by a succession of genetically related deposits - intertidal, supratidal and aeolian/continental depositional environments - and bounded at its base and top by unconformities. This sequence records sea-levels high-stands associated with the formation of a shoreline marked by a cliff in the case of OH3 and OH4. The unconformities or sequence boundaries mark the regression of the shoreline due to sea-level fall and the continentalisation of the coast. Thus, OH1 to OH4 Members are correlative to sea-levels high-stands of the main global glacio-eustatic cycles as inferred from the marine isotope stage (MIS) record and are preserved at positive elevations due to the regional tectonic uplift affecting Atlantic Morocco.

OHF predates the Anfa Formation (AF) whose Members AF1 and AF2 are correlated to MIS 13 even 15 (Fig. 2A).

The OH4 deposits predates the continental cave deposits of the GH (Fig. 2A). OSL analyzes on GH-CCC-unit 4 yielded ages from 391 ± 32 ka to 420 ± 34 ¹³. A hominin tooth provided a laser abrasion ICP-MS age of $501 +89/-66$ ka¹³. Biostratigraphic data point towards the first part of the Middle Pleistocene^{14,15}. OSL dating of quartz provided an age range between 360 ka to 470 ka (370 ± 58 to 440 ± 38 ka) for the aeolianite OH5 intercalated between the lower units (3-4) and the upper (1-2) of the GH-CCC¹⁶. The stratigraphic position, the facies and the dating allow to correlate this aeolianite with MIS 11 AF3 Member of the Anfa Formation.

The OH1-Bed2 microfauna, particularly the rodents, suggest a placement of the faunal assemblage between the fauna of Aïn Hanech and that of Tighennif in Algeria, i.e, representing the second half of the Early Pleistocene, but probably not in its terminal part^{14,15}. This attribution is in agreement with the results of the OSL dating, which provide an age between 0.8 and 1.2 Ma¹⁶.

As continental infillings of the GH cavity have been dated to 0.5-0.6 Ma^{12,13,16} in accordance with biostratigraphic data^{14,15}, OH4 sea-level high-stand associated with the palaeoshoreline is undoubtedly much older than MIS 15. Thus, the OH4 to OH1 Members records sea-level high-stands at least MIS 17 to older, much older if the record is not complete. Nevertheless, since it is difficult to estimate what the large hiatus corresponding to the embedding of about ten meters of the Anfa formation base platform in the Oulad Hamida Formation, and the quartzitic basement, may represent in terms of unrecorded cycles, it cannot be ruled out that these sea-levels high-stands of the OH formation are much older.

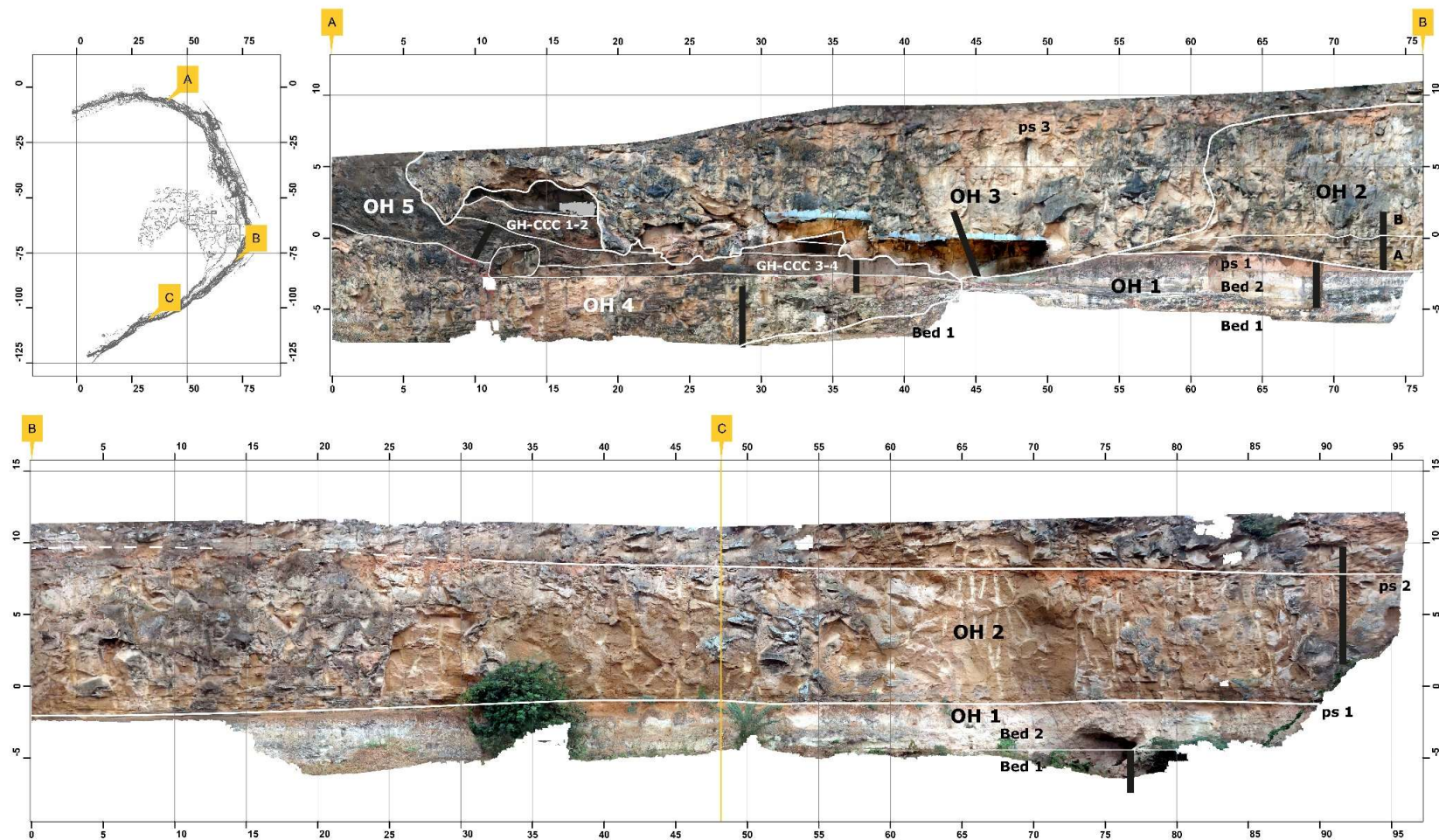


Fig. S1. Oulad Hamida Formation at ThI (photogrammetry and CAD S. Sanz-Laliberté and D. Lefèvre). The black bars indicate the location of magnetostratigraphical samples.

2. Thin sections' micromorphology of OH1 Bed2 - ThI-L

2.1 Methods. Twenty-seven samples were extracted during 1990 excavation from a test pit section in squares U25 (L1 to L5 base) and U28 (L5) of the lithic-bearing stratigraphic section of ThI-L site, OHF Member 1 (OH1), Bed 2. Five samples only were selected from archaeostratigraphic units L1 (9065), L2 (9062) and L5 (9039, 9043, 9054) to manufacture large thin sections (13,5 x 5,5 cm) at the micromorphology facility of Institut du Quaternaire from Bordeaux University (M. El Graoui). They were cut from oriented blocks of sediments vaccum-impregnated with polyester resin, following the process described by Guilloré^{17,18}.

This preliminary observation was intended first to give support to the interpretation of the field evidence about the depositional and post-depositional processes leading to the formation of each unit and second to search for the occurrence of mineral and organic anthropogenic debris related to human or animal activities¹⁹⁻²². Micromorphological studies of thin sections employed an optical petrographic microscope Olympus BX41 equipped with a digital camera Olympus E420. Thin sections were observed at various magnifications (20x, 40x, 100x, 200x, 400x) under plane polarized light (PPL), cross-polarized light (XPL), and oblique incident light (OIL). Additionally, thin sections have been observed under oblique incident radiation (epifluorescence) of ultraviolet (UV) and blue (BLF) lights using a mercury burner (HBO lamp) 100 W, mostly to detect the occurrence of phosphatic features and to assess the degree of bone fragments preservation²³. The description of thin sections is summarized in Table S1 that follows the terminology suggested by Stoops²⁴. Data interpretation follows the concepts on the formation of natural and anthropogenic layers summarized in Courty et al.²⁵, Nicosia and Stoops²⁶, and Stoops et al.²⁷.

2.2 Results. From the sedimentological point of view, Bed 2 presents distinct sedimentary environments that corresponds to facies related to the evolution of nearshore environments.

The lowermost part of the sequence (L1) consists of a packed accumulation of sand-sized, subangular quartz grains with occasional occurrence of glauconite grains, and common to scarce coarse bioclasts (Supplementary Fig. S2). The latter are in part dissolved and testified by moldic voids, pseudomorphic of bioclasts. In some cases, dissolution voids are partially filled by sparitic or micritic cement (Supplementary Fig. S3). The micromass consists of a variable quantity of micrite; in the lower part of L1 the micritic groundmass is almost absent and calcite nodules are present (Supplementary Fig. S2).

The following L2 unit alternates levels consisting of carbonatic mud with interspersed scarce sand-sized quartz grains and very rare bioclasts (Supplementary Fig. S2) displaying calcitic coatings, to levels with abundant sand-sized quartz grains, ghosts of carbonatic clasts, and calcitic pedorelicts (with altered margins) in a micromass of micritic to sparitic calcite (Supplementary Fig. S2). The porosity is generally low in L2 and related to construction voids and occasionally by bioturbation voids (common to scarce channels; Supplementary Fig. S2). Occasional compact microlayers are evident (Supplementary Fig. S4). In L2 altered bone fragments and phosphatic impregnation on the groundmass are occasionally present (Supplementary Fig. S4).

The uppermost part of the sequence (L5) consists of accumulations of coarse sand, which is constituted mostly by subangular quartz grains and occasionally other minerals including glauconite (Supplementary Fig. S2), interspersed in a calcitic micromass. Unit L5 displays a weak to moderate preferential orientation of the coarse constituents, which is detectable thanks to the occurrence of aligned dissolution voids after shell fragments (Supplementary Fig. S5). In the lower part of L5, a thin layer of laminar to stromatolithic calcite is present. Bioturbation is evident in this part of the sequence and the occurrence of Fe-rich oxy-hydroxides staining mineral grains and the rim of voids and impregnating the groundmass in the lower part of L5 is a further evidence of pedogenesis (Supplementary Fig. S3). Anthropogenic debris are occasionally present; in L5 they are represented by fragments of knapped lithic artifacts and bone fragments and phosphatic

impregnation of the groundmass, which can have an animal origin (Supplementary Fig. S5). A few, very small fragments of charcoal are also present, but their attribution to intentional human firing is not possible.

The sedimentary facies observed at the microscale suggest the interplay of distinct sedimentation mechanism in charge of the accumulation of Bed 2. All processes happened in nearshore environments thanks to the interplay between wind and fluvial sedimentation. The basal unit L1 formed after the accumulation of aeolian sand constituted by quartz grains, glauconite grains, and bioclasts (e.g., shell fragments, bryozoan, echinoderm, foraminifera, red algae) deflated presumably from the emerged shelf. The subsequent layer L2 shows a transition towards fluvial processes and the unit likely accreted in correspondence of a system of low to medium energy channels alternated to swamps. In such conditions, decantation of clay and precipitation of calcite occurred in swamp to lake environments, whereas coarse layers suggest increased energy of the system and the onset of a channel system. Likely, it was a braided system that accumulated carbonatic sand-sized grains, limestone fragments, and pedorelicts resulting from the dismantling of the carbonatic mud of the swamp environment. Finally, thin sections from layer L5 suggest a further shift in the sedimentary system and a new onset of wind sedimentation with the accretion of dunes. The shape and size of quartz grains is compatible with the aeolian sedimentary environment and the presence of glauconite grains and abundant bioclast moulds support the interpretation of this unit as eolianites.

All deposits identified in the L5 to L1 sequence suffered strong post-depositional modification. Evidence of bioturbation is evident along the whole sequence as much a huge mobilization and reprecipitation of calcite. Bioclasts in the L5 wind-accreted unit are completely dissolved resulting in abundant dissolution/moldic voids; the same happened to carbonatic grains from the L2 unit, which are represented by micrite envelopes²⁸. Calcite reprecipitated as micrite cementing the micromass or occasionally as sparite; in many cases, secondary calcite formed bridges among grains and precipitated inside the voids of former mineral grains and bioclasts^{19,28}. As common in carbonatic soils of the Mediterranean area, the typical calcitic crystallitic b-fabric is the combination between calcite inherited from sedimentary parent material and gradual precipitation of micrite in the micromass and filling of pore space between grains by precipitated silt- and clay-size pedogenic carbonate crystals²⁹⁻³². Incipient formation of calcite nodules is evident in the basal part of the sequence (L1). Bioturbation is evident in deposits related to wind sedimentation suggesting a moderate vegetal cover. Also, carbonatic mud observed under the microscope display moderate to weak occurrence of bioturbation (channel voids) due to vegetation or invertebrates. L5 suffered initial pedogenesis under warm environmental conditions during episodes of subaerial exposure; this is suggested by the occurrence of Fe-oxyhydroxides impregnating the groundmass and forming coatings on grains and voids³³⁻³⁵. Warm conditions after the deposition of the sand deposit of L5 are further confirmed by the occurrence of micritic undulated laminar layers that can be interpreted as thin calcrete^{28,36}. Such processes (calcite redistribution and Fe-bearing pedofeatures) are common in Pleistocene eolianites deposits from the Mediterranean region and elsewhere³⁷⁻⁴⁰ and likely promoted by the transpiration of dune plants^{28,34,36}.

Compact layers detected in L2 and repeated alignments of elongated constituents in L5 are syndepositional features likely related to runoff or eolian processes even if trampling associated to human occupation of the site could also be suggested^{41,42}. The accumulation of bone fragments is also due to animal and/or human accumulators. Observation of bone fragments under BLF light suggests that they are moderately altered and partially impregnated by Fe-oxyhydroxides. The fluorescence light highlighted the presence of accumulation of phosphates in the groundmass of L5 and (less abundant) L2, likely formed after weathering under warm conditions of bone fragments^{23,43,44}. Finally, the occurrence of lithic fragments^{45,46} confirms an in situ knapping activity already revealed by the excavation.

2.3 Conclusion. The observation of thin sections from sediments of ThI-L under the microscope highlighted the major sedimentary properties of the deposit and strong post-depositional and

taphonomic processes affecting the whole sequence. The final product is a sedimentary sequence alternating coarse siliciclastic to bioclastic sands and calcareous mudstones. The formation of the sequence is likely related to the interplay of littoral processes that include sedimentation in low energy channel interchanged to swamps along backshore environments, alternated to periods of enhanced aeolian sedimentation. Moreover, the whole sequence displays strong evidence of pedogenesis and diagenesis, including huge calcite mobilization and redistribution and bioturbation, resulting in layers with huge accumulation of micritic cement in the groundmass and abundant dissolution cavities related to pristine calcitic constituents (mineral grains and bioclasts). In the uppermost part of the sequence (unit L5), evidence of pedogenesis during warm episodes of subaerial exposure and increased vegetation cover are preserved.

A limited human overprint on sedimentation and taphonomy of deposits is supposed in two distinct layers. In the uppermost part of L5, biogenic/anthropogenic indicators⁴⁷ are interspersed in the groundmass and include fragments of knapped lithic artefacts and minute fragments of altered bones. In the same unit, very small charcoal fragments of unknown origin have been identified. In the same layer a weak to moderate preferential orientation and alignment of dissolution voids (mould of shell fragments) was detected but more investigations are necessary before attributing them to repeating trampling on the same surface rather to ordinary bioturbation. Moderately preserved fragments of altered bones were also identified in layer L2; under fluorescence light and the same thin section displays evidence of phosphatic impregnation of the groundmass, which is generally related to the deep weathering of bone fragments and the same unit displays occasional evidence of compaction features that could be associated to trampled surfaces. However, one must keep in mind that these low energy channels and swamps environment was at least heavily frequented by hippos and crocodiles.

Table S1. Summary of micromorphological properties of samples.

| Sample | Layer | Depth (cm) | Mineral constituents | Micromass | Organic and anthropogenic constituents | Voids | c/f related distribution | b-fabric | Microstructure | Pedofeatures |
|-----------|--------|------------|---------------------------------------------------------------------------------------------------------------------------------------------------------------------|--------------------------------------------------------------------------------------------------------------------|---------------------------------------------------------------------------------------------------------------------------|------------------------------------------------------------------------------------------------------------------|-----------------------------------------------------------------|----------------------------------|--------------------|---------------------------------------------------------------------------------------------------------------------------------------------------------------------------------------------------------------------------------------------------------------------------------------------------------------------------------------------------------------------------------------------------------------------------------------------------------------------|
| 9039 | L5 | -223–233 | Common to abundant sand-sized quartz grains, subangular to poorly rounded; very scarce igneous grains; scarce altered bioclasts | Brownish grey clayey micromass impregnated of calcite | Scarce, small bone fragments, partially weathered; scarce fragments of knapped lithic; very rare small charcoal fragments | Common vughs; scarce channels and planes; common mouldic voids after bioclasts dissolution, occasionally aligned | Single spaced porphyric | Crystallitic to undifferentiated | Massive to complex | Common crystalline pedofeatures related to calcite dissolution and redistribution, including sparitic and micritic coatings on voids and clasts, infillings of mouldic voids, hypocoatings, and impregnation of the groundmass; scarce phosphatic impregnation on the groundmass; weak evidence of Fe-oxyhydroxides impregnation on the groundmass and around discrete elements; weak Mn-rich oxyhydroxides impregnation on bone fragments; scarce passage features |
| 9043 | L5 | -283–273 | Common to abundant sand-sized quartz grains, subangular to poorly rounded; scarce glauconite clasts; very scarce igneous grains; scarce altered bioclasts | Brownish grey clayey micromass impregnated of calcite | Scarce, small bone fragments, partially weathered | Common vughs; rare to scarce channels and planes; common mouldic voids after bioclasts dissolution | Single spaced to close porphyric | Undifferentiated | Massive to complex | Common crystalline pedofeatures related to calcite dissolution and redistribution, including sparitic and micritic coatings on voids and clasts, infillings of mouldic voids, hypocoatings, and impregnation of the groundmass; scarce calcite nodules; weak evidence of Fe-oxyhydroxides impregnation on the groundmass and around discrete elements; weak Mn-rich oxyhydroxides impregnation on bone fragments; scarce passage features |
| 9054 | L5-L4 | -326–335 | Common sand-sized quartz grains, subangular to poorly rounded; common carbonatic clasts; very scarce altered bioclasts | Brownish grey clayey micromass impregnated of calcite; in the upper part, weakly micritic ovoidular laminar layers | | Common vughs; scarce to common channels and planes; common mouldic voids after bioclasts dissolution | Single to double spaced porphyric; occasionally close porphyric | Crystallitic to undifferentiated | Massive to complex | Common crystalline pedofeatures related to calcite dissolution and redistribution, including sparitic and micritic coatings on voids and clasts, infillings of voids, hypocoatings, and impregnation of the groundmass; scarce calcite nodules; common Fe-oxyhydroxides impregnation on the groundmass and around discrete elements |
| 9062 haut | L23 | -402–414 | Scarce to common sand-sized quartz grains, subangular to poorly rounded; common to scarce carbonatic clasts; very rare bioclasts | very scarce micritic micromass | Scarce, small bone fragments, partially weathered | Common vughs; scarce channels and planes; scarce mouldic voids after limestone clasts and bioclasts dissolution | Close porphyric | Crystallitic | Massive to complex | Common crystalline pedofeatures related to calcite dissolution and redistribution, including sparitic and micritic coatings on voids and clasts, infillings of voids (including mouldic voids), hypocoatings, and impregnation of the groundmass; scarce calcite nodules; ripening layers; in the lower part of the sample, calcitic pedorelicts with erosional margins and Fe-impregnation; tion of the groundmass; |
| 9062 bas | L23 | -417–429 | Scarce to common sand-sized quartz grains, subangular to poorly rounded; common to scarce carbonatic clasts; scarce rock fragments (limestone); very rare bioclasts | Brownish grey clayey micromass impregnated of calcite | | Common vughs; scarce channels and planes; scarce mouldic voids after limestone clasts and bioclasts dissolution | Close to sulge spaced porphyric | Crystallitic | Massive to complex | Common crystalline pedofeatures related to calcite dissolution and redistribution, including sparitic and micritic coatings on voids and clasts, infillings of voids (including mouldic voids), hypocoatings, and impregnation of the groundmass; scarce calcite nodules; calcitic pedorelicts with erosional margins and Fe-impregnation; tion of the groundmass; scarce lithorelicts |
| 9065 haut | L1 top | -455–467 | Common to abundant sand-sized quartz grains, subangular to poorly rounded; very scarce igneous grains; scarce altered bioclasts | Brownish grey clayey micromass impregnated of calcite | | Common vughs; scarce channels and planes; common mouldic voids after bioclasts dissolution | Single spaced to close porphyric | Crystallitic to undifferentiated | Massive to complex | Common crystalline pedofeatures related to calcite dissolution and redistribution, including sparitic and micritic coatings on voids and clasts, infillings of mouldic voids, hypocoatings, and impregnation of the groundmass; scarce calcite nodules; very weak Fe-oxyhydroxides impregnation on the groundmass |
| 9065 bas | L1 top | -460–472 | Common to abundant sand-sized quartz grains, subangular to poorly rounded; scarce glauconite clasts; very scarce igneous grains; scarce altered bioclasts | Scarce brownish grey clayey micromass impregnated of calcite | | Common vughs; scarce channels and planes; common mouldic voids after bioclasts dissolution | Close porphyric | Crystallitic to undifferentiated | Massive to complex | Common crystalline pedofeatures related to calcite dissolution and redistribution, including sparitic and micritic coatings on voids and clasts, infillings of mouldic voids, hypocoatings, and impregnation of the groundmass; scarce calcite nodules; common abundant calcitic nodules |

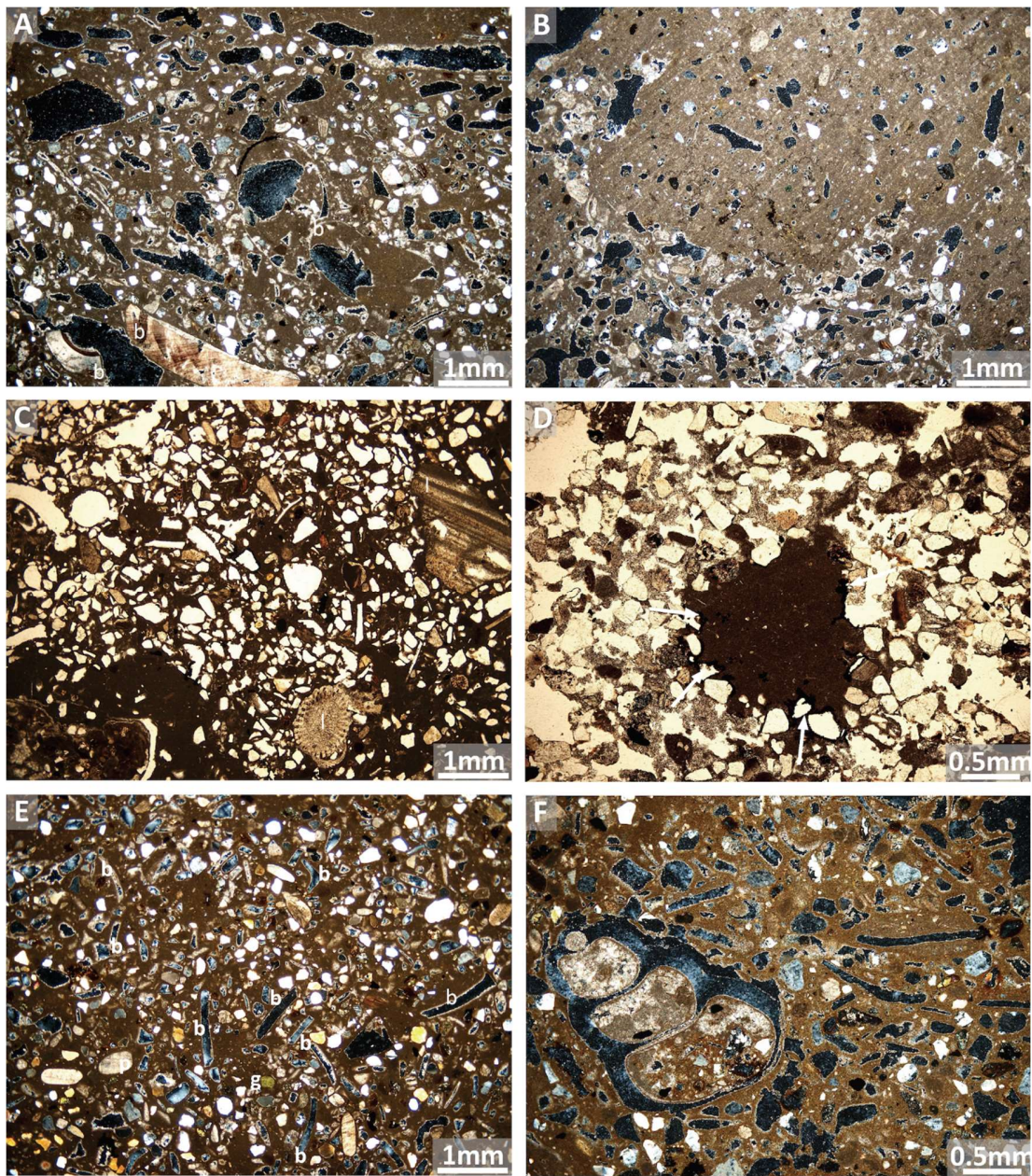


Fig. S2. General aspect of the observed thin sections from layers L1–L5 illustrating variations in the groundmass and constituents that reflects changes in sedimentary environments. (A) Single spaced porphyric c/f related distribution of the sandy L1 unit; notice the occurrence of common bioclasts (B) (XPL). (B) Open porphyric c/f related distribution of the carbonatic mud in L2 (XPL). (C) Close to single spaced porphyric c/f related distribution of the sandy layer in L1 related to moderate energy fluvial system; notice the occurrence of lithorelicts (l) (PPL). (D) A pedorelict (a micrite nodule with altered margins indicated by the arrows) in the L1 unit (PPL). (E) Close to single spaced porphyric c/f related distribution of the sandy L5 unit; notice the occurrence of subangular quartz grains, glauconite grains (g), and common bioclasts (B) (XPL). (F) A detail of the voids pseudomorphs of shell fragments with partial reprecipitation of micrite in L5 (XPL).

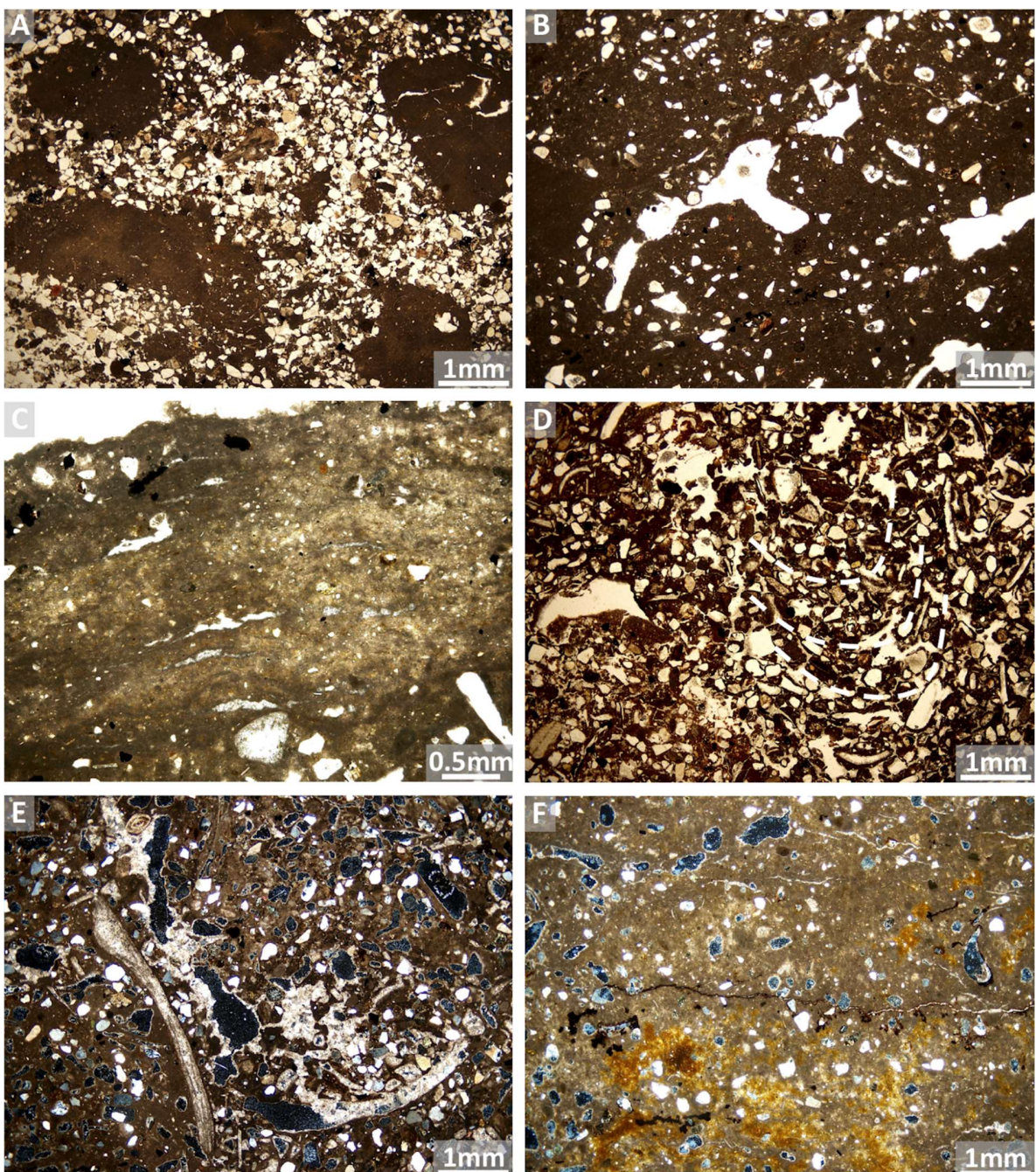


Fig. S3. Photomicrographs illustrating post-depositional processes (pedogenesis and diagenesis) affecting the sedimentary sequence of Bed 2. (A) Calcitic nodules in the sandy groundmass of L1 (PPL). (B) Channel voids due to bioturbation in the mudstone of L2 (PPL). (C) Micritic undulated laminar layer (calcrete) in L5 (PPL). (D) Dashed lines highlight a passage pedofeature (bioturbation) in L5 (PPL). (E) Strong dissolution of bioclast and reprecipitation of micrite and sparite in L5 (XPL). (F) Fe-rich oxy-hydroxides impregnating the groundmass and coating voids and grains in the lower part of L5 (XPL).

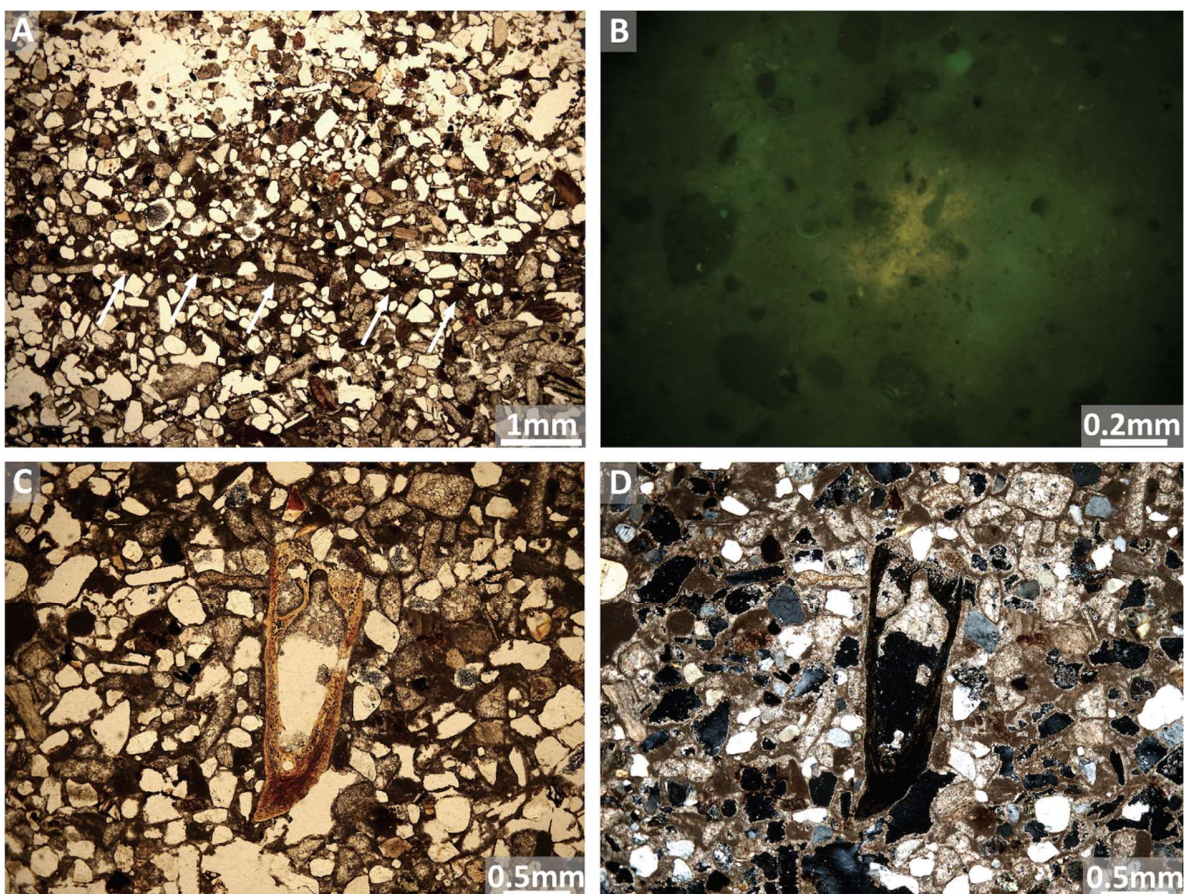


Fig. S4. Photomicrographs of some microscopic features detected unit L2. (A) Evidence of compaction (indicated by arrows) in the upper part of L1 (PPL). (B) Phosphatic impregnation on the groundmass (BLF). (C) A weakly altered bone fragment in L2; notice the abundant occurrence of moldic voids after grains dissolution with micrite envelope or secondary sparite/micrite precipitation (PPL). (D) the same of (C) in XPL.

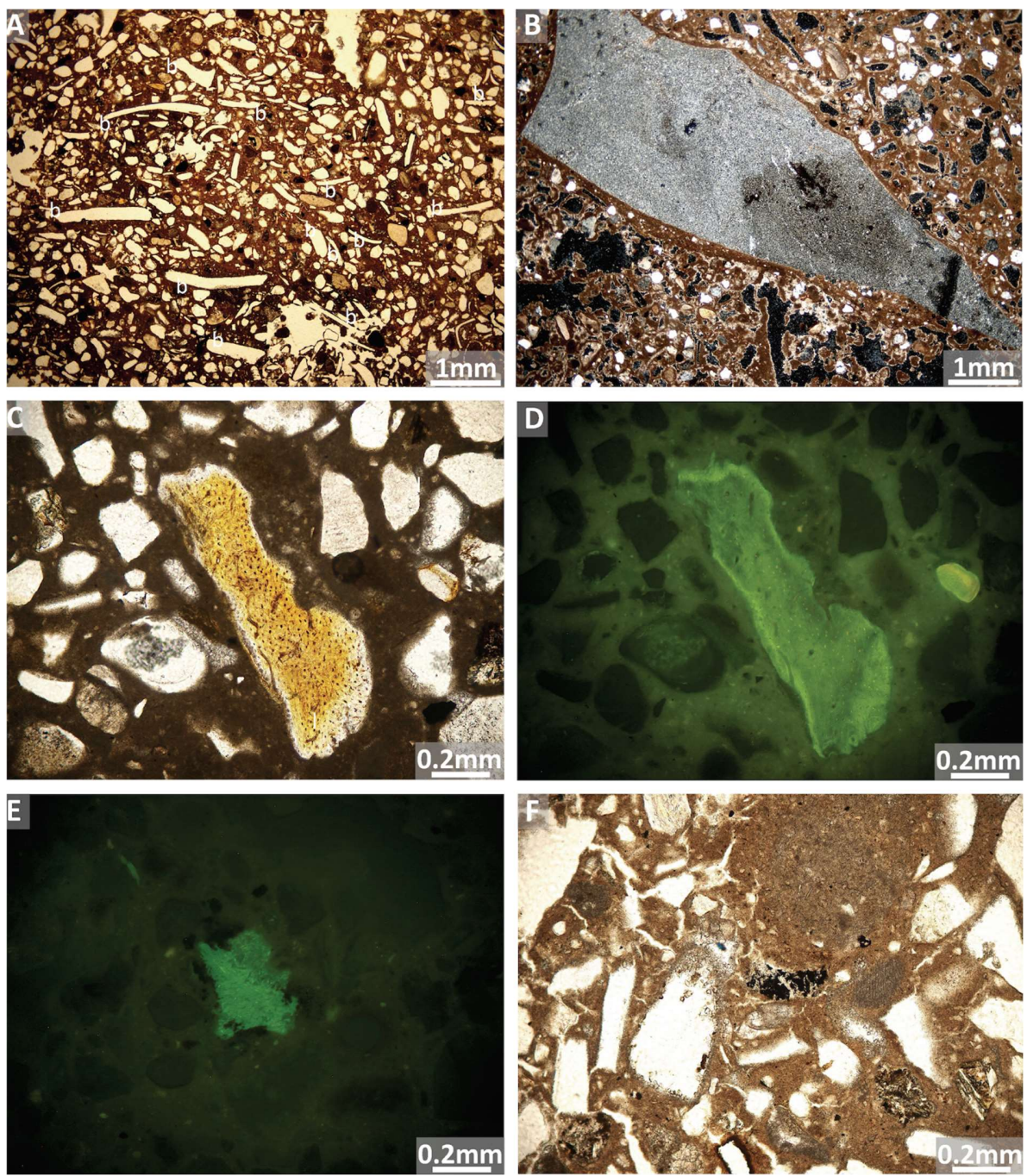


Fig. S5. Photomicrographs of some microscopic features detected in unit L5. (A) Preferential alignment of moldic voids, pseudomorphic of bioclasts (b) in the upper part of L5 (PPL). (B) A knapped lithic artifact (XPL). (C) A weakly altered bone fragment (PPL). (D) the same of (C) in BLF. (E) A bone fragment in BLF with Fe-oxyhydroxides impregnation on its margins. (F) A small fragment of charcoal (PPL).

3. Paleontology, biochronology, and zooarchaeology

3.1 Paleontology and biochronology. Large mammal remains are rare and fragmentary at ThI-L. Not unexpectedly in this environment, they are dominated by a large hippo probably identical with *Hippopotamus sirensis* from Tighennif (itself probably identical with *H. gorgops* from East Africa). A complete suid upper M3 was assigned to *Kolpochoerus maroccanus* by Geraads¹⁵, but if this species belongs in fact to *Metridiochoerus* as hypothesized by Souron⁴⁸, this tooth must in fact belong to either *K. majus* or to *K. limnetes/olduvaiensis*, all known in the East African Early Pleistocene. It is more simply built and smaller than most *K. olduvaiensis* teeth from the Early Pleistocene, slightly larger than *K. majus* teeth from the upper Konso levels⁴⁹, and more like teeth from Asbole⁵⁰ or Daka⁵¹ but we refrain from drawing biochronological conclusions from a single tooth. Bovids include a bovin, a gazelle, a medium-size alcelaphin, and a medium-size *Kobus* sp. An *Equus* and a rhino are also present, together with an Elephantidae, probably *Elephas*, although the poorly loxodont pattern of some *Loxodonta atlantica* teeth from Tighennif makes genus identification difficult.

A single tooth of *Crocidura* sp. is documented. An upper anterior premolar of Lagomorph (*Lepus* sp.?) is too primitive to belong to the common hare of the Middle Pleistocene of these quarries, *Trischizolagus raynali*, but could be of *Lepus*, already present at Ahl al Oughlam.

Rodents are represented by 15 teeth of which only three belong to murins, and 12 to gerbillins, suggesting rather arid environment. The absence of the dormouse *Eliomys* can be due to incomplete sampling, but that of the mole vole *Ellobius* is perhaps significant, as this genus is usually common when present. This genus is an Asian immigrant that first appears at Tighennif, suggesting that this Algerian site might be younger than ThI-L. A molar fragment of the murin *Paraethomys* differs from all other *Paraethomys* found in Morocco, including the *P. tighennifae* from other levels in Thomas and Oulad Hamida Quarries, but is reminiscent of *P. mellahae* Ameur, 1988 from Oued Mellah, an Algerian site earlier than Tighennif, according to Ameur⁵². A few teeth document two unnamed species of *Gerbillus*, both different from the species known at *Grotte à Hominidés*, at *Grotte des Rhinocéros* of the nearby Oulad Hamida 1 Quarry and at Tighennif⁸. The evolutionary grade of the smaller form is intermediate between those of *G. minutus* from the Plio-Pleistocene and of *G. campestris* of the Middle Pleistocene.

On the whole, the mammalian fauna from ThI-L is too poor to be confidently dated by biochronology, but it significantly differs from those of GH-CCC-unit 4, and also from that of Tighennif.

It is well-known that the rodent fauna of the northwestern African Pleistocene is highly endemic⁵³, but the large mammals have strong affinities with Eastern Africa⁵⁴, although temporal resolution is too low to estimate the dates of possible dispersal events. Most of the taxa present at ThI-L may have local ancestors, except perhaps *K. majus*, which must be of East African origin, because the earlier sites of Mansourah⁵⁵ and Aïn Hanech⁵⁶ yielded instead *K. olduvaiensis*, which belongs to another lineage⁴⁸.

3.2 Remarks on biochronology of Tighennif site (Algeria). The age of this site remains poorly supported. Geraads et al.⁵⁷ accepted an age close to 0.7 Ma, but it is becoming increasingly clear that this age was underestimated⁵⁸. Pickford⁵⁹ estimated its age at 1.4 ± 0.3 Ma, based upon his reassignment of the only suid from this locality to *Metridiochoerus andrewsi*, a species older than the South African *M. compactus*. This re-identification may be correct, but Pickford's biochronological conclusion is debatable, as the East African chronological range of *M. andrewsi* extends after 1 Ma. For instance, at Daka, a site well-dated at 1 Ma⁶⁰ the range of M3 length (63.7–88.1 mm, N = 4)⁶⁰ is almost the same as at Tighennif (64–83.5 mm, N = 6). We agree that Tighennif cannot be much younger than 1 Ma, but on the basis of bovids⁶¹, an age older than 1.5 is very unlikely.

3.3 Taphonomy. The faunal assemblage is highly fragmented and the bone surfaces are badly preserved. The main alterations are natural abrasion striations, desquamation, fissuring and polishing (Supplementary Fig. S6). Trampling, weathering and water flowing could be the main post-depositional agents of alteration, notably in this context of open-air deposits in wetland environments. Besides, we notice a total absence of anthropogenic and carnivorous marks, possibly due to this scarcity of legible surfaces. However, crocodile tooth marks (scores and punctures) could be identified, some on hippo remains (Supplementary Fig. S7)⁶²⁻⁶⁵.



Fig. S6. Natural notches and abrasion striations on an unidentified bone fragment (ThI-L- R27-16). Digital microscope images C. Daujeard.



Fig. S7. Crocodile tooth punctures on a fragment of a hippo talus (ThI-L-5381). Photo C. Daujeard.

Table S2. Thermal demagnetization data.

- (1) Sample = sample name
- (2) Temperature (°C)
- (3) NRM intensity (A/m)
- (4) Core Declination (°E)
- (5) Core Inclination (°)
- (6) Geographic Declination (°E)
- (7) Geographic Inclination (°)

| OH1 Bed 2 (trench South Wall, samples S004–S314) | | | | | | | | | |
|--------------------------------------------------|-----|----------|--------|--------|-------|-------|--|--|--|
| S004 | 0 | 1.72E-04 | 330.87 | 0.15 | 78.6 | -60.9 | | | |
| S004 | 100 | 1.70E-04 | 326.67 | -4.75 | 69.7 | -56.4 | | | |
| S004 | 150 | 1.88E-04 | 329.76 | -20.6 | 41.5 | -54 | | | |
| S004 | 200 | 1.80E-04 | 331.39 | -18.48 | 43.4 | -56.4 | | | |
| S004 | 225 | 1.74E-04 | 335.48 | -17.35 | 41.3 | -60.3 | | | |
| S004 | 250 | 1.70E-04 | 338.63 | -23.02 | 28.9 | -59 | | | |
| S004 | 275 | 1.57E-04 | 337.09 | -21.12 | 33.5 | -59.2 | | | |
| S004 | 300 | 1.57E-04 | 335.34 | -26.61 | 28.1 | -54.3 | | | |
| S004 | 325 | 1.44E-04 | 328.73 | -25.22 | 36.1 | -50.6 | | | |
| S004 | 350 | 1.42E-04 | 326.78 | -27.51 | 34.7 | -47.9 | | | |
| S004 | 375 | 1.27E-04 | 321.21 | -20.72 | 47.2 | -46.8 | | | |
| S004 | 400 | 1.33E-04 | 327.91 | -12.58 | 55.5 | -55.8 | | | |
| S004 | 425 | 1.33E-04 | 326.97 | -7.92 | 64 | -56.1 | | | |
| S004 | 450 | 1.39E-04 | 324.08 | -8.97 | 63.2 | -53.1 | | | |
| S004 | 475 | 1.30E-04 | 318.47 | -10.8 | 62.2 | -47.3 | | | |
| S004 | 500 | 1.10E-04 | 306.29 | -10.25 | 65.6 | -35.6 | | | |
| S004 | 525 | 1.28E-04 | 303.07 | -16.39 | 58.9 | -31.6 | | | |
| S004 | 550 | 1.19E-04 | 322.48 | -2.35 | 74.4 | -52.4 | | | |
| S004 | 575 | 1.19E-04 | 323.24 | -22.69 | 43.3 | -47.7 | | | |
| S004 | 600 | 1.48E-04 | 327.84 | -20.92 | 42.6 | -52.3 | | | |
| S004 | 625 | 1.38E-04 | 327.95 | -30.92 | 29.8 | -46.6 | | | |
| S004 | 650 | 1.42E-04 | 335.51 | -51.45 | 6.6 | -34.6 | | | |
| S004 | 675 | 1.51E-04 | 317.09 | -43.74 | 23.7 | -31.9 | | | |
| S010 | 0 | 2.76E-04 | 316.18 | 76.46 | 161.8 | -9.7 | | | |
| S010 | 100 | 2.60E-04 | 293.42 | 74.97 | 157.4 | -5.9 | | | |
| S010 | 150 | 2.39E-04 | 302.09 | 72.58 | 156.4 | -9.2 | | | |
| S010 | 200 | 2.22E-04 | 321.24 | 70.78 | 159 | -14.9 | | | |
| S010 | 225 | 2.14E-04 | 320.01 | 70.92 | 158.8 | -14.5 | | | |
| S010 | 250 | 2.16E-04 | 322.53 | 71.67 | 159.9 | -14.5 | | | |
| S010 | 275 | 1.97E-04 | 325.54 | 70.88 | 160.2 | -15.7 | | | |
| S010 | 300 | 1.89E-04 | 330.75 | 69.85 | 161.1 | -17.5 | | | |
| S010 | 325 | 1.83E-04 | 342.74 | 70.43 | 165.3 | -18.7 | | | |
| S010 | 350 | 1.73E-04 | 352.25 | 65.85 | 167.8 | -23.9 | | | |
| S010 | 375 | 1.60E-04 | 354.75 | 67.48 | 169.1 | -22.4 | | | |
| S010 | 400 | 1.55E-04 | 348.35 | 71.22 | 167.4 | -18.4 | | | |
| S010 | 425 | 1.42E-04 | 351.65 | 69.87 | 168.2 | -19.9 | | | |
| S010 | 450 | 1.23E-04 | 346.74 | 66.33 | 165.5 | -23 | | | |
| S010 | 475 | 1.08E-04 | 345.84 | 63.25 | 164.3 | -25.9 | | | |
| S010 | 500 | 1.08E-04 | 339.23 | 67.08 | 162.8 | -21.4 | | | |
| S010 | 525 | 1.15E-04 | 330.98 | 63.95 | 157.9 | -22.6 | | | |
| S010 | 550 | 8.64E-05 | 339.05 | 63 | 161 | -25.1 | | | |
| S010 | 575 | 7.37E-05 | 338.18 | 63.64 | 160.8 | -24.3 | | | |
| S010 | 600 | 6.87E-05 | 301.97 | 87.28 | 169 | -1.4 | | | |
| S010 | 625 | 5.83E-05 | 321.69 | 77.78 | 163.6 | -9.6 | | | |
| S010 | 650 | 5.52E-05 | 232.22 | 68.98 | 154.4 | 12.7 | | | |
| S010 | 675 | 5.29E-05 | 290.11 | 71.74 | 154.1 | -6.2 | | | |
| S010 | 700 | 2.72E-04 | 341.23 | 71.87 | 142.3 | -17.1 | | | |
| S010 | 725 | 2.61E-04 | 347.22 | 67.98 | 143.2 | -21.4 | | | |
| S040 | 150 | 2.71E-04 | 350.56 | 64.81 | 143.9 | -24.8 | | | |
| S040 | 200 | 2.61E-04 | 344.08 | 61.32 | 139.8 | -27.5 | | | |
| S040 | 225 | 2.49E-04 | 347.52 | 60.92 | 141.4 | -28.3 | | | |
| S040 | 250 | 2.44E-04 | 341.12 | 58.94 | 137.3 | -29.2 | | | |
| S040 | 275 | 2.34E-04 | 340.97 | 64.2 | 139.3 | -24.3 | | | |
| S040 | 300 | 2.08E-04 | 341.64 | 63.26 | 139.3 | -25.3 | | | |
| S040 | 325 | 1.92E-04 | 334.95 | 58.37 | 133.7 | -28.4 | | | |
| S040 | 350 | 1.81E-04 | 337.46 | 59.99 | 135.8 | -27.5 | | | |
| S040 | 375 | 1.71E-04 | 328.94 | 58.38 | 130.7 | -26.7 | | | |
| S040 | 400 | 1.49E-04 | 332.5 | 57.28 | 131.8 | -28.7 | | | |
| S040 | 425 | 1.37E-04 | 332.86 | 56.12 | 131.3 | -29.7 | | | |
| S040 | 450 | 1.34E-04 | 321.08 | 54.56 | 124.2 | -26.8 | | | |
| S040 | 475 | 1.24E-04 | 315.53 | 54.48 | 121.7 | -24.5 | | | |
| S040 | 500 | 1.00E-04 | 311.36 | 42.94 | 109.4 | -28.9 | | | |
| S040 | 525 | 1.29E-04 | 303.88 | 45.61 | 109.2 | -23 | | | |
| S040 | 550 | 1.61E-04 | 312.2 | 42.67 | 109.5 | -29.6 | | | |
| S040 | 575 | 1.31E-04 | 315.34 | 38.29 | 106.6 | -33.9 | | | |
| S040 | 600 | 1.23E-04 | 305.15 | 34.43 | 98.3 | -28.4 | | | |
| S040 | 625 | 9.86E-05 | 303.34 | 31.17 | 94.2 | -28.1 | | | |
| S040 | 650 | 1.14E-04 | 299.53 | 29.1 | 90.9 | -25.5 | | | |
| S040 | 675 | 1.04E-04 | 301.44 | 38.57 | 101.3 | -24.1 | | | |
| S040 | 700 | 1.34E-04 | 270.27 | 25.39 | 98.7 | -0.2 | | | |
| S040 | 725 | 1.26E-04 | 274.21 | 23.15 | 96.5 | -3.9 | | | |
| S040 | 750 | 1.18E-04 | 281.43 | 12.48 | 86 | -11.2 | | | |

Table S2. Thermal demagnetization data.

- (1) Sample = sample name
- (2) Temperature (°C)
- (3) NRM intensity (A/m)
- (4) Core Declination (°E)
- (5) Core Inclination (°)
- (6) Geographic Declination (°E)
- (7) Geographic Inclination (°)

| | | | | | | | | | | | | | |
|------|-----|----------|--------|--------|-------|-------|------|-----|----------|--------|-------|-------|-------|
| S204 | 450 | 1.05E-04 | 266.74 | 33.72 | 113.1 | 8.8 | S240 | 225 | 6.49E-04 | 269.37 | 78.42 | 161.6 | 6 |
| S204 | 475 | 9.93E-05 | 261.75 | 36.27 | 115.3 | 13.1 | S240 | 250 | 5.85E-04 | 259.07 | 78.29 | 161.7 | 8.1 |
| S204 | 500 | 7.76E-05 | 279.99 | 30.76 | 112.4 | -2.8 | S240 | 275 | 4.96E-04 | 277.12 | 77.57 | 160.9 | 4.3 |
| S204 | 525 | 7.60E-05 | 266.07 | 9.96 | 89.4 | 5.7 | S240 | 300 | 4.55E-04 | 298.26 | 78.87 | 163.5 | 0.7 |
| S204 | 550 | 7.53E-05 | 251.43 | 17.21 | 94.7 | 20.8 | S240 | 325 | 4.19E-04 | 275.7 | 78.54 | 161.8 | 4.8 |
| S204 | 575 | 8.71E-05 | 252.4 | -3.43 | 73.3 | 16.6 | S240 | 350 | 3.47E-04 | 274.61 | 77.36 | 160.6 | 4.8 |
| S204 | 600 | 8.89E-05 | 266.88 | -0.11 | 79.6 | 3 | S240 | 375 | 3.25E-04 | 276.48 | 78.26 | 161.6 | 4.6 |
| S204 | 625 | 8.61E-05 | 250.81 | -1.11 | 75.3 | 18.6 | S240 | 400 | 2.77E-04 | 259.3 | 76.82 | 160.2 | 8.3 |
| S204 | 650 | 6.63E-05 | 263.55 | -28.47 | 51.2 | 0.3 | S240 | 425 | 2.62E-04 | 271.13 | 79.45 | 162.7 | 5.7 |
| S204 | 675 | 4.50E-05 | 300.38 | -49.83 | 29.3 | -27.8 | S240 | 450 | 2.41E-04 | 254.29 | 81.31 | 164.8 | 8.3 |
| S215 | 0 | 5.35E-04 | 217.96 | 74.52 | 166.4 | 17.1 | S240 | 475 | 2.34E-04 | 241.19 | 80.92 | 165.2 | 10.3 |
| S215 | 100 | 5.04E-04 | 229.75 | 77.4 | 166.4 | 13 | S240 | 500 | 1.71E-04 | 246.45 | 72.14 | 156.5 | 12.8 |
| S215 | 150 | 4.21E-04 | 245.33 | 79.08 | 166.2 | 9.5 | S240 | 525 | 1.83E-04 | 251.28 | 80.26 | 163.9 | 9 |
| S215 | 200 | 3.25E-04 | 235.39 | 81.76 | 169.4 | 9.6 | S240 | 550 | 1.46E-04 | 241.15 | 74.41 | 159.3 | 13.3 |
| S215 | 225 | 2.81E-04 | 255.41 | 78.51 | 165.1 | 7.8 | S240 | 575 | 1.17E-04 | 248.9 | 64.89 | 149.2 | 14.3 |
| S215 | 250 | 2.43E-04 | 213.01 | 87.36 | 174.8 | 7.2 | S240 | 600 | 9.32E-05 | 262.19 | 65.52 | 148.7 | 8.7 |
| S215 | 275 | 2.02E-04 | 253.29 | 81.76 | 168.3 | 7.3 | S240 | 625 | 4.75E-05 | 184.14 | 64.13 | 171.2 | 31.8 |
| S215 | 300 | 1.68E-04 | 251.23 | 81.33 | 168 | 7.7 | S240 | 650 | 9.98E-05 | 252.38 | 85.38 | 168.8 | 7.4 |
| S215 | 325 | 1.22E-04 | 186.03 | 81.59 | 175.4 | 13.4 | S240 | 675 | 5.23E-05 | 299.94 | 75.41 | 160.7 | -1.4 |
| S215 | 350 | 1.21E-04 | 128.5 | 80.81 | 183.6 | 10.7 | S253 | 0 | 1.43E-03 | 312.96 | 83.78 | 163.6 | 12.7 |
| S215 | 375 | 1.08E-04 | 147.61 | 77.54 | 183.2 | 15.5 | S253 | 100 | 1.52E-03 | 317.5 | 82.57 | 163.2 | 11.5 |
| S215 | 400 | 9.89E-05 | 210.51 | 78.42 | 170.2 | 14.9 | S253 | 150 | 1.25E-03 | 338.49 | 79.14 | 164.3 | 6.9 |
| S215 | 425 | 1.07E-04 | 197.73 | 80.92 | 173.4 | 13.6 | S253 | 200 | 1.02E-03 | 343.78 | 78.51 | 165.1 | 5.9 |
| S215 | 450 | 7.61E-05 | 164.24 | 65.8 | 183.5 | 28.2 | S253 | 225 | 9.16E-04 | 347.97 | 77.97 | 165.8 | 5.2 |
| S215 | 475 | 8.58E-05 | 98.73 | 62.15 | 204.1 | 8.5 | S253 | 250 | 8.16E-04 | 346.41 | 78.02 | 165.5 | 5.3 |
| S215 | 500 | 6.37E-05 | 99.02 | 59.24 | 207 | 8.9 | S253 | 275 | 6.95E-04 | 339.43 | 77.6 | 163.9 | 5.4 |
| S215 | 525 | 6.08E-05 | 66.54 | 62.51 | 201.5 | -6.1 | S253 | 300 | 6.19E-04 | 346.74 | 78.42 | 165.6 | 5.7 |
| S215 | 550 | 3.48E-05 | 52.86 | 37.64 | 220.4 | -25 | S253 | 325 | 5.13E-04 | 7.37 | 76.78 | 170 | 3.9 |
| S215 | 575 | 4.22E-05 | 79.39 | 16.57 | 248.6 | -8.7 | S253 | 350 | 4.29E-04 | 2.41 | 77.42 | 168.8 | 4.4 |
| S215 | 600 | 4.21E-05 | 73.54 | 23.89 | 240.4 | -12.9 | S253 | 375 | 3.79E-04 | 357.85 | 74.2 | 167.7 | 1.2 |
| S215 | 625 | 8.33E-05 | 61.77 | -10.44 | 275.5 | -28.6 | S253 | 400 | 3.32E-04 | 10.07 | 77.05 | 170.5 | 4.2 |
| S215 | 650 | 2.93E-05 | 50.01 | -40.23 | 312 | -33 | S253 | 425 | 2.98E-04 | 1.84 | 80.71 | 168.6 | 7.7 |
| S215 | 675 | 1.99E-05 | 352.33 | -56.41 | 1.7 | -38.2 | S253 | 450 | 2.43E-04 | 32.95 | 78 | 174.8 | 6.8 |
| S221 | 0 | 7.65E-04 | 208.86 | 79.74 | 165.2 | 13 | S253 | 475 | 2.41E-04 | 32.24 | 79.17 | 174.1 | 7.8 |
| S221 | 100 | 6.49E-04 | 211.06 | 83.52 | 166.9 | 9.5 | S253 | 500 | 1.88E-04 | 69.09 | 82.48 | 175.5 | 14.2 |
| S221 | 150 | 5.06E-04 | 257.45 | 87.62 | 168 | 4.5 | S253 | 525 | 1.98E-04 | 72.69 | 81.14 | 177 | 14.2 |
| S221 | 200 | 4.02E-04 | 311.47 | 87.09 | 168.1 | 2.1 | S253 | 550 | 1.54E-04 | 89.07 | 79.48 | 179.3 | 16.5 |
| S221 | 225 | 3.36E-04 | 343.99 | 85.29 | 169 | -0.5 | S253 | 575 | 1.14E-04 | 109.36 | 47.88 | 212.8 | 25.4 |
| S221 | 250 | 2.84E-04 | 357.18 | 87.42 | 170.2 | 1.4 | S253 | 600 | 7.78E-05 | 127.95 | 44.01 | 214.9 | 38.8 |
| S221 | 275 | 2.37E-04 | 29.72 | 81.78 | 174.4 | -3.1 | S253 | 625 | 8.85E-05 | 110.31 | 9.44 | 254.8 | 22 |
| S221 | 300 | 2.17E-04 | 25.79 | 80.46 | 174.4 | -4.6 | S253 | 650 | 5.72E-05 | 101.85 | 17.77 | 244.2 | 16 |
| S221 | 325 | 1.83E-04 | 10.76 | 83.67 | 171.5 | -2.2 | S253 | 675 | 4.63E-05 | 159.31 | 24.49 | 233.6 | 69.3 |
| S221 | 350 | 1.49E-04 | 0.34 | 79.6 | 170.3 | -6.4 | S268 | 0 | 2.74E-03 | 174.33 | 88.2 | 160.5 | 13.8 |
| S221 | 375 | 1.26E-04 | 32.42 | 70.96 | 180.6 | -12.1 | S268 | 100 | 2.51E-03 | 81.44 | 88.77 | 161.5 | 11.8 |
| S221 | 400 | 1.10E-04 | 33.51 | 71 | 180.9 | -11.8 | S268 | 150 | 2.09E-03 | 4.53 | 85.93 | 160.6 | 7.9 |
| S221 | 425 | 9.89E-05 | 38.62 | 56.42 | 192.1 | -21.9 | S268 | 200 | 1.67E-03 | 12.14 | 84.68 | 161.4 | 6.8 |
| S221 | 450 | 1.14E-04 | 57.61 | 54.6 | 200.7 | -14.6 | S268 | 225 | 1.48E-03 | 9.44 | 84.67 | 161.2 | 6.7 |
| S221 | 475 | 9.32E-05 | 68.78 | 42.91 | 214.7 | -12.5 | S268 | 250 | 1.33E-03 | 8.86 | 83.47 | 161.3 | 5.5 |
| S221 | 500 | 6.88E-05 | 54.19 | 30.77 | 222.2 | -27.8 | S268 | 275 | 1.09E-03 | 11.33 | 81.55 | 161.9 | 3.7 |
| S221 | 525 | 5.03E-05 | 32.75 | 24.52 | 216.8 | -47.3 | S268 | 300 | 9.97E-04 | 8.06 | 82.69 | 161.3 | 4.8 |
| S221 | 550 | 8.66E-05 | 55.16 | 10.05 | 245.5 | -33.3 | S268 | 325 | 8.50E-04 | 7.39 | 82.29 | 161.3 | 4.4 |
| S221 | 575 | 7.72E-05 | 51.27 | 11.79 | 242.4 | -36.6 | S268 | 350 | 7.21E-04 | 5.64 | 81.62 | 161.1 | 3.7 |
| S221 | 600 | 7.03E-05 | 43.45 | -13.45 | 275.6 | -46.1 | S268 | 375 | 6.19E-04 | 11.65 | 82.17 | 161.9 | 4.3 |
| S221 | 625 | 8.57E-05 | 73.36 | -18.88 | 278.8 | -17 | S268 | 400 | 5.66E-04 | 13.15 | 80.08 | 162.5 | 2.3 |
| S221 | 650 | 8.72E-05 | 40.54 | -26.78 | 29.5 | -45.1 | S268 | 425 | 5.04E-04 | 17.98 | 80.32 | 163.3 | 2.8 |
| S221 | 675 | 1.11E-04 | 41.42 | -16.98 | 281.2 | -47.4 | S268 | 450 | 4.40E-04 | 4.59 | 78.83 | 161.2 | 0.9 |
| S230 | 0 | 7.58E-04 | 243.7 | 74.17 | 162.4 | 17.6 | S268 | 475 | 4.22E-04 | 11.98 | 82.35 | 161.9 | 4.5 |
| S230 | 100 | 7.81E-04 | 255.42 | 78.41 | 165.7 | 13.7 | S268 | 500 | 3.12E-04 | 15.31 | 80.06 | 162.9 | 2.4 |
| S230 | 150 | 5.94E-04 | 272.58 | 76.79 | 163.9 | 10.1 | S268 | 525 | 3.22E-04 | 32.25 | 83.26 | 163.9 | 6.3 |
| S230 | 200 | 4.41E-04 | 289.83 | 75.27 | 163.4 | 5.7 | S268 | 550 | 2.41E-04 | 44.35 | 79.62 | 167.5 | 4.5 |
| S230 | 225 | 3.70E-04 | 295.8 | 72.86 | 161.9 | 3.2 | S268 | 575 | 1.99E-04 | 53.46 | 68.82 | 177.2 | -0.9 |
| S230 | 250 | 3.10E-04 | 286.56 | 71.1 | 159.1 | 5.2 | S268 | 600 | 1.11E-04 | 26.94 | 64.23 | 171.9 | -11.1 |
| S230 | 275 | 2.16E-04 | 301.52 | 66.03 | 157 | -2 | S268 | 625 | 1.43E-04 | 49.44 | 44.57 | 194.9 | -17.9 |
| S230 | 300 | 2.07E-04 | 307.02 | 63.66 | 156.4 | -5.2 | S268 | 650 | 8.84E-05 | 67.63 | 54.7 | 192.6 | -2.6 |
| S230 | 325 | 1.51E-04 | 306.66 | 55.69 | 150 | -9.9 | S268 | 675 | 1.09E-04 | 27.98 | 48.45 | 180.3 | -24.7 |
| S230 | 350 | 1.24E-04 | 300.65 | 46.4 | 140 | -11.9 | S273 | 25 | 2.26E-03 | 304.13 | 84.34 | 161.5 | 9.8 |
| S230 | 375 | 1.02E-04 | 294.3 | 35.76 | 128 | -12.5 | S273 | 100 | 2.18E-03 | 310.82 | 83.56 | 161.4 | 8.7 |
| S230 | 400 | 7.33E-05 | 295.75 | 31.02 | 124.1 | -15.5 | S273 | 150 | 1.77E-03 | 331.15 | 80.21 | 161.6 | 4.4 |
| S230 | 425 | 6.76E-05 | 287.24 | 30.45 | 120.8 | -8.9 | S273 | 200 | 1.47E-03 | 337.1 | 78.33 | 161.8 | 2.2 |
| S230 | 450 | 5.85E-05 | 314.66 | 30.58 | 132.4 | -29.8 | S273 | 225 | 1.33E-03 | 342.19 | 77.8 | 162.6 | 1.4 |
| S230 | 475 | 4.21E-05 | 319 | 15.45 | 119.6 | -41.5 | S273 | 250 | 1.20E-03 | 350.19 | 77.16 | 164.1 | 0.3 |
| S230 | 500 | 6.43E-05 | 318.61 | -4.76 | 92.6 | -48.6 | S273 | 275 | 9.68E-04 | 356.45 | 75.26 | 165.4 | -1.7 |
| S230 | 525 | 5.44E-05 | 330.4 | -23.84 | 58.8 | -59.1 | S273 | 300 | 8.48E-04 | 356.41 | 74.32 | 165.3 | -2.7 |
| S230 | 550 | 8.55E-05 | 333.64 | -61.03 | 12.8 | -36.4 | S273 | 325 | 7.41E-04 | 354.45 | 72.79 | 164.6 | -4.1 |
| S230 | 575 | 8.01E-05 | 310.27 | -53.76 | 29.4 | -31.9 | S273 | 350 | 6.59E-04 | 3.24 | 72.16 | 167.3 | -4.8 |
| S230 | 600 | 9.10E-05 | 290.31 | -64.59 | 22.4 | -18.6 | S273 | 375 | 5.82E-04 | 3.98 | 70.59 | 167.6 | -6.4 |
| S230 | 625 | 8.54E-05 | 359.66 | -60.56 | 357.5 | -40.4 | S273 | 400 | 5.09E-04 | 15.15 | 67.96 | 172</ | |

Table S2. Thermal demagnetization data.

- (1) Sample = sample name
- (2) Temperature (°C)
- (3) NRM intensity (A/m)
- (4) Core Declination (°E)
- (5) Core Inclination (°)
- (6) Geographic Declination (°E)
- (7) Geographic Inclination (°)

| | | | | | | | | | | | | | |
|------|-----|----------|--------|-------|-------|-------|-------|-----|----------|--------|---------|-------|-------|
| S281 | 575 | 1.74E-04 | 346.35 | 77.88 | 159.4 | 1.2 | oh2_3 | 300 | 5.62E-03 | 167.4 | -10.8 | 167.4 | -10.8 |
| S281 | 600 | 1.04E-04 | 314.17 | 70.38 | 148.3 | -0.9 | oh2_3 | 325 | 5.00E-03 | 170 | -11.4 | 170 | -11.4 |
| S281 | 625 | 8.19E-05 | 21.75 | 47.4 | 178.6 | -26.6 | oh2_3 | 350 | 4.76E-03 | 170 | -7.9 | 170 | -7.9 |
| S281 | 650 | 8.46E-05 | 11.17 | 59.31 | 168.2 | -17.1 | oh2_3 | 375 | 4.61E-03 | 170.4 | -12.6 | 170.4 | -12.6 |
| S281 | 675 | 1.06E-04 | 20.31 | 73.59 | 167.9 | -2.4 | oh2_3 | 400 | 4.57E-03 | 172.3 | -8.8 | 172.3 | -8.8 |
| S287 | 25 | 3.63E-03 | 296.15 | 84.49 | 158.2 | 11.5 | oh2_3 | 425 | 4.33E-03 | 172.9 | -4.3 | 172.9 | -4.3 |
| S287 | 100 | 3.20E-03 | 305.93 | 81.76 | 156.5 | 9.1 | oh2_3 | 450 | 4.10E-03 | 175.5 | 6.5 | 175.5 | 6.5 |
| S287 | 150 | 2.56E-03 | 321.84 | 78.72 | 156.3 | 5 | oh2_3 | 475 | 4.46E-03 | 168.2 | -8.7 | 168.2 | -8.7 |
| S287 | 200 | 2.11E-03 | 326.66 | 77.48 | 156.4 | 3.5 | oh2_3 | 500 | 4.40E-03 | 161 | -14.7 | 161 | -14.7 |
| S287 | 225 | 1.92E-03 | 326.03 | 76.21 | 155.6 | 2.5 | oh2_3 | 525 | 4.03E-03 | 164.1 | -6.9 | 164.1 | -6.9 |
| S287 | 250 | 1.71E-03 | 323.47 | 75.88 | 154.9 | 2.5 | oh2_3 | 550 | 3.26E-03 | 148.6 | -2.9 | 148.6 | -2.9 |
| S287 | 275 | 1.38E-03 | 328.01 | 73.52 | 154.6 | -0.1 | oh2_3 | 575 | 3.39E-03 | 163.4 | -13.6 | 163.4 | -13.6 |
| S287 | 300 | 1.21E-03 | 331.04 | 67.87 | 152.7 | -5.5 | oh2_3 | 600 | 3.05E-03 | 156.7 | -3.4 | 156.7 | -3.4 |
| S287 | 325 | 1.10E-03 | 322.42 | 71.6 | 152.2 | -0.8 | oh2_3 | 625 | 3.21E-03 | 162.1 | -18.5 | 162.1 | -18.5 |
| S287 | 350 | 9.24E-04 | 316.77 | 70.12 | 149.8 | -0.7 | oh2_3 | 650 | 3.34E-03 | 154.2 | 11 | 154.2 | 11 |
| S287 | 375 | 8.25E-04 | 319.7 | 69.19 | 150 | -2.1 | oh2_3 | 675 | 2.81E-03 | 146.5 | -7.5 | 146.5 | -7.5 |
| S287 | 400 | 7.30E-04 | 314.67 | 69.1 | 148.6 | -1 | oh2_4 | 0 | 5.89E-03 | 341.1 | 10.7 | 341.1 | 10.7 |
| S287 | 425 | 6.72E-04 | 312.4 | 67.82 | 147.1 | -1.3 | oh2_4 | 100 | 5.54E-03 | 341.2 | 7.5 | 341.2 | 7.5 |
| S287 | 450 | 6.21E-04 | 316.49 | 67.76 | 148.2 | -2.4 | oh2_4 | 150 | 4.66E-03 | 343 | 2.6 | 343 | 2.6 |
| S287 | 475 | 5.99E-04 | 319.89 | 66.48 | 148.3 | -4.3 | oh2_4 | 200 | 4.34E-03 | 345.2 | 1.6 | 345.2 | 1.6 |
| S287 | 500 | 5.44E-04 | 318.44 | 63.92 | 146.2 | -5.8 | oh2_4 | 225 | 4.00E-03 | 344.3 | 1.9 | 344.3 | 1.9 |
| S287 | 525 | 4.53E-04 | 306.18 | 62.31 | 141.2 | -3 | oh2_4 | 250 | 3.61E-03 | 340.6 | 0.3 | 340.6 | 0.3 |
| S287 | 550 | 3.42E-04 | 318.38 | 63.48 | 145.9 | -6.2 | oh2_4 | 275 | 3.49E-03 | 344.6 | -3.1 | 344.6 | -3.1 |
| S287 | 575 | 2.47E-04 | 305.87 | 56.01 | 136.1 | -6.7 | oh2_4 | 300 | 3.00E-03 | 344.7 | -8 | 344.7 | -8 |
| S287 | 600 | 1.88E-04 | 294.56 | 47.51 | 125.2 | -5.4 | oh2_4 | 325 | 2.61E-03 | 346.3 | -6.2 | 346.3 | -6.2 |
| S287 | 625 | 1.10E-04 | 298.61 | 56.06 | 133.9 | -3.4 | oh2_4 | 350 | 2.38E-03 | 345.4 | -9.3 | 345.4 | -9.3 |
| S287 | 650 | 1.57E-04 | 309.01 | 36.49 | 121.5 | -20.3 | oh2_4 | 375 | 2.24E-03 | 338.4 | -11.5 | 338.4 | -11.5 |
| S287 | 675 | 1.12E-04 | 290.21 | 40.25 | 117.2 | -5.7 | oh2_4 | 400 | 2.44E-03 | 342 | -8.4 | 342 | -8.4 |
| S299 | 25 | 3.94E-03 | 223.48 | 85.18 | 159.9 | 13.5 | oh2_4 | 425 | 2.18E-03 | 339.1 | -13.6 | 339.1 | -13.6 |
| S299 | 100 | 3.74E-03 | 253.91 | 85.7 | 159.1 | 11.2 | oh2_4 | 450 | 1.57E-03 | 348.5 | 21.3 | 348.5 | 21.3 |
| S299 | 150 | 3.02E-03 | 295.17 | 84.12 | 157.9 | 7.5 | oh2_4 | 475 | 1.74E-03 | 339.2 | -20 | 339.2 | -20 |
| S299 | 200 | 2.56E-03 | 305.17 | 83.8 | 158.2 | 6.4 | oh2_4 | 500 | 2.00E-03 | 324.3 | -28.6 | 324.3 | -28.6 |
| S299 | 225 | 2.28E-03 | 309.36 | 82.54 | 157.5 | 5.2 | oh2_4 | 525 | 2.08E-03 | 323.7 | -21 | 323.7 | -21 |
| S299 | 250 | 2.02E-03 | 310.46 | 82.67 | 157.7 | 5.2 | oh2_4 | 550 | 1.21E-03 | 343.6 | -32.6 | 343.6 | -32.6 |
| S299 | 275 | 1.56E-03 | 312.13 | 82.76 | 157.9 | 5.1 | oh2_4 | 575 | 1.14E-03 | 350.7 | -22.9 | 350.7 | -22.9 |
| S299 | 300 | 1.39E-03 | 309.23 | 82.05 | 157.1 | 4.9 | oh2_4 | 600 | 4.17E-04 | 17.3 | 5.6 | 17.3 | 5.6 |
| S299 | 325 | 1.27E-03 | 310.31 | 82.25 | 157.4 | 4.9 | oh2_4 | 625 | 3.78E-04 | 27.4 | 21.2 | 27.4 | 21.2 |
| S299 | 350 | 1.04E-03 | 304.53 | 79.96 | 155 | 4.2 | oh2_4 | 650 | 4.78E-04 | 256.3 | 9.1 | 256.3 | 9.1 |
| S299 | 375 | 9.33E-04 | 302.61 | 79.76 | 154.6 | 4.4 | oh2_4 | 675 | 1.59E-03 | 321.7 | -63.8 | 321.7 | -63.8 |
| S299 | 400 | 7.78E-04 | 287.61 | 77.89 | 151.7 | 6.2 | S352 | 0 | 1.08E-02 | 98.956 | 36.225 | 181.5 | 7.8 |
| S299 | 425 | 1.00E-03 | 330.22 | 72.34 | 154.6 | -5.4 | S352 | 100 | 9.88E-03 | 103.61 | 31.562 | 185.9 | 12.1 |
| S299 | 450 | 6.18E-04 | 285.38 | 79.5 | 153.1 | 7.1 | S352 | 150 | 7.09E-03 | 98.659 | 32.51 | 185.3 | 7.8 |
| S299 | 475 | 6.22E-04 | 294.14 | 76.34 | 150.8 | 4.2 | S352 | 200 | 5.41E-03 | 92.591 | 35.103 | 182.9 | 2.7 |
| S299 | 500 | 4.68E-04 | 275.36 | 76.65 | 149.8 | 8.5 | S352 | 250 | 5.37E-03 | 92.869 | 35.02 | 183 | 2.9 |
| S299 | 525 | 4.18E-04 | 280.61 | 76.17 | 149.6 | 7.2 | S352 | 300 | 4.05E-03 | 95.277 | 38.851 | 179.1 | 4.7 |
| S299 | 550 | 3.74E-04 | 281.5 | 73.61 | 147.1 | 6.4 | S352 | 350 | 3.88E-03 | 93.479 | 31.88 | 186.1 | 3.5 |
| S299 | 575 | 2.40E-04 | 271.06 | 71.68 | 144.7 | 9.2 | S352 | 400 | 3.00E-03 | 105.76 | 45.689 | 171.4 | 11.7 |
| S299 | 600 | 1.30E-04 | 279.82 | 61.46 | 135.1 | 4.1 | S352 | 425 | 2.90E-03 | 90.225 | 28.421 | 189.6 | 0.7 |
| S299 | 625 | 8.44E-05 | 290.31 | 64.78 | 139.7 | 0.7 | S352 | 475 | 2.74E-03 | 94.217 | 37.34 | 180.6 | 4 |
| S299 | 650 | 1.16E-04 | 255.72 | 45.44 | 117.9 | 17.1 | S352 | 500 | 2.63E-03 | 99.97 | 42.17 | 175.5 | 8 |
| S299 | 675 | 1.45E-04 | 280.28 | 29.25 | 103.9 | -3.9 | S352 | 550 | 2.66E-03 | 105.02 | 43.246 | 173.9 | 11.6 |
| S314 | 25 | 6.04E-03 | 31.25 | 82.48 | 162.2 | 8.5 | S352 | 575 | 1.95E-03 | 112.34 | 37.567 | 178.5 | 18.2 |
| S314 | 100 | 5.43E-03 | 5.19 | 80.61 | 159.1 | 5.6 | S352 | 600 | 2.19E-03 | 106.99 | 37.307 | 179.6 | 14.1 |
| S314 | 150 | 4.41E-03 | 349.63 | 79.38 | 156.4 | 4.5 | S352 | 625 | 1.23E-03 | 186.73 | 16.591 | 105.3 | 73.1 |
| S314 | 200 | 3.72E-03 | 32.8 | 77.59 | 159 | 2.6 | S352 | 650 | 4.91E-04 | 311.91 | 62.958 | 107.3 | -16.7 |
| S314 | 225 | 3.27E-03 | 0.12 | 77.7 | 158.3 | 2.7 | S352 | 675 | 6.83E-04 | 105.22 | 51.783 | 165.3 | 10.1 |
| S314 | 250 | 3.01E-03 | 352.15 | 77.14 | 156.5 | 2.3 | S372 | 0 | 6.90E-03 | 80.401 | 0.6646 | 168.2 | -9.4 |
| S314 | 275 | 2.40E-03 | 342.97 | 77.53 | 154.7 | 3.1 | S372 | 100 | 7.30E-03 | 79.787 | -4.2449 | 173 | -10.6 |
| S314 | 300 | 2.02E-03 | 345.6 | 75.71 | 154.8 | 1.1 | S372 | 150 | 5.95E-03 | 71.596 | -8.0193 | 176.1 | -19.1 |
| S314 | 325 | 1.74E-03 | 342.76 | 75.54 | 154 | 1.2 | S372 | 200 | 5.37E-03 | 57.348 | -4.5896 | 170.9 | -32.9 |
| S314 | 350 | 1.48E-03 | 344.94 | 73.99 | 154.2 | -0.5 | S372 | 250 | 5.14E-03 | 53.644 | -4.46 | 170.4 | -36.6 |
| S314 | 375 | 1.30E-03 | 332.58 | 74.66 | 151.3 | 1.3 | S372 | 300 | 4.57E-03 | 46.253 | -8.0476 | 174.4 | -44.2 |
| S314 | 400 | 1.11E-03 | 334.94 | 73.8 | 151.5 | 0.3 | S372 | 350 | 4.54E-03 | 46.969 | -4.1682 | 169.2 | -43.2 |
| S314 | 425 | 6.81E-04 | 288.31 | 78.92 | 147.6 | 11.3 | S372 | 400 | 4.45E-03 | 43.452 | 0 | 162.7 | -46.1 |
| S314 | 450 | 8.82E-04 | 325.14 | 74.85 | 149.7 | 2.4 | S372 | 425 | 4.39E-03 | 42.036 | 3.922 | 156.7 | -46.6 |
| S314 | 475 | 8.68E-04 | 323.35 | 73.85 | 148.7 | 1.9 | S372 | 450 | 4.25E-03 | 42.992 | 4.3179 | 156.5 | -45.6 |
| S314 | 500 | 6.57E-04 | 322.02 | 69.97 | 146.1 | -1 | S372 | 475 | 4.22E-03 | 39.806 | 2.1726 | 158.4 | -49.2 |
| S314 | 525 | 5.44E-04 | 301.07 | 68.33 | 139.8 | 3.2 | S372 | 500 | 3.98E-03 | 37.938 | 4.8966 | 153.6 | -50.3 |
| S314 | 550 | 4.59E-04 | 305.36 | 69.22 | 141.4 | 2.5 | S372 | 525 | 4.03E-03 | 41.882 | 0.99526 | 160.8 | -47.5 |
| S314 | 575 | 2.80E-04 | 290.39 | 50.26 | 121.5 | -0.9 | S372 | 550 | 4.21E-03 | 35.617 | 1.4978 | 157.9 | -53.5 |
| S314 | 600 | 1.63E-04 | 272.16 | 13.49 | 81.9 | 1.4 | S372 | 575 | 4.00E-03 | 36.87 | 2.2906 | 157.1 | -52 |
| S314 | 625 | 1.45E-04 | 274.63 | -2.94 | 66.6 | -5.2 | S372 | 600 | 2.88E-03 | 37.036 | 17.141 | 136.2 | -46.2 |
| S314 | 650 | 1.85E-04 | 268.92 | 2.71 | 70.6 | 1.7 | S372 | 625 | 1.05E-03 | 6.3775 | -14.019 | 218.8 | -80.6 |
| S314 | 675 | 1.98E-04 | 286.58 | -7.66 | 60.5 | -0.6 | S372 | 650 | 1.10E-03 | 262.45 | 36.953 | 26.4 | 10.2 |
| | | | | | | | oh2_2 | 0 | 1.97E-02 | 170.8 | 0.2 | 170.8 | 0.2 |
| | | | | | | | oh2_2 | 100 | 1.77E-02 | 169.5 | 0.4 | 169.5 | 0.4 |
| | | | | | | | oh2_2 | 150 | 1.49E-02 | 170.8 | -2.9 | 170.8 | -2.9 |
| | | | | | | | oh2_2 | 200 | 1.30E-02 | 168.6 | -3.3 | 168.6 | -3. |

Table S2. Thermal demagnetization data.

- (1) Sample = sample name
- (2) Temperature (°C)
- (3) NRM intensity (A/m)
- (4) Core Declination (°E)
- (5) Core Inclination (°)
- (6) Geographic Declination (°E)
- (7) Geographic Inclination (°)

| | | | | | | | | | | | | | |
|-------|------|----------|--------|---------|-------|-------|------|-----|----------|--------|----------|-------|-------|
| oh2_5 | 350 | 2.14E-03 | 217.2 | 6.9 | 217.2 | 6.9 | S436 | 500 | 2.96E-03 | 48.25 | -14.091 | 160.8 | -42.3 |
| oh2_5 | 375 | 1.99E-03 | 217.6 | 7.4 | 217.6 | 7.4 | S436 | 525 | 2.53E-03 | 40.32 | -16.528 | 165.2 | -49.8 |
| oh2_5 | 400 | 1.67E-03 | 209 | 12.9 | 209 | 12.9 | S436 | 550 | 2.84E-03 | 44.893 | -13.289 | 159.9 | -45.6 |
| oh2_5 | 425 | 1.54E-03 | 212.2 | 1.9 | 212.2 | 1.9 | S436 | 575 | 2.26E-03 | 40.31 | -22.15 | 173.7 | -48.8 |
| oh2_5 | 450 | 1.49E-03 | 227.4 | -30.4 | 227.4 | -30.4 | S436 | 600 | 3.55E-03 | 41.898 | -35.884 | 191.5 | -42.7 |
| oh2_5 | 475 | 1.39E-03 | 201.6 | 5.6 | 201.6 | 5.6 | S436 | 625 | 3.19E-03 | 37.809 | -17.127 | 166.7 | -52.1 |
| oh2_5 | 500 | 1.27E-03 | 196.4 | 4.2 | 196.4 | 4.2 | S436 | 650 | 2.43E-03 | 17.763 | -0.23621 | 126.2 | -70.7 |
| oh2_5 | 525 | 2.04E-03 | 200.6 | 25.9 | 200.6 | 25.9 | S436 | 650 | 8.64E-04 | 202.32 | 0.33168 | 311.1 | 66.5 |
| oh2_5 | 550 | 1.31E-03 | 213.3 | 42 | 213.3 | 42 | S436 | 675 | 1.00E-03 | 38.279 | -50.697 | 209.6 | -36.9 |
| oh2_5 | 575 | 1.56E-03 | 166.7 | 44.7 | 166.7 | 44.7 | S436 | 0 | 1.54E-03 | 141.82 | 61.17 | 77.7 | 21.3 |
| oh2_5 | 600 | 7.31E-04 | 179 | -16.3 | 179 | -16.3 | S436 | 100 | 1.37E-03 | 136.84 | 58.955 | 81.2 | 21.2 |
| oh2_5 | 625 | 1.84E-03 | 144.3 | 53.8 | 144.3 | 53.8 | S436 | 150 | 9.11E-04 | 126.54 | 51.841 | 91.1 | 20.7 |
| oh2_5 | 650 | 1.35E-03 | 81.1 | 85.5 | 81.1 | 85.5 | S436 | 200 | 8.11E-04 | 98.242 | 44.452 | 104.2 | 5.2 |
| oh2_5 | 675 | 1.70E-03 | 214.6 | 64.1 | 214.6 | 64.1 | S436 | 250 | 6.28E-04 | 105.56 | 58.534 | 89.5 | 7.2 |
| S386 | 0 | 7.43E-03 | 87.982 | 6.183 | 161.6 | -3.6 | S453 | 300 | 7.90E-04 | 57.636 | 51.56 | 93 | -20.3 |
| S386 | 100 | 7.45E-03 | 89.846 | 5.3893 | 161.9 | -1.6 | S453 | 350 | 6.49E-04 | 35.142 | 70.289 | 70.7 | -17 |
| S386 | 150 | 4.97E-03 | 78.437 | 10.43 | 159.9 | -13.9 | S453 | 400 | 6.18E-04 | 252.55 | 27.049 | 357.4 | 15 |
| S386 | 200 | 5.09E-03 | 76.929 | 8.3518 | 162.4 | -14.8 | S453 | 425 | 4.73E-04 | 229.96 | 37.342 | 14.3 | 30.1 |
| S386 | 250 | 3.36E-03 | 78.791 | 6.3143 | 163.9 | -12.5 | S453 | 450 | 4.83E-04 | 154.28 | 28.038 | 97.4 | 51.9 |
| S386 | 300 | 3.44E-03 | 73.333 | 10.552 | 161 | -18.8 | S453 | 475 | 6.59E-04 | 53.276 | 76.2 | 70.2 | -9.2 |
| S386 | 350 | 3.00E-03 | 69.845 | 18.651 | 153.3 | -23.7 | S453 | 500 | 5.51E-04 | 171.54 | 57.124 | 64.4 | 31.5 |
| S386 | 400 | 3.04E-03 | 68.235 | 18.222 | 154 | -25.1 | S453 | 550 | 1.53E-03 | 1.7993 | 68.057 | 59.7 | -22.9 |
| S386 | 450 | 2.93E-03 | 62.751 | 26.382 | 145.5 | -31.1 | S453 | 575 | 7.12E-04 | 330.96 | 32.346 | 20.9 | -48.4 |
| S386 | 475 | 2.80E-03 | 62.534 | 24.018 | 148.2 | -31.1 | S453 | 600 | 7.37E-04 | 13.285 | 66.327 | 64.8 | -24 |
| S386 | 500 | 1.93E-03 | 64.538 | 23.999 | 148.1 | -29.3 | S453 | 625 | 7.67E-04 | 110.65 | 79.56 | 68.8 | 2.7 |
| S386 | 525 | 2.71E-03 | 69.775 | 26.472 | 144.8 | -24.9 | S453 | 650 | 3.06E-04 | 47.203 | -16.106 | 171.3 | -40.4 |
| S386 | 550 | 2.66E-03 | 59.927 | 32.917 | 137.8 | -33.7 | S453 | 675 | 1.58E-04 | 77.758 | 21.681 | 127.1 | -11.7 |
| S386 | 575 | 2.83E-03 | 43.819 | 14.506 | 162.9 | -47.8 | S471 | 0 | 7.73E-04 | 307.2 | 20.441 | 353.1 | -34.5 |
| S386 | 600 | 2.05E-03 | 50.346 | 18.937 | 155.7 | -42 | S471 | 100 | 7.51E-04 | 279.93 | 8.6577 | 336.8 | -9.8 |
| S386 | 625 | 2.61E-03 | 48.932 | 18.643 | 156.2 | -43.4 | S471 | 150 | 6.62E-04 | 250.85 | -16.763 | 310.3 | 18.3 |
| S386 | 650 | 2.63E-03 | 61.631 | 30.145 | 141.1 | -32.2 | S471 | 200 | 7.86E-04 | 269.92 | -17.558 | 310.4 | 0.1 |
| S386 | 675 | 7.16E-04 | 49.588 | -15.637 | 197.5 | -31.7 | S471 | 250 | 7.74E-04 | 274.35 | -27.725 | 300.2 | -3.9 |
| oh2_1 | 0 | 1.14E-02 | 155.1 | 15.4 | 155.1 | 15.4 | S471 | 300 | 8.43E-04 | 274.56 | -29.962 | 298 | -3.9 |
| oh2_1 | 100 | 1.05E-02 | 156.5 | 12.6 | 156.5 | 12.6 | S471 | 350 | 8.36E-04 | 252.9 | -21.985 | 305.1 | 15.8 |
| oh2_1 | 150 | 8.77E-03 | 158.1 | 12.1 | 158.1 | 12.1 | S471 | 400 | 9.23E-04 | 269.4 | -21.95 | 306 | 0.6 |
| oh2_1 | 200 | 7.68E-03 | 154.4 | 10.1 | 154.4 | 10.1 | S471 | 450 | 1.02E-03 | 279.23 | -14.844 | 313 | -8.9 |
| oh2_1 | 225 | 7.07E-03 | 158.5 | 9.6 | 158.5 | 9.6 | S471 | 475 | 1.02E-03 | 261.04 | -14.185 | 313.6 | 8.7 |
| oh2_1 | 250 | 6.07E-03 | 153.9 | 8.8 | 153.9 | 8.8 | S471 | 500 | 1.04E-03 | 263.56 | -5.8558 | 322.1 | 6.4 |
| oh2_1 | 275 | 5.53E-03 | 153.7 | 8 | 153.7 | 8 | S471 | 525 | 9.03E-04 | 261.74 | -23.367 | 304.4 | 7.6 |
| oh2_1 | 300 | 5.08E-03 | 151.5 | 12.8 | 151.5 | 12.8 | S471 | 550 | 6.52E-04 | 298.11 | 23.397 | 354.1 | -25.6 |
| oh2_1 | 325 | 4.47E-03 | 148.2 | 8.2 | 148.2 | 8.2 | S471 | 575 | 1.66E-03 | 278.54 | -50.985 | 276.7 | -5.4 |
| oh2_1 | 350 | 4.06E-03 | 149.3 | 6.6 | 149.3 | 6.6 | S471 | 600 | 6.24E-04 | 245.18 | -32.042 | 293.4 | 20.8 |
| oh2_1 | 375 | 3.70E-03 | 149.2 | 9.6 | 149.2 | 9.6 | S471 | 625 | 6.22E-04 | 263.62 | -32.912 | 294.9 | 5.3 |
| oh2_1 | 400 | 3.31E-03 | 145.6 | 10.6 | 145.6 | 10.6 | S471 | 650 | 5.25E-04 | 257.15 | 10.198 | 338.5 | 12.6 |
| oh2_1 | 425 | 3.19E-03 | 145.8 | 9.7 | 145.8 | 9.7 | S471 | 675 | 2.69E-04 | 113.63 | -86.272 | 234.6 | 1.5 |
| oh2_1 | 450 | 2.88E-03 | 157.1 | -17.7 | 157.1 | -17.7 | S486 | 0 | 1.09E-03 | 154.27 | 43.339 | 96.3 | 49.9 |
| oh2_1 | 475 | 2.51E-03 | 150.5 | -0.9 | 150.5 | -0.9 | S486 | 100 | 7.79E-04 | 114.52 | -2.7956 | 164.5 | 23.6 |
| oh2_1 | 500 | 3.02E-03 | 145.3 | 25.6 | 145.3 | 25.6 | S486 | 150 | 6.48E-04 | 117.38 | -34.307 | 197.3 | 16 |
| oh2_1 | 525 | 1.86E-03 | 140 | 4.1 | 140 | 4.1 | S486 | 200 | 4.81E-04 | 117.96 | -43.33 | 205.8 | 12.5 |
| oh2_1 | 550 | 1.42E-03 | 163.3 | 47.1 | 163.3 | 47.1 | S486 | 250 | 4.81E-04 | 163.27 | -37.382 | 229.6 | 40.1 |
| oh2_1 | 575 | 1.26E-03 | 189.7 | -45.9 | 189.7 | -45.9 | S486 | 300 | 4.95E-04 | 74.148 | -31.698 | 187.2 | -18.7 |
| oh2_1 | 600 | 1.38E-03 | 131.8 | 32.2 | 131.8 | 32.2 | S486 | 350 | 1.77E-04 | 86.332 | -47.296 | 203.6 | -9.8 |
| oh2_1 | 625 | 9.04E-04 | 144.5 | 0.4 | 144.5 | 0.4 | S486 | 400 | 3.75E-04 | 67.949 | -76.856 | 234.4 | -14.7 |
| oh2_1 | 650 | 1.28E-03 | 151.5 | 12.8 | 151.5 | 12.8 | S486 | 425 | 5.60E-04 | 154.4 | -70.674 | 238.7 | 7.5 |
| oh2_1 | 675 | 9.45E-04 | 81.7 | 31.7 | 81.7 | 31.7 | S486 | 450 | 4.51E-04 | 122.88 | -74.837 | 234.3 | -1.6 |
| oh2_1 | 700 | 3.19E-04 | 324 | -40.5 | 324 | -40.5 | S486 | 475 | 7.50E-04 | 194.01 | -39.58 | 260.8 | 38.7 |
| oh2_1 | 750 | 2.91E-04 | 333.8 | -24.4 | 333.8 | -24.4 | S486 | 500 | 5.43E-04 | 246.13 | -62.903 | 271.6 | 1.5 |
| oh2_1 | 800 | 2.28E-04 | 307 | -55.8 | 307 | -55.8 | S486 | 525 | 7.03E-04 | 117.15 | -75.563 | 234.2 | -3.2 |
| oh2_1 | 850 | 2.94E-04 | 329 | -47.2 | 329 | -47.2 | S486 | 550 | 5.68E-04 | 114.13 | -57.452 | 217.5 | 4 |
| oh2_1 | 900 | 2.91E-04 | 330.3 | -51.8 | 330.3 | -51.8 | S486 | 575 | 7.20E-04 | 120.14 | -69.608 | 229.5 | 0.5 |
| oh2_1 | 950 | 2.52E-04 | 329.4 | -43.9 | 329.4 | -43.9 | S510 | 0 | 1.28E-04 | 77.814 | 43.932 | 126.8 | 1.2 |
| oh2_1 | 1000 | 2.80E-04 | 342.2 | -47.7 | 342.2 | -47.7 | S510 | 100 | 1.94E-04 | 44.716 | -35.76 | 208.8 | -44.5 |
| oh2_1 | 1050 | 1.91E-04 | 0.6 | -24.9 | 0.6 | -24.9 | S510 | 150 | 2.62E-04 | 15.542 | -47.88 | 244.3 | -53.7 |
| oh2_1 | 1100 | 2.28E-04 | 307 | -55.8 | 307 | -55.8 | S510 | 200 | 3.33E-04 | 2.0214 | -59.257 | 260.5 | -44.7 |
| oh2_1 | 1150 | 2.94E-04 | 329 | -47.2 | 329 | -47.2 | S510 | 250 | 3.93E-04 | 43.264 | -65.404 | 242.6 | -30.9 |
| oh2_1 | 1200 | 3.57E-04 | 357.2 | -19.5 | 357.2 | -19.5 | S510 | 300 | 4.02E-04 | 36.781 | -71.349 | 249.4 | -28.5 |
| oh2_1 | 1250 | 4.00E-04 | 342 | -50.9 | 342 | -50.9 | S510 | 350 | 3.88E-04 | 306.32 | -68.033 | 281.6 | -26.1 |
| oh2_1 | 1300 | 4.57E-04 | 285.3 | -46.2 | 285.3 | -46.2 | S510 | 400 | 3.80E-04 | 343.63 | -54.647 | 275.9 | -47.4 |
| oh2_1 | 1350 | 4.22E-04 | 215.4 | 60.7 | 215.4 | 60.7 | S510 | 450 | 3.60E-04 | 325.45 | -34.552 | 312.4 | -52.7 |
| oh2_1 | 1400 | 3.72E-04 | 305.6 | -23 | 305.6 | -23 | S510 | 475 | 5.55E-04 | 309.95 | -51.461 | 297.8 | -35.3 |
| oh2_1 | 1450 | 3.50E-04 | 19.8 | 15.4 | 19.8 | 15.4 | S510 | 500 | 3.78E-04 | 311.16 | -59.851 | 288.5 | -32 |
| oh2_1 | 1500 | 1.15E-03 | 233.9 | -57.4 | 233.9 | -57.4 | S510 | 525 | 4.42E-04 | 314.82 | -59.754 | 287.4 | -33.6 |
| oh2_1 | 1550 | 9.81E-04 | 239.6 | -55.1 | 239.6 | -55.1 | S510 | 550 | 7.82E-04 | 337.93 | 18.402 | 47.5 | -51 |
| oh2_1 | 1600 | 5.94E-04 | 238.9 | 4.3 | 238.9 | 4.3 | S510 | 575 | 7.62E-04 | 15.043 | -5.0446 | 142.3 | -72.7 |
| oh2_1 | 1650 | 1.17E-03 | 204.1 | -78.9 | 204.1 | -78.9 | S510 | 600 | 3.29E-04 | 282.99 | -71.058 | 281.4 | -17.4 |
| oh2_1 | 1700 | 5.25E-04 | 198.7 | 1 | 198.7 | 1 | S510 | 625 | 4.33E-04 | 10.036 | -33.357 | 238.5 | -68.6 |
| oh | | | | | | | | | | | | | |

Table S2. Thermal demagnetization data.

- (1) Sample = sample name
- (2) Temperature (°C)
- (3) NRM intensity (A/m)
- (4) Core Declination (°E)
- (5) Core Inclination (°)
- (6) Geographic Declination (°E)
- (7) Geographic Inclination (°)

| | | | | | | | | | | | | | | |
|--------------|-----|----------|--------|----------|-------|-------|---------|-----|----------|--------|---------|-------|-------|--|
| S1701 | 150 | 3.28E-03 | 264.69 | -55.953 | 8.7 | -11.9 | 3BOH221 | 450 | 4.84E-04 | 74,899 | -66.16 | 208.7 | -9.7 | |
| S1701 | 200 | 1.46E-03 | 190.41 | -26.451 | 347.1 | 44.4 | 3BOH221 | 475 | 3.32E-04 | 28,896 | -58.046 | 214.6 | -31.4 | |
| S1701 | 250 | 4.62E-03 | 216.52 | -55.952 | 353.8 | 9.9 | 3BOH221 | 500 | 3.98E-04 | 52,896 | -42.516 | 189.6 | -29.4 | |
| S1701 | 300 | 9.44E-03 | 180.94 | -42.535 | 334.8 | 29.5 | 3BOH221 | 550 | 5.88E-04 | 49,943 | -37.276 | 185 | -33.6 | |
| S1701 | 350 | 4.12E-03 | 172.5 | -46.532 | 328.3 | 25.1 | 3BOH221 | 575 | 6.15E-04 | 330.43 | -48.275 | 257 | -39 | |
| S1701 | 400 | 4.12E-03 | 251.9 | -82.363 | 341.5 | -15.5 | 3BOH221 | 600 | 5.31E-04 | 29,393 | -60.311 | 215.8 | -29.4 | |
| S1701 | 425 | 1.82E-03 | 222.68 | -21.308 | 22.6 | 32.6 | 3BOH221 | 625 | 6.66E-04 | 158.49 | -63.742 | 222 | 20.4 | |
| S1701 | 450 | 8.45E-04 | 212.87 | 31.533 | 94.8 | 57.4 | 3BOH221 | 650 | 4.72E-04 | 249.9 | -19.543 | 300.1 | 17.4 | |
| S1701 | 475 | 7.96E-04 | 187.37 | -21.531 | 344.7 | 49.8 | 3BOH221 | 650 | 8.66E-05 | 18,544 | 39,965 | 71.4 | -42.8 | |
| S1701 | 500 | 4.40E-04 | 208.08 | -27.918 | 5.2 | 36.6 | 3BOH281 | 0 | 8.26E-04 | 198.7 | 75,569 | 12.3 | 13.7 | |
| S1701 | 550 | 3.19E-04 | 141.25 | 17.12 | 239.3 | 53.1 | 3BOH281 | 100 | 7.59E-04 | 125.11 | 84,084 | 21.8 | 3.4 | |
| S1701 | 575 | 6.18E-04 | 267.67 | 6,1302 | 69.1 | 4.1 | 3BOH281 | 150 | 7.94E-04 | 132.67 | 83,704 | 21.6 | 4.3 | |
| S1701 | 600 | 4.29E-04 | 224.37 | 41,659 | 105.8 | 45.5 | 3BOH281 | 200 | 8.52E-04 | 49,821 | 82,055 | 23.1 | -5.1 | |
| 3BOH281 | 250 | | | | | | 3BOH281 | 250 | 8.45E-04 | 38,919 | 75,82 | 26 | -11 | |
| OH3-B | | | | | | | | | | | | | | |
| 3BOH30 | 0 | 1.22E-03 | 197.08 | 48.95 | 331.3 | 44.7 | 3BOH281 | 350 | 8.87E-04 | 17,669 | 72,937 | 22.3 | -15.5 | |
| 3BOH30 | 100 | 7.00E-04 | 204.6 | 21,617 | 292.7 | 61.5 | 3BOH281 | 400 | 8.12E-04 | 2,6838 | 76,309 | 17.7 | -13.7 | |
| 3BOH30 | 150 | 3.64E-04 | 157.43 | 17,761 | 46.9 | 65 | 3BOH281 | 450 | 8.34E-04 | 339.76 | 72,443 | 20.7 | -18.4 | |
| 3BOH30 | 200 | 4.61E-04 | 203.09 | 24,192 | 298.8 | 61.3 | 3BOH281 | 475 | 1.07E-03 | 342.52 | 29,298 | 348.8 | -56.3 | |
| 3BOH30 | 250 | 3.18E-04 | 116.65 | 17.74 | 60.1 | 27.2 | 3BOH281 | 500 | 5.23E-04 | 326.49 | 59.84 | 359.2 | -24.8 | |
| 3BOH30 | 300 | 2.25E-04 | 123.23 | 72.047 | 2.5 | 15.5 | 3BOH281 | 525 | 1.39E-03 | 10,437 | 67.01 | 21.4 | -22.6 | |
| 3BOH30 | 350 | 3.16E-04 | 244.01 | 64,794 | 323.5 | 16.3 | 3BOH281 | 550 | 9.96E-04 | 349.28 | 64,073 | 11.8 | -25.4 | |
| 3BOH30 | 400 | 3.90E-04 | 45,327 | 17,633 | 48.3 | -39.4 | 3BOH281 | 575 | 8.43E-04 | 325.7 | 60,223 | 359.1 | -24.2 | |
| 3BOH30 | 425 | 3.47E-04 | 322.45 | -21.855 | 229.6 | -50.4 | 3BOH281 | 600 | 7.86E-04 | 353.69 | 72,503 | 15 | -17.4 | |
| 3BOH30 | 450 | 3.96E-04 | 224.03 | -77.831 | 175.4 | 2.8 | 3BOH281 | 625 | 1.01E-03 | 331.19 | 83,496 | 13.9 | -5.7 | |
| 3BOH30 | 475 | 2.11E-04 | 265.64 | 1,6319 | 258.2 | 4.5 | 3BOH281 | 650 | 5.57E-04 | 286.61 | -11,698 | 274.8 | -16.3 | |
| 3BOH30 | 500 | 1.56E-04 | 296.43 | 14,306 | 275.5 | -23.8 | 3BOH281 | 675 | 1.57E-04 | 328.14 | 32,313 | 337.2 | -45.9 | |
| 3BOH30 | 550 | 1.33E-04 | 289.61 | 3,3747 | 262.7 | -19.1 | 3BOH308 | 0 | 1.02E-03 | 141.03 | 27,832 | 58.3 | 42.8 | |
| 3BOH30 | 575 | 3.58E-04 | 168.35 | 33,946 | 6.6 | 60 | 3BOH308 | 100 | 6.01E-04 | 123.35 | -22,185 | 124.5 | 31 | |
| 3BOH30 | 600 | 3.52E-04 | 261.8 | 20,478 | 276.8 | 9.8 | 3BOH308 | 150 | 5.68E-04 | 113.42 | -23,547 | 124 | 21.8 | |
| 3BOH30 | 625 | 1.04E-03 | 40,537 | -73,801 | 156 | -18.1 | 3BOH308 | 200 | 5.30E-04 | 112.42 | -18,953 | 119 | 21.5 | |
| 3BOH57 | 0 | 9.30E-04 | 189.5 | 67.5 | 337.2 | 17.2 | 3BOH308 | 250 | 4.65E-04 | 109.53 | -14,969 | 114.5 | 19.1 | |
| 3BOH58 | 100 | 5.72E-04 | 238.6 | 74.4 | 327.7 | 3.2 | 3BOH308 | 300 | 5.97E-04 | 111.21 | -5,5745 | 104.6 | 21.2 | |
| 3BOH59 | 150 | 2.66E-04 | 334.8 | 54.4 | 323 | -36.6 | 3BOH308 | 350 | 6.03E-04 | 110.85 | 4,1847 | 94.1 | 20.7 | |
| 3BOH61 | 250 | 2.47E-04 | 333 | 62.4 | 327 | -29.2 | 3BOH308 | 425 | 5.07E-04 | 110.44 | -2,0337 | 100.8 | 20.5 | |
| 3BOH62 | 300 | 2.50E-04 | 329.3 | 67.9 | 328.9 | -23.8 | 3BOH308 | 450 | 2.03E-04 | 92,741 | -22.25 | 121.2 | 2.9 | |
| 3BOH63 | 350 | 3.48E-04 | 204.9 | 74.5 | 334.5 | 9 | 3BOH308 | 475 | 2.81E-04 | 100.91 | 5,1011 | 93.6 | 10.8 | |
| 3BOH64 | 400 | 2.40E-04 | 314.4 | 56.8 | 314.9 | -27 | 3BOH308 | 500 | 3.42E-04 | 72,827 | -28,107 | 128.4 | -14.6 | |
| 3BOH65 | 425 | 3.58E-04 | 12.5 | 34.5 | 0.9 | -58.3 | 3BOH308 | 525 | 2.93E-04 | 112.98 | 17,497 | 79.7 | 21.5 | |
| 3BOH66 | 450 | 4.62E-04 | 301 | 41 | 294.7 | -26.4 | 3BOH308 | 550 | 3.12E-04 | 114.54 | -13,529 | 113.4 | 24.1 | |
| 3BOH67 | 475 | 3.96E-04 | 319.5 | 31.8 | 291.3 | -43.6 | 3BOH388 | 0 | 1.00E-03 | 181.88 | -19,332 | 264.1 | 69.6 | |
| 3BOH68 | 500 | 3.12E-04 | 310.5 | 29.8 | 285 | -37.2 | 3BOH388 | 100 | 8.87E-04 | 165.14 | -31.53 | 236.9 | 54.5 | |
| 3BOH69 | 525 | 5.80E-04 | 301.9 | 46.2 | 300.4 | -25.3 | 3BOH388 | 150 | 9.57E-04 | 140.1 | -31,214 | 213 | 40.3 | |
| 3BOH70 | 550 | 3.16E-04 | 310.5 | -3.6 | 242.1 | -39.8 | 3BOH388 | 200 | 9.02E-04 | 138.41 | -36,385 | 217.5 | 36.3 | |
| 3BOH71 | 575 | 4.99E-04 | 310.2 | 4.1 | 252.2 | -40.4 | 3BOH388 | 250 | 1.07E-03 | 143.85 | -22,034 | 204.4 | 47.9 | |
| 3BOH72 | 600 | 6.68E-04 | 306.5 | 14.3 | 265.1 | -36.6 | 3BOH388 | 300 | 1.14E-03 | 147.83 | -20,554 | 205.2 | 51.8 | |
| 3BOH73 | 625 | 3.63E-04 | 316.7 | 44.6 | 304.3 | -35.3 | 3BOH388 | 350 | 1.05E-03 | 129.16 | -25,059 | 200.7 | 34.4 | |
| 3BOH94 | 0 | 1.02E-03 | 225.39 | 43,696 | 330 | 28.9 | 3BOH388 | 400 | 1.08E-03 | 139.66 | -20,115 | 199.4 | 45.2 | |
| 3BOH94 | 100 | 6.51E-04 | 236.22 | 56,066 | 337.1 | 16.3 | 3BOH388 | 425 | 8.61E-04 | 137.39 | -25.24 | 204.6 | 41.2 | |
| 3BOH94 | 150 | 5.69E-04 | 241.65 | 54,468 | 334.1 | 14.3 | 3BOH388 | 450 | 9.64E-04 | 138.13 | -23,988 | 203.5 | 42.3 | |
| 3BOH94 | 200 | 4.31E-04 | 253.93 | 73,441 | 350.1 | 2.6 | 3BOH388 | 475 | 7.00E-04 | 144.73 | -21,106 | 203.7 | 49 | |
| 3BOH94 | 250 | 4.02E-04 | 315.91 | 70,574 | 352.1 | -15.8 | 3BOH388 | 500 | 8.62E-04 | 136.96 | -33,049 | 213.2 | 37.1 | |
| 3BOH94 | 300 | 3.23E-04 | 300.21 | 55,498 | 335 | -18.3 | 3BOH388 | 550 | 1.14E-03 | 115.11 | -16,603 | 187.6 | 23.7 | |
| 3BOH94 | 350 | 3.47E-04 | 353.2 | 59,256 | 1.9 | -32.5 | 3BOH388 | 575 | 7.42E-04 | 139.99 | -23,082 | 203.4 | 44.2 | |
| 3BOH94 | 400 | 4.20E-04 | 332.29 | 74,564 | 358.6 | -15.6 | 3BOH388 | 600 | 7.81E-04 | 125.87 | -27,711 | 202.5 | 30.7 | |
| 3BOH94 | 450 | 3.82E-04 | 316.25 | 20,845 | 303.2 | -43.4 | 3BOH388 | 625 | 1.12E-03 | 150.45 | -45,597 | 233.5 | 36.6 | |
| 3BOH94 | 475 | 6.75E-04 | 331.56 | 58,277 | 349.3 | -29.5 | 3BOH388 | 650 | 1.57E-04 | 157.66 | -27,306 | 223.5 | 54.5 | |
| 3BOH94 | 500 | 6.33E-04 | 314.02 | 66,995 | 348.8 | -17.7 | 3BOH388 | 675 | 2.75E-04 | 295.2 | 65,814 | 56.9 | -9.1 | |
| 3BOH94 | 525 | 1.11E-03 | 338.34 | 13,976 | 306.4 | -65.5 | 3BOH428 | 0 | 1.06E-03 | 202.6 | 47,668 | 333.7 | 38.4 | |
| 3BOH94 | 550 | 3.94E-04 | 337.07 | 39,756 | 340 | -46.9 | 3BOH428 | 100 | 7.17E-04 | 221.96 | 65,856 | 336.3 | 17.7 | |
| 3BOH94 | 575 | 6.85E-04 | 335.58 | 22,669 | 14.7 | -69.1 | 3BOH428 | 150 | 5.61E-04 | 211.82 | 57,973 | 334.7 | 26.8 | |
| 3BOH94 | 600 | 4.90E-04 | 355.66 | 30,269 | 358.2 | -61.4 | 3BOH428 | 200 | 6.38E-04 | 254.77 | 46,175 | 310.2 | 10.5 | |
| 3BOH94 | 625 | 2.31E-04 | 301.01 | -0.74403 | 273.9 | -31 | 3BOH428 | 250 | 4.15E-04 | 239.26 | 71,853 | 337.3 | 9.2 | |
| 3BOH94 | 650 | 9.25E-04 | 227.03 | 52,822 | 337.4 | 22.6 | 3BOH428 | 300 | 6.30E-04 | 245.66 | 72,97 | 337.4 | 6.9 | |
| 3BOH94 | 675 | 2.89E-04 | 309.17 | 15.257 | 293.9 | -38.2 | 3BOH428 | 350 | 6.69E-04 | 267.45 | 76,408 | 339.4 | 0.6 | |
| 3BOH136 | 0 | 1.67E-03 | 219.31 | 58,211 | 330.6 | 36 | 3BOH428 | 400 | 5.62E-04 | 292.09 | 70,939 | 335.2 | -7.1 | |
| 3BOH136 | 100 | 9.69E-04 | 218.32 | 28,484 | 294.6 | 51.2 | 3BOH428 | 425 | 4.65E-04 | 237.34 | 53,308 | 320.9 | 18.8 | |
| 3BOH136 | 150 | 9.87E-04 | 215.71 | 30,572 | 298.9 | 52.7 | 3BOH428 | 450 | 4.54E-04 | 275.92 | 68,705 | 331.8 | -2.1 | |
| 3BOH136 | 200 | 8.83E-04 | 232.25 | 21,634 | 282.5 | 39.6 | 3BOH428 | 475 | 5.38E-04 | 263.31 | -32,237 | 295.4 | 5.7 | |
| 3BOH136 | 250 | 4.23E-04 | 282.51 | 22,062 | 289.4 | -6.4 | 3BOH428 | 500 | 6.04E-04 | 319.27 | 54,496 | 328 | -26.1 | |
| 3BOH136 | 300 | 4.37E-04 | 252.53 | 10,286 | 271.5 | 19.1 | 3BOH428 | 525 | 5.86E-04 | 279.96 | 28,63 | 292 | -8.7 | |
| 3BOH136 | 350 | 4.16E-04 | 210.06 | 14,462 | 271.4 | 60.8 | 3BOH428 | 550 | 3.83E-04 | 281.83 | 47,49 | 311.1 | -8 | |
| 3BOH136 | 400 | 6.37E-04 | 193.51 | 23,986 | 307.6 | 73.1 | 3BOH428 | 575 | 5.45E-04 | 292.53 | 30,431 | 295.5 | -19.3 | |
| 3BOH136 | 400 | 6.48E-0 | | | | | | | | | | | | |

Table S2. Thermal demagnetization data.

- (1) Sample = sample name
- (2) Temperature (°C)
- (3) NRM intensity (A/m)
- (4) Core Declination (°E)
- (5) Core Inclination (°)
- (6) Geographic Declination (°E)
- (7) Geographic Inclination (°)

| | | | | | | | | | | | | | |
|--------|-----|----------|---------|----------|-------|-------|--------|-----|----------|--------|---------|-------|-------|
| 4OH454 | 675 | 4.96E-03 | 275.12 | 28.283 | 196.2 | -1.6 | 4OH578 | 250 | 5.92E-03 | 259.53 | -55.484 | 286.7 | 7.6 |
| 4OH468 | 0 | 1.33E-02 | 132.59 | -15.314 | 12.7 | 40.4 | 4OH578 | 300 | 4.39E-03 | 265.29 | -63.708 | 278.8 | 3.9 |
| 4OH468 | 100 | 8.46E-03 | 140.02 | -33.749 | 38.2 | 38.9 | 4OH578 | 350 | 4.20E-03 | 234.85 | -31.111 | 307 | 30.7 |
| 4OH468 | 150 | 7.76E-03 | 142.52 | -41.845 | 47.7 | 35.4 | 4OH578 | 400 | 6.28E-03 | 266.26 | -44.874 | 297.6 | 4.1 |
| 4OH468 | 200 | 6.83E-03 | 161.89 | -41.902 | 62.7 | 44.1 | 4OH578 | 425 | 4.53E-03 | 259.98 | -58.668 | 283.6 | 6.9 |
| 4OH468 | 250 | 5.59E-03 | 183.79 | -60.812 | 83.6 | 28.1 | 4OH578 | 450 | 3.85E-03 | 248.65 | -68.198 | 273 | 9.6 |
| 4OH468 | 300 | 5.99E-03 | 208.15 | -57.236 | 98.2 | 27.5 | 4OH578 | 475 | 3.21E-03 | 239.9 | -75.616 | 265.1 | 9.1 |
| 4OH468 | 350 | 6.83E-03 | 212.13 | -69.866 | 92.5 | 16 | 4OH578 | 500 | 3.81E-03 | 229.88 | -72.223 | 266.4 | 13.3 |
| 4OH468 | 400 | 5.19E-03 | 201.65 | -56.377 | 95.1 | 30 | 4OH578 | 550 | 5.44E-03 | 224.3 | -77.68 | 261.2 | 10.8 |
| 4OH468 | 425 | 4.69E-03 | 215.24 | -52.131 | 105.4 | 29.2 | 4OH578 | 575 | 4.89E-03 | 211.66 | -73.235 | 261.6 | 16.2 |
| 4OH468 | 450 | 4.62E-03 | 217.2 | -58.738 | 101.5 | 23.5 | 4OH578 | 600 | 2.47E-03 | 191.69 | -61.371 | 258.9 | 30 |
| 4OH468 | 475 | 5.64E-03 | 215.12 | -63.07 | 97.7 | 20.8 | 4OH578 | 625 | 2.42E-03 | 222.33 | -38.095 | 294.1 | 37.1 |
| 4OH468 | 500 | 5.06E-03 | 233.18 | -65.045 | 101.8 | 13.7 | | | | | | | |
| 4OH468 | 550 | 5.21E-03 | 188.2 | -63.645 | 85.5 | 25.1 | | | | | | | |
| 4OH468 | 575 | 5.65E-03 | 243.97 | -59.179 | 109.6 | 12.1 | 5OH130 | 0 | 1.79E-02 | 67.04 | 63.749 | 5.1 | 24.6 |
| 4OH468 | 600 | 4.84E-03 | 215.9 | -57.632 | 101.7 | 24.8 | 5OH130 | 100 | 1.03E-02 | 60.573 | 58.446 | 7.3 | 18.8 |
| 4OH468 | 625 | 5.47E-03 | 213.42 | -50.372 | 105.8 | 31.3 | 5OH130 | 150 | 6.68E-03 | 45.292 | 51.414 | 5.1 | 7.8 |
| 4OH468 | 650 | 3.03E-03 | 218.1 | -37.159 | 120.2 | 38.1 | 5OH130 | 200 | 5.04E-03 | 32.113 | 55.915 | 356 | 7.8 |
| 4OH468 | 675 | 1.18E-03 | 243.5 | -0.82776 | 170.1 | 26.5 | 5OH130 | 250 | 4.23E-03 | 38.876 | 66.928 | 353.6 | 19 |
| 4OH483 | 0 | 5.44E-03 | 132.06 | 76.769 | 354.4 | 6.8 | 5OH130 | 300 | 3.24E-03 | 20.045 | 60.896 | 348.3 | 10.2 |
| 4OH483 | 100 | 3.51E-03 | 45.599 | 54.64 | 11.8 | -25.7 | 5OH130 | 350 | 1.44E-03 | 64.867 | 71.953 | 357.2 | 28.8 |
| 4OH483 | 150 | 4.19E-03 | 12.369 | 56.149 | 352.9 | -34.9 | 5OH130 | 400 | 2.13E-03 | 2.596 | 55.871 | 340 | 3.9 |
| 4OH483 | 200 | 2.96E-03 | 340.95 | 6.2095 | 267.6 | -70.5 | 5OH130 | 425 | 1.90E-03 | 322 | 77.684 | 329.9 | 28 |
| 4OH483 | 250 | 3.04E-03 | 354.7 | 4.5244 | 280.2 | -84.1 | 5OH130 | 450 | 1.78E-03 | 5.69 | 71.878 | 340.4 | 20 |
| 4OH483 | 300 | 2.29E-03 | 343.01 | -9.0563 | 221.1 | -69.8 | 5OH130 | 475 | 1.67E-03 | 326.79 | 63.884 | 324 | 15.2 |
| 4OH483 | 350 | 3.14E-03 | 353.03 | -27.048 | 177.1 | -60.2 | 5OH130 | 500 | 1.72E-03 | 303.55 | 58.405 | 311.3 | 17.2 |
| 4OH483 | 400 | 2.40E-03 | 9.6599 | -6.2246 | 115 | -77.3 | 5OH130 | 525 | 1.19E-03 | 265.12 | 56.401 | 297.2 | 33.4 |
| 4OH483 | 425 | 3.63E-03 | 358.42 | -2.2078 | 185.1 | -85.5 | 5OH130 | 550 | 1.00E-03 | 300.47 | 31.681 | 291.3 | -1 |
| 4OH483 | 450 | 3.02E-03 | 0.57678 | 9.3371 | 348.9 | -82.6 | 5OH130 | 575 | 1.21E-03 | 280.55 | 57.595 | 302.5 | 26.3 |
| 4OH483 | 475 | 3.56E-03 | 14.273 | -6.9473 | 106.8 | -73.2 | 5OH130 | 600 | 1.30E-03 | 271.96 | 42.056 | 284.7 | 23.1 |
| 4OH483 | 500 | 3.11E-03 | 357.97 | 5.1579 | 311.8 | -86.2 | 5OH130 | 625 | 1.31E-03 | 282.87 | 59.906 | 305.4 | 26.4 |
| 4OH483 | 550 | 3.97E-03 | 10.913 | -2.4571 | 96.7 | -78.2 | 5OH130 | 650 | 8.21E-04 | 219.22 | 45.509 | 275.7 | 60.1 |
| 4OH483 | 575 | 3.44E-03 | 2.6864 | 7.5094 | 10.3 | -83.9 | 5OH130 | 675 | 8.65E-04 | 222.66 | 48.582 | 281.5 | 57.7 |
| 4OH483 | 600 | 3.01E-03 | 0.3807 | 0 | 153.7 | -88 | 5OH181 | 0 | 1.46E-02 | 250.24 | 42.374 | 315.4 | 29.6 |
| 4OH484 | 0 | 6.04E-03 | 272.98 | -27.086 | 314.4 | -2.7 | 5OH181 | 100 | 6.75E-03 | 260.1 | 39.908 | 314 | 21.8 |
| 4OH484 | 100 | 3.43E-03 | 5.1783 | -20.479 | 237.9 | -68.9 | 5OH181 | 150 | 5.37E-04 | 258 | 35.49 | 309 | 22.5 |
| 4OH484 | 150 | 3.67E-03 | 355.28 | -7.1978 | 284.6 | -81.4 | 5OH181 | 200 | 5.21E-03 | 261.76 | 35.192 | 309.4 | 19.5 |
| 4OH484 | 200 | 4.01E-03 | 18.957 | -17.997 | 206.5 | -64.1 | 5OH181 | 250 | 3.02E-03 | 254.15 | 33.152 | 305.7 | 25.1 |
| 4OH484 | 250 | 3.63E-03 | 27.553 | -1.8924 | 165.6 | -62.4 | 5OH181 | 300 | 2.52E-03 | 245.47 | 34.526 | 305.9 | 32.4 |
| 4OH484 | 300 | 4.49E-03 | 29.33 | -7.8045 | 177.1 | -59.7 | 5OH181 | 350 | 2.12E-03 | 259.84 | 29.743 | 303.4 | 19.6 |
| 4OH484 | 350 | 3.35E-03 | 40.135 | 4.628 | 154.3 | -49.6 | 5OH181 | 400 | 1.76E-03 | 249.96 | 28.027 | 299.3 | 27.5 |
| 4OH484 | 400 | 4.43E-03 | 25.753 | -4.7863 | 172.4 | -63.8 | 5OH181 | 425 | 1.44E-03 | 230.02 | 16.79 | 280.5 | 42.8 |
| 4OH484 | 425 | 4.04E-03 | 43.191 | -4.9811 | 165.9 | -46.7 | 5OH181 | 450 | 9.74E-04 | 250.84 | 22.196 | 293.2 | 25.3 |
| 4OH484 | 450 | 3.43E-03 | 30.935 | -6.3693 | 173.8 | -58.5 | 5OH181 | 475 | 1.23E-03 | 238.55 | 29.816 | 299.3 | 37.7 |
| 4OH484 | 475 | 3.67E-03 | 44.007 | -0.78046 | 162.6 | -46 | 5OH181 | 500 | 1.04E-03 | 254.41 | -1.214 | 271.1 | 13.8 |
| 4OH484 | 500 | 3.33E-03 | 45.249 | -12.145 | 178.4 | -43.5 | 5OH181 | 525 | 1.02E-03 | 266.68 | 1.801 | 278.9 | 3.8 |
| 4OH484 | 525 | 3.24E-03 | 41.917 | -20.988 | 191.4 | -44 | 5OH181 | 550 | 1.13E-03 | 257.41 | -3.8174 | 270 | 10 |
| 4OH484 | 550 | 3.23E-03 | 27.121 | -3.5492 | 169.2 | -62.7 | 5OH181 | 600 | 5.59E-04 | 222.09 | 26.323 | 292.4 | 51.8 |
| 4OH484 | 575 | 3.11E-03 | 34.1 | -4.2383 | 169 | -55.7 | 5OH215 | 0 | 9.47E-03 | 136.92 | 26.669 | 80.6 | 44.6 |
| 4OH484 | 600 | 2.85E-03 | 36.505 | -7.6636 | 174.2 | -52.8 | 5OH215 | 100 | 5.38E-03 | 142.16 | 28.896 | 75.1 | 48.2 |
| 4OH484 | 625 | 1.03E-03 | 28.172 | 8.6327 | 143.7 | -60.6 | 5OH215 | 150 | 4.03E-03 | 139.79 | 35.112 | 68.4 | 43.6 |
| 4OH484 | 650 | 1.28E-03 | 24.825 | -19.473 | 201.6 | -58.8 | 5OH215 | 200 | 3.25E-03 | 132.22 | 31.706 | 75.8 | 39.2 |
| 4OH484 | 675 | 1.63E-03 | 32.851 | 8.7718 | 358 | -57.4 | 5OH215 | 250 | 2.52E-03 | 148.58 | 35.656 | 62.1 | 49.4 |
| 4OH508 | 0 | 5.70E-03 | 258.89 | -53.747 | 286.5 | 9 | 5OH215 | 300 | 2.13E-03 | 133.97 | 40.603 | 64.7 | 37.1 |
| 4OH508 | 100 | 3.00E-03 | 304.35 | -71.379 | 265.9 | -7.5 | 5OH215 | 350 | 1.60E-03 | 143.96 | 22.864 | 83 | 51.9 |
| 4OH508 | 150 | 3.76E-03 | 55.088 | -71.845 | 235.6 | -7.4 | 5OH215 | 400 | 1.38E-03 | 135.58 | 65.877 | 39.7 | 23.6 |
| 4OH508 | 200 | 4.50E-03 | 41.9 | -40.954 | 214.1 | -31.8 | 5OH215 | 425 | 1.47E-03 | 161.76 | 75.302 | 26.4 | 20.9 |
| 4OH508 | 250 | 5.95E-03 | 45.659 | -51.676 | 221.7 | -23.1 | 5OH215 | 450 | 1.05E-03 | 181.42 | 72.113 | 21 | 24.9 |
| 4OH508 | 300 | 5.62E-03 | 55.849 | -47.564 | 214.1 | -19.9 | 5OH215 | 475 | 1.12E-03 | 139.09 | 55.438 | 47.4 | 31.7 |
| 4OH508 | 350 | 5.44E-03 | 60.328 | -44.564 | 209.8 | -18.4 | 5OH215 | 500 | 1.40E-03 | 150.35 | 70.191 | 32.1 | 24 |
| 4OH508 | 400 | 5.34E-03 | 52.82 | -46.289 | 214 | -22.3 | 5OH215 | 550 | 1.40E-03 | 245.04 | 74.083 | 6.7 | 13.4 |
| 4OH508 | 425 | 5.96E-03 | 60.779 | -43.214 | 208.3 | -18.6 | 5OH215 | 575 | 9.78E-04 | 334.18 | 87.981 | 20.6 | 5.2 |
| 4OH508 | 450 | 6.61E-03 | 65.124 | -38.681 | 202.7 | -17.2 | 5OH215 | 600 | 1.06E-03 | 259.9 | 85.983 | 17.5 | 7.7 |
| 4OH508 | 475 | 6.33E-03 | 64.99 | -38.696 | 202.7 | -17.3 | 5OH215 | 625 | 8.04E-04 | 20.134 | 14.337 | 64.6 | -60.8 |
| 4OH508 | 500 | 6.48E-03 | 66.977 | -37.475 | 201 | -16.1 | 5OH244 | 0 | 5.47E-03 | 233.54 | 24.045 | 320.5 | 37.6 |
| 4OH508 | 525 | 6.65E-03 | 65.611 | -38.754 | 202.6 | -16.8 | 5OH244 | 100 | 2.63E-03 | 222.55 | 35.765 | 338.5 | 44.3 |
| 4OH508 | 550 | 6.69E-03 | 73.593 | -35.438 | 197.6 | -11.5 | 5OH244 | 150 | 2.57E-03 | 216.44 | 19.323 | 316.3 | 53.9 |
| 4OH508 | 575 | 6.69E-03 | 69.113 | -35.212 | 198.3 | -15.1 | 5OH244 | 200 | 1.62E-03 | 207 | 39.427 | 353 | 52.8 |
| 4OH508 | 600 | 6.56E-03 | 67.868 | -38.254 | 201.6 | -15.3 | 5OH244 | 250 | 1.56E-03 | 171.41 | 55.456 | 35.4 | 45 |
| 4OH508 | 625 | 6.86E-03 | 64.045 | -37.3 | 201.6 | -18.4 | 5OH244 | 300 | 1.53E-03 | 173.09 | 29.342 | 46.9 | 70.6 |
| 4OH508 | 650 | 5.30E-04 | 289.96 | -40.312 | 297.9 | -13.1 | 5OH244 | 350 | 1.47E-03 | 154.83 | 45.736 | 55.5 | 49.2 |
| 4OH528 | 0 | 1.68E-02 | 233.71 | -4.857 | 338.9 | 36.5 | 5OH244 | 400 | 1.03E-03 | 66.267 | 82.911 | 35.1 | 8.1 |
| 4OH528 | 100 | 8.70E-03 | 248.31 | 14.586 | 358.2 | 19.2 | 5OH244 | 425 | 9.51E-04 | 153.91 | 37.262 | 65.9 | 54.8 |
| 4OH528 | 150 | 8.98E-03 | 256.68 | 5.3039 | 347.3 | 12.6 | 5OH244 | 450 | 9.74E-04 | 145.0 | | | |

Table S2. Thermal demagnetization data.

- (1) Sample = sample name
- (2) Temperature (°C)
- (3) NRM intensity (A/m)
- (4) Core Declination (°E)
- (5) Core Inclination (°)
- (6) Geographic Declination (°E)
- (7) Geographic Inclination (°)

| | | | | | | |
|-------|-----|----------|--------|--------|-------|-------|
| oh298 | 575 | 1.70E-05 | 101.26 | -43.37 | 232.8 | 1.2 |
| oh298 | 600 | 1.94E-05 | 172.52 | 4.54 | 224.1 | 80.8 |
| oh305 | 0 | 3.61E-05 | 239.81 | 27.05 | 25 | 38.2 |
| oh305 | 100 | 3.16E-05 | 238.5 | 61.03 | 69.6 | 41.9 |
| oh305 | 150 | 3.30E-05 | 276.13 | 80.2 | 92.1 | 29.5 |
| oh305 | 200 | 3.42E-05 | 321.06 | 78.91 | 95.8 | 22.2 |
| oh305 | 225 | 3.79E-05 | 314.56 | 77.3 | 93.6 | 21.7 |
| oh305 | 250 | 4.00E-05 | 321.45 | 77.35 | 94.9 | 20.8 |
| oh305 | 275 | 3.80E-05 | 336.75 | 77.64 | 98.1 | 19.5 |
| oh305 | 300 | 3.37E-05 | 333.75 | 67.68 | 93.4 | 10.6 |
| oh305 | 325 | 3.04E-05 | 315.05 | 70.72 | 89.2 | 16.6 |
| oh305 | 350 | 2.98E-05 | 318.12 | 73.81 | 92 | 18.5 |
| oh305 | 375 | 2.89E-05 | 315.11 | 58.35 | 81.4 | 6.9 |
| oh305 | 400 | 2.94E-05 | 314.36 | 56.98 | 80.2 | 6 |
| oh305 | 425 | 2.85E-05 | 334.56 | 58.21 | 90.2 | 1.7 |
| oh305 | 450 | 2.91E-05 | 331.54 | 62.19 | 90.4 | 6 |
| oh305 | 475 | 2.55E-05 | 334.23 | 52.31 | 87.8 | -3.7 |
| oh305 | 500 | 1.69E-05 | 338.33 | 54.6 | 90.9 | -2.4 |
| oh305 | 525 | 2.69E-05 | 324.76 | 43.44 | 78.2 | -8.9 |
| oh305 | 550 | 1.38E-05 | 336.25 | 66.91 | 94.1 | 9.6 |
| oh305 | 575 | 1.69E-05 | 237.09 | 62.63 | 71.9 | 42.2 |
| oh305 | 600 | 1.27E-05 | 311.77 | 70.12 | 87.9 | 16.9 |
| oh305 | 625 | 2.65E-05 | 292.6 | 41.09 | 59 | 5.2 |
| oh305 | 650 | 9.86E-06 | 352.21 | -14.28 | 78.4 | -71.8 |
| oh305 | 675 | 1.11E-05 | 357.04 | 72.07 | 102.3 | 13.1 |
| oh325 | 0 | 1.83E-04 | 211.33 | -29.06 | 333.1 | 23.8 |
| oh325 | 100 | 1.58E-04 | 211.96 | -34.83 | 330.6 | 18.5 |
| oh325 | 150 | 1.29E-04 | 218.12 | -35.2 | 334.9 | 15.6 |
| oh325 | 200 | 1.20E-04 | 208.81 | -34.94 | 328.1 | 19.6 |
| oh325 | 225 | 1.09E-04 | 215.93 | -31.18 | 335.6 | 19.9 |
| oh325 | 250 | 1.14E-04 | 210.98 | -31.19 | 331.7 | 22.1 |
| oh325 | 275 | 1.02E-04 | 209.6 | -30.22 | 331 | 23.5 |
| oh325 | 300 | 9.27E-05 | 214.6 | -25.36 | 337.9 | 25.5 |
| oh325 | 325 | 8.70E-05 | 206.42 | -21.5 | 332.7 | 32.6 |
| oh325 | 350 | 9.40E-05 | 196.2 | -18.66 | 323.1 | 38.9 |
| oh325 | 375 | 9.94E-05 | 214.35 | -14.83 | 344.6 | 34.3 |
| oh325 | 400 | 9.27E-05 | 213.16 | -20.08 | 339.9 | 30.6 |
| oh325 | 425 | 9.37E-05 | 206.79 | -19.02 | 334.5 | 34.6 |
| oh325 | 450 | 9.73E-05 | 224.59 | -19.64 | 349.8 | 24.4 |
| oh325 | 475 | 1.05E-04 | 229.7 | -14.87 | 357.3 | 24.4 |
| oh325 | 500 | 9.26E-05 | 237.04 | -15.32 | 2 | 18.8 |
| oh325 | 525 | 9.40E-05 | 229.04 | -28.79 | 346.5 | 14.9 |
| oh325 | 550 | 1.02E-04 | 254.15 | -16.56 | 11 | 4.8 |
| oh325 | 575 | 9.02E-05 | 258.14 | -32.02 | 359.9 | -6.6 |
| oh325 | 600 | 1.17E-04 | 247.46 | -24.16 | 1.1 | 5.6 |
| oh325 | 625 | 9.42E-05 | 249.81 | -35.21 | 353.4 | -2.5 |
| oh325 | 650 | 1.04E-04 | 246 | -24.77 | 359.9 | 6.3 |
| oh325 | 675 | 1.05E-04 | 260.25 | -18.09 | 12.8 | -0.9 |
| oh345 | 0 | 1.43E-04 | 178.28 | -25.2 | 296 | 47.8 |
| oh345 | 100 | 1.35E-04 | 176.85 | -24.07 | 293.9 | 48.8 |
| oh345 | 150 | 1.21E-04 | 172.69 | -23.6 | 288.1 | 48.8 |
| oh345 | 200 | 1.16E-04 | 172.73 | -23.07 | 288 | 49.3 |
| oh345 | 225 | 1.13E-04 | 172.37 | -23.83 | 287.7 | 48.5 |
| oh345 | 250 | 1.16E-04 | 181.21 | -19.07 | 300.2 | 53.9 |
| oh345 | 275 | 1.10E-04 | 183.16 | -14.35 | 304.1 | 58.5 |
| oh345 | 300 | 1.11E-04 | 174.19 | 0.24 | 278.8 | 72.3 |
| oh345 | 325 | 1.07E-04 | 172.86 | -12.9 | 284.6 | 59.3 |
| oh345 | 350 | 1.05E-04 | 180.36 | -26.01 | 298.8 | 47 |
| oh345 | 375 | 1.07E-04 | 174.55 | -13.25 | 287.9 | 59.3 |
| oh345 | 400 | 1.10E-04 | 175.25 | -16.6 | 290.1 | 56.1 |
| oh345 | 425 | 1.07E-04 | 176.65 | -3.09 | 288.6 | 69.6 |
| oh345 | 450 | 9.59E-05 | 176.28 | -3.54 | 287.8 | 69.1 |
| oh345 | 475 | 1.00E-04 | 177.59 | -10.62 | 293.2 | 62.3 |
| oh345 | 500 | 9.86E-05 | 177.74 | 3.28 | 288.9 | 76.1 |
| oh345 | 525 | 8.17E-05 | 180.04 | 11.55 | 298.7 | 84.5 |
| oh345 | 550 | 7.68E-05 | 192.18 | -2.29 | 331.4 | 67.3 |
| oh345 | 575 | 8.33E-05 | 185.58 | 11.24 | 342.2 | 82.1 |
| oh345 | 600 | 8.53E-05 | 172.19 | 2.47 | 269.6 | 73.6 |
| oh345 | 625 | 8.36E-05 | 175.13 | 23.93 | 150.8 | 81.7 |
| oh345 | 650 | 8.53E-05 | 171.99 | 5.35 | 263.4 | 76 |
| oh345 | 675 | 8.81E-05 | 183.17 | 16.49 | 19.2 | 86.9 |

Table S3. Magnetostratigraphic data.

Sample = sample name.
 cm = elevation of sample from section base in cm.
 NRM = natural remanent magnetization of sample at room temperature in mA/m (10E-3 A/m) and 10cc volume.
 SUS = volume magnetic susceptibility in 10E-6 SI.
 A_LT = low unblocking temperature in °C of magnetic component A.
 A_HT = high unblocking temperature in °C of magnetic component A.
 A_Dec = mean declination in °E of magnetic component A.
 A_Inc = mean inclination in ° of magnetic component A.
 C_LT = low unblocking temperature in °C of characteristic magnetic component C.
 C_HT = high unblocking temperature in °C of characteristic magnetic component C.
 C_MAD = maximum angular deviation of characteristic magnetic component C.
 C_Dec = mean declination in °E of characteristic magnetic component C.
 C_Inc = mean inclination in ° of characteristic magnetic component C.
 C_VGP = virtual geomagnetic pole latitude in ° of characteristic magnetic component C.

| Sample | cm | NRM | SUS | A_LT | A_HT | A_Dec | A_Inc | C_LT | C_HT | C_MAD | C_Dec | C_Inc | C_VGP |
|--------------------------------------|--------|--------|-------|------|------|-------|-------|------|------|-------|-------|-------|-------|
| OH1 Bed1 (below trench base): | | | | | | | | | | | | | |
| S-30 | -30.0 | 0.066 | 10.1 | | | | | 100 | 425 | 9.2 | 246.3 | -9.0 | -22.2 |
| S-41 | -41.0 | 0.300 | 9.9 | | | | | 100 | 450 | 26.5 | 171.4 | -33.5 | -72.9 |
| S-62 | -62.0 | 0.311 | 8.6 | 0 | 100 | 352.9 | 7.1 | 100 | 350 | 7.0 | 227.1 | -53.8 | -51.3 |
| S-77 | -77.0 | 0.252 | 11.5 | 0 | 100 | 353.4 | 36.0 | 100 | 350 | 7.0 | 227.1 | -53.8 | -51.3 |
| S-91 | -91.0 | 0.159 | 10.8 | | | | | | | | | | |
| S-109 | -109.0 | 0.335 | 17.7 | | | | | | | | | | |
| S-134 | -134.0 | 0.218 | 13.6 | 0 | 100 | 27.1 | 22.8 | 100 | 400 | 31.1 | 195.8 | -21.5 | -63.3 |
| S-180 | -180.0 | 0.376 | 13.3 | 0 | 100 | 314.4 | 14.6 | 100 | 350 | 7.0 | 227.1 | -53.8 | -51.3 |
| OH1 Bed2 Trench South Wall: | | | | | | | | | | | | | |
| s004 | 4.0 | 0.172 | 153.3 | | | | | 350 | 575 | 11.3 | 176.1 | -18.5 | -65.6 |
| s010 | 10.0 | 0.276 | 132.9 | | | | | 275 | 475 | 10.3 | 156.0 | -21.0 | -58.4 |
| s014 | 14.0 | 0.274 | 157.1 | | | | | 100 | 475 | 17.1 | 162.7 | -33.5 | -68.3 |
| s040 | 40.0 | 0.272 | 180.3 | | | | | 150 | 425 | 12.7 | 150.8 | -31.1 | -58.9 |
| s043 | 43.0 | 0.333 | 185.7 | | | | | 150 | 500 | 20.1 | 187.4 | -27.0 | -69.6 |
| s050 | 50.0 | 0.375 | 171.9 | | | | | 150 | 600 | 11.6 | 153.6 | 10.2 | -43.9 |
| s054 | 54.0 | 0.134 | 170.7 | | | | | 150 | 425 | 17.5 | 181.4 | 1.4 | -55.7 |
| s058 | 58.0 | 0.157 | 160.3 | | | | | 150 | 500 | 11.6 | 153.6 | 10.2 | -43.9 |
| s061 | 61.0 | 0.101 | 104.1 | | | | | 100 | 475 | 17.1 | 162.7 | -33.5 | -68.3 |
| s110 | 110.0 | 0.230 | 132.1 | 0 | 100 | 45.0 | 13.7 | 150 | 650 | 7.5 | 181.4 | 1.4 | -55.7 |
| s113 | 113.0 | 0.140 | 94.6 | | | | | 250 | 500 | 11.6 | 153.6 | 10.2 | -43.9 |
| s117 | 117.0 | 0.244 | 110.8 | | | | | 150 | 600 | 17.5 | 177.1 | 14.4 | -49.0 |
| s124 | 124.0 | 0.123 | 83.8 | | | | | 150 | 425 | 9.9 | 169.3 | 12.4 | -48.9 |
| s131 | 131.0 | 0.157 | 89.3 | | | | | 225 | 400 | 13.6 | 143.9 | -21.0 | -49.9 |
| s135 | 135.0 | 0.108 | 87.3 | 0 | 100 | 320.0 | 67.0 | 225 | 325 | 12.2 | 173.0 | -2.0 | -56.8 |
| s140 | 140.0 | 0.077 | 73.6 | | | | | 150 | 400 | 14.8 | 150.8 | 13.9 | -40.8 |
| s146 | 146.0 | 0.120 | 65.4 | | | | | 225 | 600 | 18.3 | 156.2 | 8.7 | -45.9 |
| s152 | 152.0 | 0.197 | 104.9 | | | | | 200 | 575 | 16.3 | 164.6 | -8.1 | -57.2 |
| s160 | 160.0 | 0.183 | 97.4 | | | | | 150 | 425 | 13.6 | 150.2 | 4.7 | -44.4 |
| s164 | 164.0 | 0.117 | 95.0 | | | | | 150 | 350 | 13.2 | 161.6 | 3.9 | -50.5 |
| s171 | 171.0 | 0.146 | 104.4 | | | | | 150 | 400 | 11.9 | 151.0 | 8.5 | -43.3 |
| s176 | 176.0 | 0.176 | 110.8 | | | | | 225 | 400 | 22.9 | 165.4 | -20.5 | -63.4 |
| s181 | 181.0 | 0.396 | 111.7 | | | | | 250 | 500 | 10.0 | 181.1 | 5.6 | -53.6 |
| s187 | 187.0 | 0.370 | 128.8 | | | | | 200 | 525 | 5.1 | 156.6 | 1.9 | -49.0 |
| s204 | 204.0 | 0.588 | 181.3 | | | | | 225 | 400 | 7.1 | 159.2 | 12.7 | -45.4 |
| s215 | 215.0 | 0.535 | 182.9 | | | | | 250 | 400 | 14.4 | 167.0 | 0.9 | -53.8 |
| s221 | 221.0 | 0.765 | 214.3 | | | | | 200 | 425 | 6.1 | 171.0 | -1.3 | -56.0 |
| s230 | 230.0 | 0.758 | 226.4 | 0 | 100 | 33.9 | 38.3 | 275 | 425 | 7.9 | 172.5 | 1.1 | -55.1 |
| s234 | 234.0 | 0.840 | 180.4 | | | | | 200 | 350 | 5.7 | 169.2 | 7.3 | -51.4 |
| s240 | 240.0 | 1.098 | 220.1 | | | | | 225 | 475 | 7.6 | 160.7 | 4.6 | -49.8 |
| s253 | 253.0 | 1.434 | 323.9 | 0 | 100 | 336.5 | 7.5 | 225 | 550 | 4.3 | 162.2 | 3.4 | -50.9 |
| s268 | 268.0 | 2.739 | 447.2 | | | | | 275 | 525 | 2.9 | 160.9 | 4.6 | -49.8 |
| s273 | 273.0 | 2.255 | 418.5 | | | | | 275 | 600 | 5.0 | 160.2 | -0.9 | -52.0 |
| s281 | 281.0 | 2.658 | 488.2 | 0 | 100 | 317.4 | 51.3 | 250 | 575 | 2.2 | 159.7 | 6.7 | -48.4 |
| s287 | 287.0 | 3.634 | 526.2 | | | | | 275 | 625 | 5.3 | 156.8 | -0.8 | -50.3 |
| s299 | 299.0 | 3.936 | 549.6 | | | | | 250 | 650 | 2.3 | 159.6 | 4.6 | -49.3 |
| s314 | 314.0 | 6.043 | 669.3 | | | | | 200 | 550 | 3.0 | 160.8 | 2.5 | -50.8 |
| OH1 Bed2 Trench North Wall: | | | | | | | | | | | | | |
| n007 | 7.0 | 0.086 | 108.1 | | | | | 150 | 525 | 22.3 | 163.7 | -1.8 | -53.9 |
| n011 | 11.0 | 0.021 | 89.0 | 0 | 150 | 8.6 | 71.2 | 150 | 300 | 20.2 | 214.3 | -3.9 | -45.0 |
| n015 | 15.0 | 0.100 | 103.8 | | | | | 150 | 300 | 20.2 | 214.3 | -3.9 | -45.0 |
| n019 | 19.0 | 0.114 | 109.0 | 0 | 100 | 6.7 | 14.8 | 250 | 475 | 25.3 | 139.6 | -25.2 | -48.1 |
| n023 | 23.0 | 0.050 | 140.6 | 0 | 150 | 39.5 | 68.9 | 250 | 450 | 11.4 | 134.8 | -18.4 | -42.1 |
| n069 | 69.0 | 0.250 | 191.8 | | | | | 225 | 350 | 17.6 | 198.6 | -39.6 | -70.2 |
| n072 | 72.0 | 0.139 | 183.8 | | | | | 225 | 350 | 17.6 | 198.6 | -39.6 | -70.2 |
| n074 | 74.0 | 0.117 | 192.9 | | | | | 225 | 350 | 17.6 | 198.6 | -39.6 | -70.2 |
| n077 | 77.0 | 0.159 | 190.2 | 0 | 100 | 308.8 | 29.3 | 225 | 525 | 18.9 | 161.4 | -27.7 | -64.7 |
| n082 | 82.0 | 0.155 | 188.7 | 0 | 100 | 38.2 | 0.6 | 300 | 400 | 20.1 | 148.3 | -21.2 | -53.2 |
| OH2: | | | | | | | | | | | | | |
| s333 | 333.0 | 0.798 | 164.3 | | | | | 200 | 525 | 7.5 | 180.4 | -1.3 | -57.1 |
| OH2 Hand Sample 03.19 (oh2_3) | 347.0 | 10.980 | 144.4 | | | | | 100 | 550 | 5.6 | 171.1 | -6.7 | -58.6 |
| OH2 Hand Sample 04.19 (oh2_4) | 351.0 | 5.885 | 168.8 | 0 | 100 | 339.2 | 51.5 | 150 | 475 | 7.6 | 346.2 | 15.4 | 61.3 |
| S352 | 352.0 | 10.830 | 186.0 | | | | | 100 | 675 | 7.2 | 183.5 | 8.1 | -52.2 |
| S372 | 372.0 | 6.896 | 203.9 | 0 | 100 | 49.0 | 17.1 | 200 | 650 | 18.6 | 174.2 | -34.5 | -74.5 |
| OH2 Hand Sample 02.19 (oh2_2) | 376.0 | 19.660 | 168.1 | | | | | 150 | 650 | 10.2 | 164.8 | 3.7 | -51.8 |
| OH2 Hand Sample 05.19 (oh2_5) | 383.0 | 4.418 | 161.0 | | | | | 150 | 425 | 16.7 | 205.6 | 2.3 | -47.7 |

| | | | | | | | | | | | | |
|-----------------|--------|---------|-------|-----|-----|-------|------|-----|-------|-------|-------|-------|
| S386 | 386.0 | 7.428 | 194.4 | | | | 150 | 675 | 12.8 | 155.9 | -24.0 | -59.6 |
| OH2 Hand Sample | 01.19 | (oh2_1) | | | | | 100 | 500 | 8.2 | 162.7 | 11.2 | -47.5 |
| 391.0 | 11.370 | 131.7 | | | | | | | | | | |
| OH2 Hand Sample | 06.19 | (oh2_6) | | | | | 100 | 600 | 26.7 | 165.4 | 16.7 | -45.7 |
| 401.0 | 0.319 | 19.3 | | | | | 100 | 650 | 12.5 | 170.4 | -47.9 | -80.6 |
| S409 | 409.0 | 3.177 | 218.1 | | | | 200 | 425 | 20.2 | 130.0 | -16.4 | -37.6 |
| S436 | 436.0 | 2.855 | 249.7 | | | | | | | | | |
| S453 | 453.0 | 1.544 | 91.5 | 0 | 150 | 60.3 | 20.5 | | | | | |
| S471 | 471.0 | 0.773 | 96.2 | | | | 100 | 450 | 23.2 | 171.2 | 20.0 | -45.3 |
| S486 | 486.0 | 1.093 | 115.3 | | | | 100 | 350 | 19.4 | 231.6 | -12.6 | -35.1 |
| S510 | 510.0 | 0.128 | 48.0 | | | | 400 | 8.3 | 196.5 | 2.0 | -52.1 | |
| S520 | 520.0 | 1.324 | 91.8 | | | | | | | | | |
| S548 | 548.0 | 1.354 | 94.3 | 0 | 150 | 35.7 | 43.2 | 150 | | | | |
| S565 | 565.0 | 0.405 | 48.1 | 0 | 100 | 52.2 | 62.7 | 100 | | | | |
| S598 | 598.0 | 5.212 | 137.1 | | | | 100 | 300 | 12.9 | 169.8 | 5.6 | -52.4 |
| S605 | 605.0 | 0.957 | 96.0 | 0 | 200 | 25.5 | 25.0 | | | | | |
| S625 | 625.0 | 1.181 | 102.0 | 0 | 200 | 1.4 | 35.7 | | | | | |
| S663 | 663.0 | 0.770 | 60.0 | 0 | 100 | 41.0 | 53.5 | 150 | | | | |
| S709 | 709.0 | 1.067 | 80.1 | 0 | 150 | 316.9 | 36.0 | | | | | |
| S762 | 762.0 | 0.783 | 36.9 | | | | | | | | | |
| S810 | 810.0 | 0.580 | 43.1 | 0 | 150 | 329.8 | 10.3 | | | | | |
| S863 | 863.0 | 0.615 | 48.1 | | | | | | | | | |
| S939 | 939.0 | 0.738 | 81.5 | 0 | 200 | 351.9 | 64.9 | | | | | |
| S987 | 987.0 | 1.077 | 107.9 | | | | | | | | | |
| S1044 | 1044.0 | 1.101 | 106.8 | 0 | 100 | 5.0 | 58.9 | | | | | |
| S1099 | 1099.0 | 0.798 | 125.3 | 0 | 100 | 30.8 | 82.7 | 200 | 525 | 24.4 | 172.8 | -11.7 |
| S1171 | 1171.0 | 0.432 | 25.2 | | | | | | | | | |
| S1238 | 1238.0 | 0.272 | 12.2 | 0 | 200 | 334.1 | 34.4 | | | | | |
| S1281 | 1281.0 | 0.425 | 13.8 | 0 | 150 | 22.9 | 61.9 | 200 | 350 | 17.9 | 183.0 | -36.6 |
| S1309 | 1309.0 | 0.298 | 29.0 | 100 | 200 | 35.2 | 49.4 | | | | | |
| S1353 | 1353.0 | 0.184 | 22.0 | | | | | | | | | |
| S1375 | 1375.0 | 0.640 | 24.7 | 0 | 100 | 14.1 | 72.6 | 100 | 450 | 19.0 | 322.7 | 23.5 |
| S1436 | 1436.0 | 0.634 | 30.3 | | | | | | | | | |
| S1525 | 1525.0 | 1.367 | 81.1 | 0 | 100 | 43.5 | 62.2 | | | | | |
| S1569 | 1569.0 | 3.591 | 264.5 | 0 | 150 | 354.9 | 54.4 | | | | | |
| S1589 | 1589.0 | 0.868 | 43.4 | 0 | 100 | 332.4 | 13.0 | | | | | |
| S1599 | 1599.0 | 11.770 | 435.6 | 0 | 150 | 349.6 | 33.8 | | | | | |
| S1634 | 1634.0 | 20.090 | 790.1 | 0 | 150 | 347.4 | 29.9 | | | | | |
| S1701 | 1701.0 | 18.040 | 714.0 | 0 | 150 | 19.9 | 77.2 | | | | | |

OB3-B:

| | | | | | | | | | | | | |
|---------|-------|-------|------|-----|-----|-------|------|-----|-----|------|-------|------|
| 3BOH30 | 30.0 | 1.218 | 36.8 | 0 | 200 | 327.8 | 32.5 | | | | | |
| 3BOH57 | 57.0 | 0.930 | 28.3 | 0 | 250 | 339.0 | 29.2 | | | | | |
| 3BOH94 | 94.0 | 1.016 | 46.2 | 0 | 300 | 320.2 | 45.7 | | | | | |
| 3BOH136 | 136.0 | 1.666 | 55.2 | 0 | 300 | 347.1 | 42.2 | | | | | |
| 3BOH178 | 178.0 | 1.325 | 49.3 | 0 | 250 | 325.5 | 26.1 | | | | | |
| 3BOH221 | 221.0 | 1.519 | 51.2 | 0 | 200 | 341.7 | 36.5 | | | | | |
| 3BOH281 | 281.0 | 0.826 | 29.0 | | | | | | | | | |
| 3BOH308 | 308.0 | 1.019 | 35.4 | 0 | 150 | 16.6 | 31.3 | 150 | 425 | 24.0 | 210.6 | -3.4 |
| 3BOH388 | 388.0 | 0.999 | 41.4 | 0 | 150 | 4.9 | 28.7 | 350 | 650 | 16.5 | 198.1 | 36.9 |
| 3BOH428 | 428.0 | 1.055 | 55.5 | 0 | 250 | 330.4 | 54.6 | | | | | |
| 3BOH463 | 463.0 | 1.765 | 58.6 | 100 | 425 | 31.1 | 44.0 | | | | | |
| 3BOH486 | 486.0 | 0.510 | 35.2 | 100 | 200 | 29.8 | 44.7 | | | | | |
| 3BOH510 | 510.0 | 1.326 | 42.5 | 0 | 200 | 10.5 | 24.7 | | | | | |

OB3-A:

| | | | | | | | | | | | | |
|--------|-------|-------|-------|---|-----|-------|------|-----|-----|------|-------|-------|
| 3OH28 | 28.0 | 0.600 | 27.1 | 0 | 150 | 284.7 | 23.4 | | | | | |
| 3OH51 | 51.0 | 0.439 | 29.3 | | | | | | | | | |
| 3OH94 | 94.0 | 0.862 | 37.9 | 0 | 150 | 9.8 | 18.2 | | | | | |
| 3OH121 | 121.0 | 3.505 | 394.8 | 0 | 150 | 27.8 | 27.1 | 300 | 625 | 34.4 | 166.7 | -21.0 |
| 3OH144 | 144.0 | 0.328 | 27.3 | 0 | 150 | 327.0 | 24.1 | | | | | |
| 3OH172 | 172.0 | 0.563 | 36.6 | | | | | | | | | |
| 3OH212 | 212.0 | 0.427 | 23.0 | 0 | 150 | 342.7 | 27.1 | | | | | |
| 3OH229 | 229.0 | 1.156 | 50.4 | 0 | 150 | 339.3 | 27.7 | | | | | |
| 3OH246 | 246.0 | 1.272 | 38.5 | 0 | 100 | 284.8 | 51.4 | 350 | 500 | 10.9 | 180.5 | 8.6 |
| 3OH313 | 313.0 | 0.943 | 35.0 | 0 | 100 | 320.8 | 33.9 | 150 | 300 | 14.4 | 150.1 | 5.2 |
| 3OH339 | 339.0 | 1.251 | 37.9 | 0 | 300 | 18.1 | 43.5 | | | | | |
| 3OH379 | 379.0 | 0.748 | 46.5 | 0 | 200 | 333.0 | 29.9 | | | | | |
| 3OH405 | 405.0 | 7.364 | 42.5 | 0 | 200 | 23.3 | 45.6 | 250 | 475 | 3.2 | 34.9 | 41.6 |
| 3OH462 | 462.0 | 4.294 | 161.7 | 0 | 100 | 10.6 | 1.4 | 150 | 625 | 31.9 | 1.9 | 7.4 |
| 3OH490 | 490.0 | 6.235 | 53.1 | 0 | 100 | 338.3 | 16.2 | 150 | 500 | 8.8 | 312.6 | 28.6 |

OB4:

| | | | | | | | | | | | | |
|-----------------|-------|---------|--------|---|-----|-------|------|-----|-----|------|-------|-------|
| 4OH8 | 8.0 | 40.350 | 8380.1 | 0 | 150 | 358.5 | 25.1 | 250 | 675 | 8.2 | 178.6 | -33.9 |
| 4OH29 | 29.0 | 15.670 | 2124.6 | 0 | 200 | 0.8 | 25.5 | 200 | 625 | 3.1 | 183.0 | -48.6 |
| 4OH59 | 59.0 | 25.740 | 3319.5 | 0 | 150 | 6.4 | 37.8 | 300 | 675 | 6.9 | 194.6 | -21.5 |
| OH4 Hand Sample | 07.19 | (oh4_7) | | | | | | | | | | |
| | 91.0 | 12.580 | 4049.4 | 0 | 250 | 351.8 | 22.2 | 275 | 675 | 6.8 | 182.7 | -30.1 |
| 4OH96 | 96.0 | 12.340 | 2312.6 | 0 | 250 | 10.1 | 25.1 | 300 | 650 | 12.5 | 188.7 | -18.4 |
| 4OH116 | 116.0 | 3.794 | 593.8 | 0 | 150 | 10.0 | 25.5 | 250 | 675 | 8.5 | 216.8 | -43.2 |
| 4OH145 | 145.0 | 1.666 | 683.8 | 0 | 150 | 25.2 | 37.8 | 300 | 675 | 15.5 | 184.3 | -13.4 |
| OH4 Hand Sample | 08.19 | (oh4_8) | | | | | | | | | | |
| | 148.0 | 8.638 | 1942.8 | 0 | 200 | 3.7 | 23.2 | 275 | 650 | 5.3 | 181.2 | -30.0 |
| 4OH166 | 166.0 | 3.313 | 1103.2 | 0 | 200 | 356.9 | 29.2 | 350 | 675 | 6.2 | 189.5 | -21.0 |
| 4OH198 | 198.0 | 4.659 | 723.7 | 0 | 200 | 347.5 | 44.2 | 250 | 625 | 6.7 | 199.2 | -18.7 |
| OH4 Hand Sample | 09.19 | (oh4_9) | | | | | | | | | | |
| | 204.0 | 5.979 | 1097.0 | 0 | 200 | 353.8 | 42.1 | 250 | 675 | 9.3 | 178.9 | -8.3 |
| 4OH237 | 237.0 | 4.817 | 648.6 | 0 | 250 | 6.6 | 21.9 | 250 | 675 | 7.2 | 219.4 | -46.8 |
| 4OH263 | 263.0 | 5.317 | 606.9 | 0 | 300 | 11.3 | 27.2 | 450 | 650 | 11.7 | 176.4 | -2.9 |
| 4OH303 | 303.0 | 3.231 | 401.3 | 0 | 150 | 13.9 | 38.1 | 550 | 675 | 20.0 | 205.7 | -47.5 |
| 4OH363 | 363.0 | 31.040 | 3156.3 | 0 | 150 | 348.7 | 31.7 | | | | | |

| | | | | | | | | | | | | | |
|--------|-------|--------|--------|---|-----|-------|------|-----|-----|------|-------|-------|-------|
| 4OH403 | 403.0 | 9.800 | 1386.8 | 0 | 150 | 25.6 | 46.7 | 250 | 625 | 11.3 | 248.0 | -21.0 | -24.3 |
| 4OH433 | 433.0 | 7.275 | 1324.3 | 0 | 200 | 345.1 | 39.9 | 200 | 675 | 24.0 | 174.3 | -35.9 | -75.4 |
| 4OH443 | 443.0 | 19.210 | 1682.5 | | | | | 200 | 600 | 16.6 | 202.2 | -58.7 | -71.3 |
| 4OH454 | 454.0 | 25.780 | 1610.0 | 0 | 150 | 331.9 | 50.5 | 425 | 625 | 21.6 | 227.6 | -9.5 | -37.3 |
| 4OH468 | 468.0 | 13.260 | 937.2 | 0 | 250 | 342.4 | 30.2 | | | | | | |
| 4OH483 | 483.0 | 5.411 | 636.0 | 0 | 250 | 2.3 | 31.0 | 350 | 575 | 32.2 | 172.4 | 24.7 | -42.9 |
| 4OH484 | 484.0 | 6.043 | 573.0 | 0 | 150 | 320.4 | 28.8 | 200 | 675 | 12.2 | 173.6 | -56.6 | -83.7 |
| 4OH508 | 508.0 | 5.704 | 631.7 | 0 | 250 | 336.6 | 29.0 | 450 | 650 | 3.1 | 199.5 | -16.0 | -58.8 |
| 4OH528 | 528.0 | 16.760 | 836.7 | 0 | 150 | 316.5 | 53.3 | 250 | 625 | 9.0 | 8.5 | 16.2 | 63.5 |
| 4OH548 | 548.0 | 22.490 | 1139.0 | 0 | 100 | 331.6 | 45.5 | 100 | 500 | 20.9 | 300.4 | 35.7 | 35.7 |
| 4OH578 | 578.0 | 25.680 | 1175.0 | 0 | 150 | 322.6 | 7.8 | 200 | 550 | 31.9 | 345.3 | 13.9 | 60.2 |

OH5:

| | | | | | | | | | | | | | |
|--------|-------|--------|-------|---|-----|-------|------|-----|-----|------|-------|------|------|
| 5OH130 | 130.0 | 17.860 | 390.7 | 0 | 150 | 3.2 | 33.9 | 200 | 675 | 19.3 | 344.4 | 15.0 | 60.3 |
| 5OH181 | 181.0 | 14.570 | 371.8 | 0 | 200 | 317.5 | 34.5 | 250 | 550 | 20.0 | 320.7 | 29.4 | 50.4 |
| 5OH215 | 215.0 | 9.466 | 270.5 | | | | | | | | | | |
| 5OH244 | 244.0 | 5.479 | 160.7 | 0 | 200 | 311.7 | 29.1 | 250 | 525 | 28.3 | 351.3 | 43.2 | 78.7 |
| 5OH266 | 266.0 | 10.420 | 272.8 | 0 | 150 | 327.7 | 23.5 | 200 | 500 | 7.8 | 315.6 | 13.2 | 41.0 |
| 5OH291 | 291.0 | 9.466 | 396.6 | 0 | 200 | 328.0 | 8.0 | 200 | 625 | 17.5 | 321.4 | 17.8 | 46.9 |
| 5OH326 | 326.0 | 13.970 | 423.8 | 0 | 150 | 313.8 | 27.9 | 200 | 500 | 10.9 | 310.4 | 45.5 | 47.1 |
| 5OH351 | 351.0 | 19.640 | 566.0 | 0 | 150 | 312.3 | 27.9 | 350 | 525 | 6.5 | 335.5 | 11.8 | 54.2 |
| 5OH377 | 377.0 | 11.910 | 370.9 | 0 | 150 | 321.3 | 32.2 | 200 | 525 | 9.5 | 318.0 | 9.3 | 41.5 |

Sidi Abderrhamane:

| | | | | | | | | | | | | | |
|------|-------|-------|------|---|-----|-------|------|-----|-----|-------|-------|------|------|
| SA1 | 177.0 | 0.553 | 11.8 | 0 | 100 | 340.5 | 48.9 | | | | | | |
| SA2 | 206.0 | 0.906 | 35.6 | 0 | 100 | 42.6 | 14.3 | | | | | | |
| SA3 | 226.0 | 0.703 | 21.5 | | | | | | | | | | |
| SA4 | 276.0 | 2.231 | 45.8 | 0 | 100 | 356.8 | 15.3 | | | | | | |
| SA5 | 335.0 | 0.743 | 23.5 | 0 | 100 | 349.2 | 23.5 | | | | | | |
| SA6 | 361.0 | 1.829 | 38.4 | 0 | 100 | 327.1 | 36.1 | 100 | 350 | 12.6 | 336.0 | 41.7 | 67.0 |
| SA7 | 419.0 | 0.148 | 17.9 | | | | | | | | | | |
| SA8 | 434.0 | 0.733 | 25.6 | | | | | | | | | | |
| SA9 | 459.0 | 0.192 | 17.1 | | | | | | | | | | |
| SA10 | 485.0 | 1.024 | 22.9 | 0 | 100 | 347.5 | 62.0 | 100 | 450 | 16.5 | 321.9 | 59.2 | 59.1 |
| SA11 | 290.0 | 8.670 | 35.7 | | | 0 | | 450 | 5.1 | 2.3 | -0.1 | 56.3 | |
| SA12 | 304.0 | 5.882 | 21.1 | | | 0 | | 425 | 7.0 | 2.1 | -3.9 | 54.4 | |
| SA13 | 290.0 | 7.645 | 30.0 | | | 0 | | 450 | 6.2 | 355.0 | -7.1 | 52.5 | |
| SA14 | 301.0 | 4.978 | 15.9 | | | 100 | | 475 | 3.8 | 4.8 | -0.9 | 55.7 | |
| SA15 | 303.0 | 4.697 | 14.3 | | | 100 | | 500 | 9.7 | 5.2 | -7.1 | 52.5 | |
| SA16 | 305.0 | 5.326 | 20.5 | | | | | | | | | | |

Rhino Cave:

| | | | | | | | | | | | | | |
|------|-------|-------|-------|---|-----|-------|------|-----|-----|------|-------|-------|-------|
| R108 | 108.0 | 5.756 | 443.6 | 0 | 150 | 340.2 | 73.4 | | | | | | |
| R195 | 195.0 | 0.984 | 190.8 | 0 | 150 | 8.9 | 46.0 | 400 | 575 | 21.7 | 195.3 | -34.7 | -70.1 |
| R216 | 216.0 | 3.417 | 250.7 | 0 | 200 | 318.3 | 33.5 | 250 | 550 | 20.7 | 189.0 | -10.8 | -60.6 |
| R246 | 246.0 | 5.341 | 523.9 | | | | | 250 | 575 | 33.0 | 165.9 | -57.4 | -77.8 |
| R276 | 276.0 | 5.901 | 655.0 | 0 | 100 | 13.0 | 37.9 | 200 | 625 | 20.2 | 181.7 | -21.3 | -67.4 |
| R316 | 316.0 | 2.694 | 579.4 | 0 | 150 | 46.1 | 49.7 | 300 | 675 | 14.5 | 208.4 | -67.3 | -63.4 |
| R342 | 342.0 | 2.761 | 321.1 | 0 | 200 | 352.1 | 53.9 | 250 | 575 | 30.7 | 158.0 | -36.8 | -66.5 |
| R392 | 392.0 | 2.167 | 262.7 | 0 | 150 | 23.9 | 49.0 | 200 | 550 | 30.0 | 196.6 | -30.2 | -67.1 |
| R417 | 417.0 | 5.058 | 282.0 | | | | | | | | | | |
| R431 | 431.0 | 3.672 | 294.1 | 0 | 100 | 313.9 | 24.8 | | | | | | |
| R459 | 459.0 | 3.034 | 166.2 | | | | | | | | | | |

Ouled Hamida:

| | | | | | | | | | | | | | |
|-------|-------|-------|-------|---|-----|-------|------|------|--|--|--|--|--|
| oh220 | 220.0 | 0.029 | 59.2 | 0 | 100 | 334.0 | 12.4 | | | | | | |
| oh230 | 230.0 | 0.039 | 39.0 | 0 | 200 | 335.9 | 57.6 | | | | | | |
| oh237 | 237.0 | 0.041 | 51.4 | 0 | 150 | 2.3 | | 42.4 | | | | | |
| oh249 | 249.0 | 0.044 | 58.1 | 0 | 275 | 352.1 | 37.7 | | | | | | |
| oh279 | 279.0 | 0.027 | 63.8 | 0 | 225 | 330.4 | 41.1 | | | | | | |
| oh298 | 298.0 | 0.017 | 59.5 | 0 | 100 | 15.4 | 27.8 | | | | | | |
| oh305 | 305.0 | 0.036 | 81.2 | 0 | 200 | 326.6 | 14.0 | | | | | | |
| oh325 | 325.0 | 0.183 | 147.4 | 0 | 100 | 353.4 | 51.4 | | | | | | |
| oh345 | 345.0 | 0.143 | 66.4 | 0 | 150 | 329.2 | 36.7 | | | | | | |

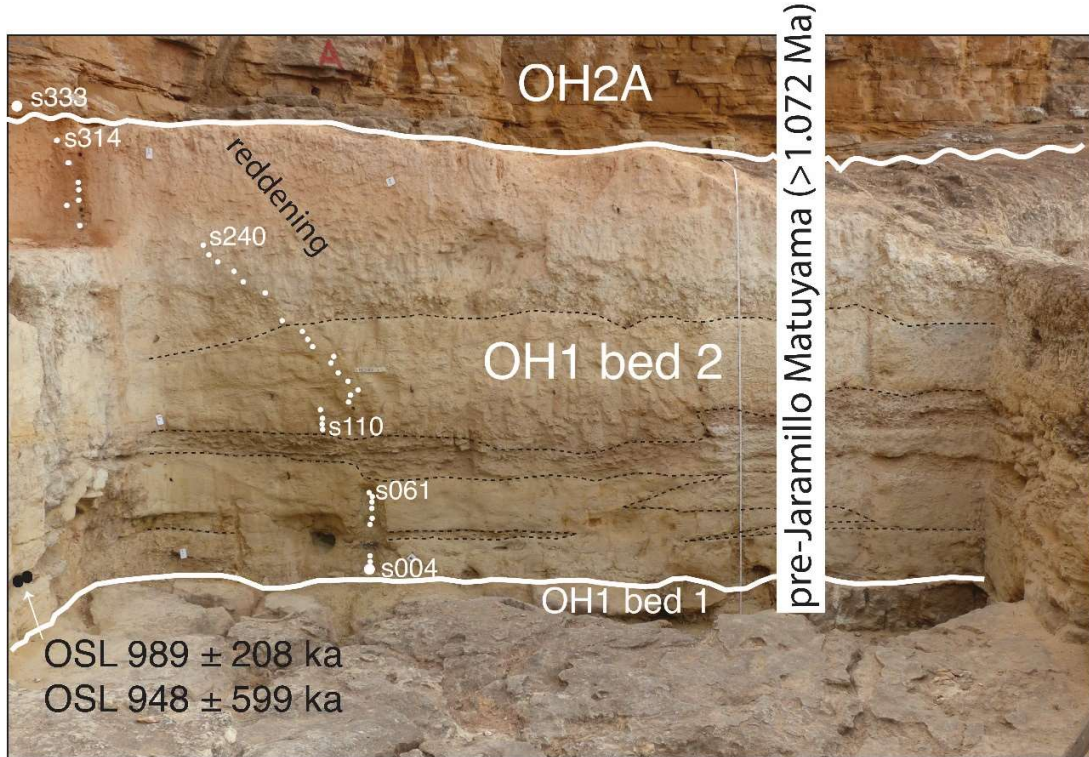


Fig. S8. Photograph of the stratigraphy of archeological section in unit OH1 Bed 2, trench south side with position of samples for magnetostratigraphy. OH1 Bed 2 is dated to the pre-Jaramillo Matuyama (>1.072 Ma) probably prior to the Cobb Mountain subchron. See main text for discussion.

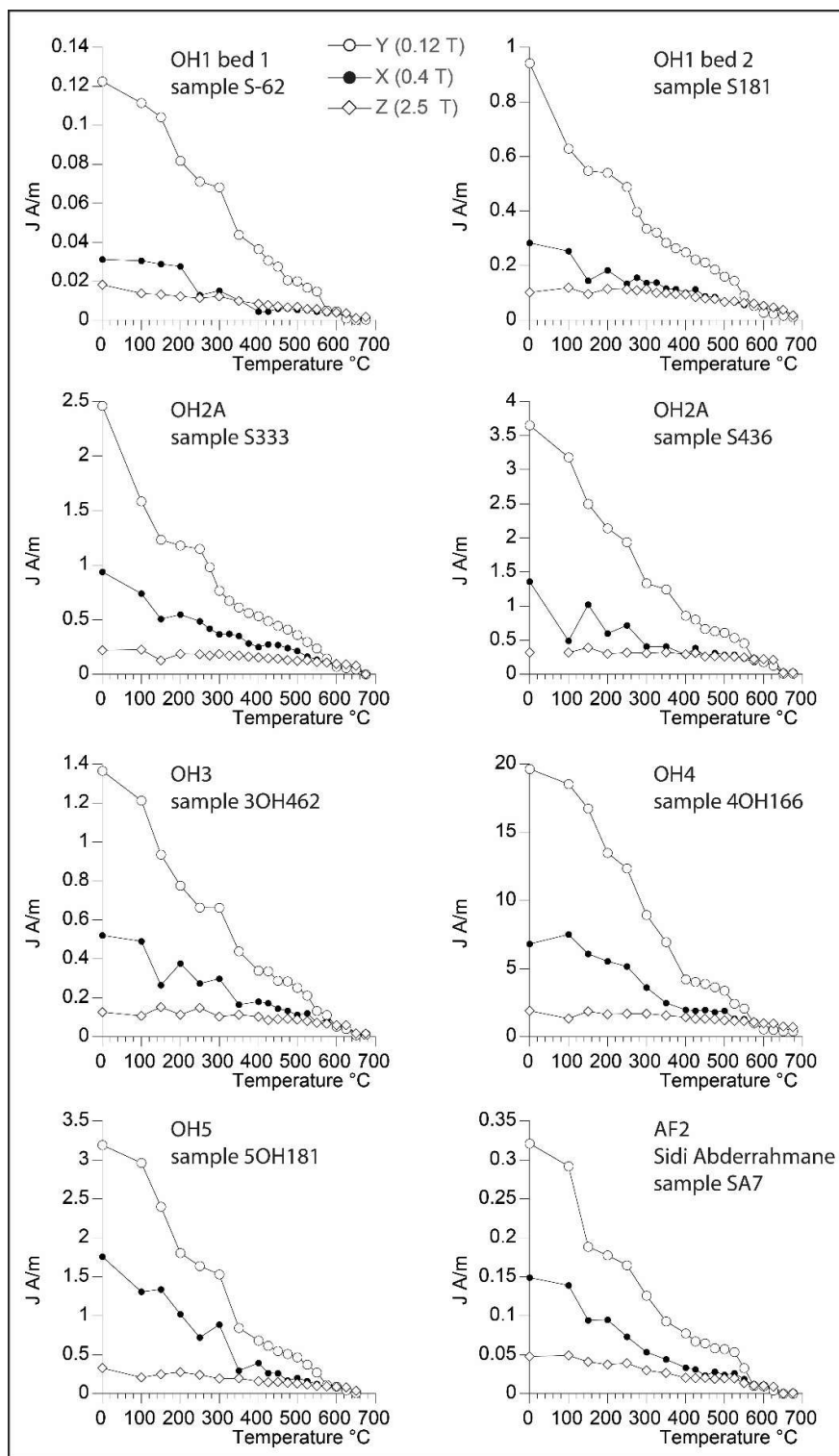


Fig. S9. Thermal demagnetization of a three component isothermal remanent magnetization (IRM) using fields of 2.5T, 0.4T, and 0.12T of selected samples from the investigated sedimentary units showing the predominance of magnetite as the carrier of the remanence coexisting with subsidiary hematite. See text for discussion.

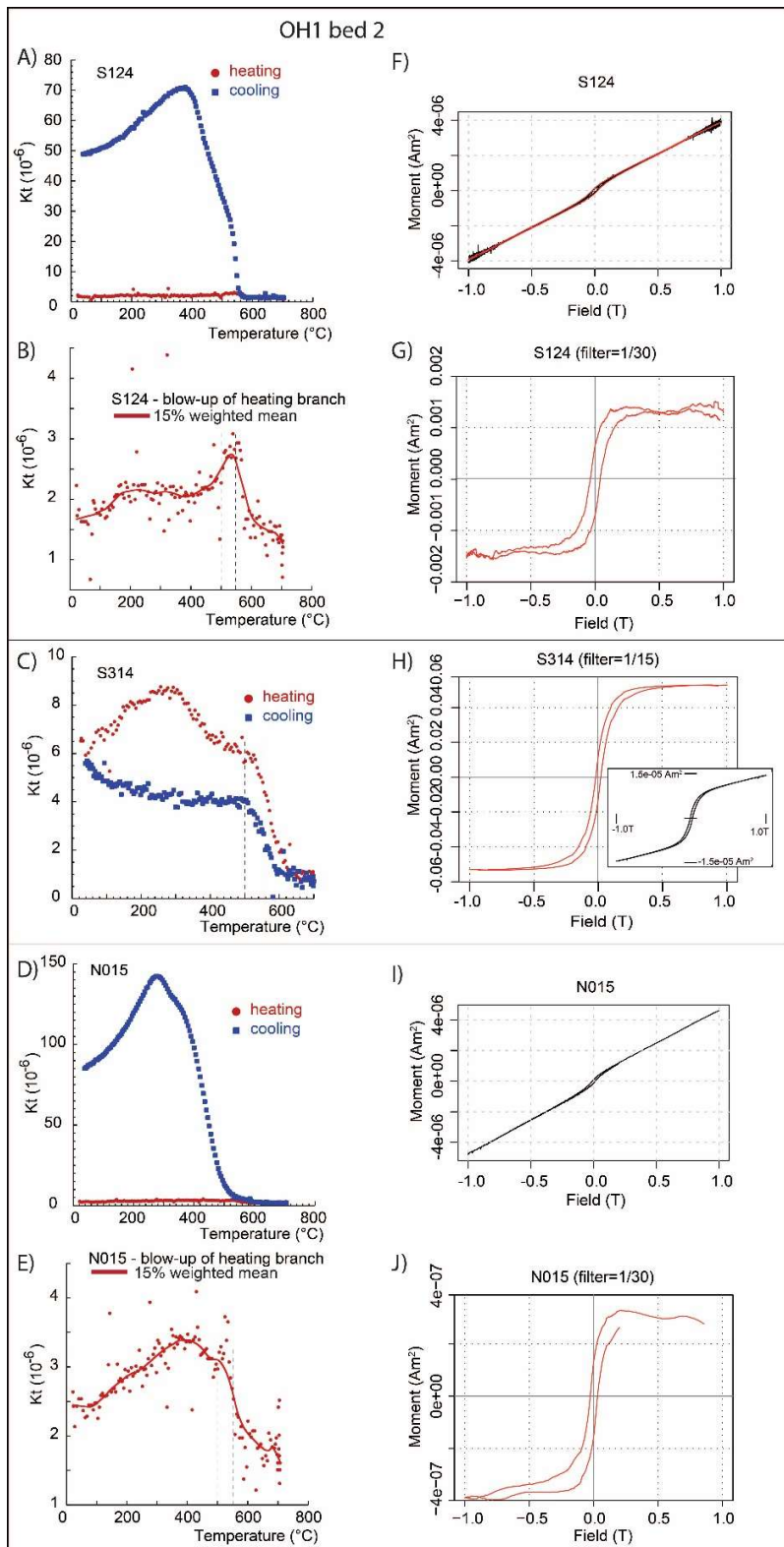


Fig. S10. Thermomagnetic (heating-cooling) cycles of magnetic susceptibility (A–E) and hysteresis experiments (F–J) on selected samples from OH1 Bed 2.

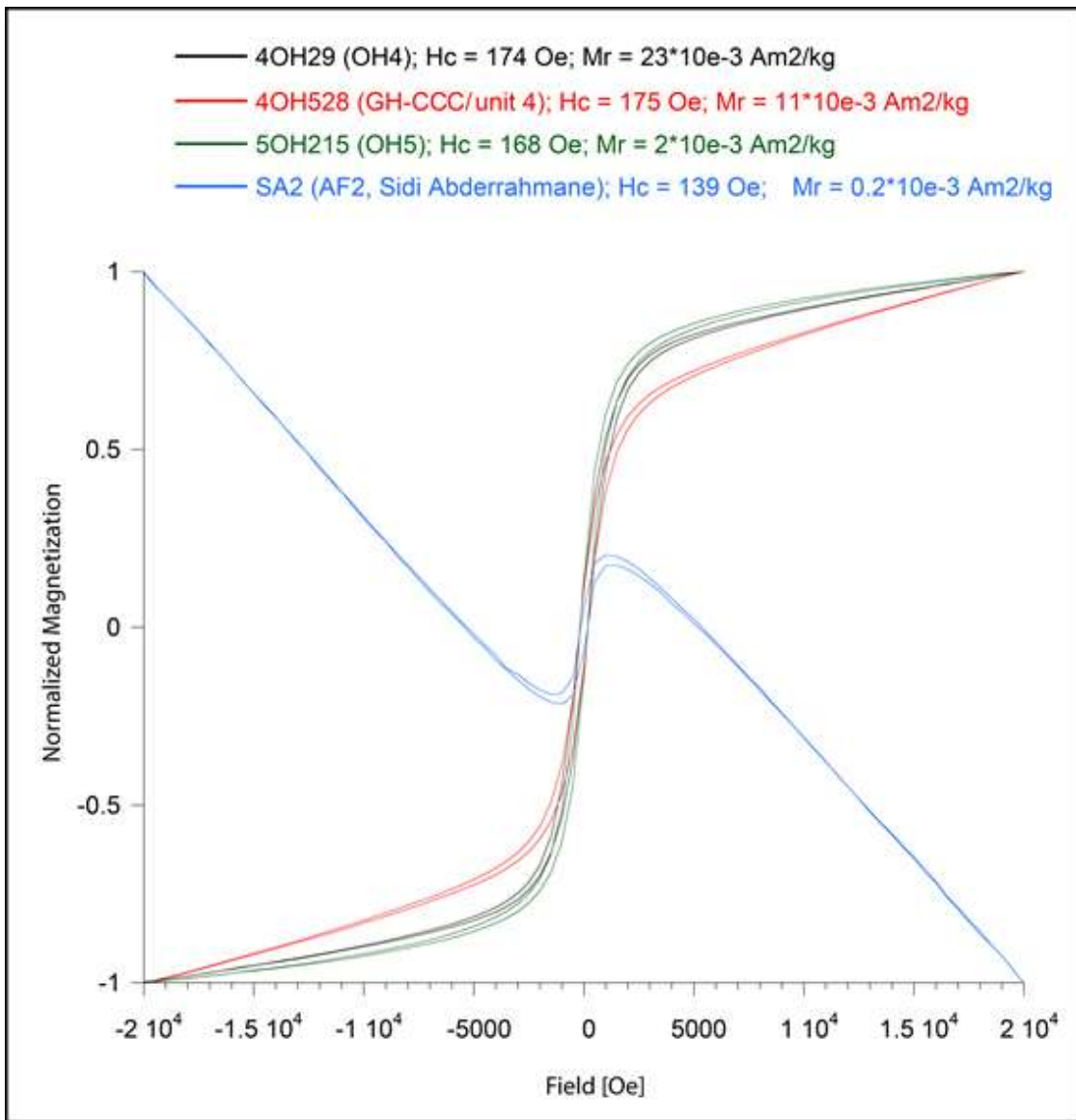


Fig. S11. Hysteresis experiments on samples from OH4, GH-CCC, OH5, and AF2 at Sidi Abderrahmane quarry. Analyses are non-corrected for paramagnetic (positive slope) or diamagnetic (negative slope) contributions.

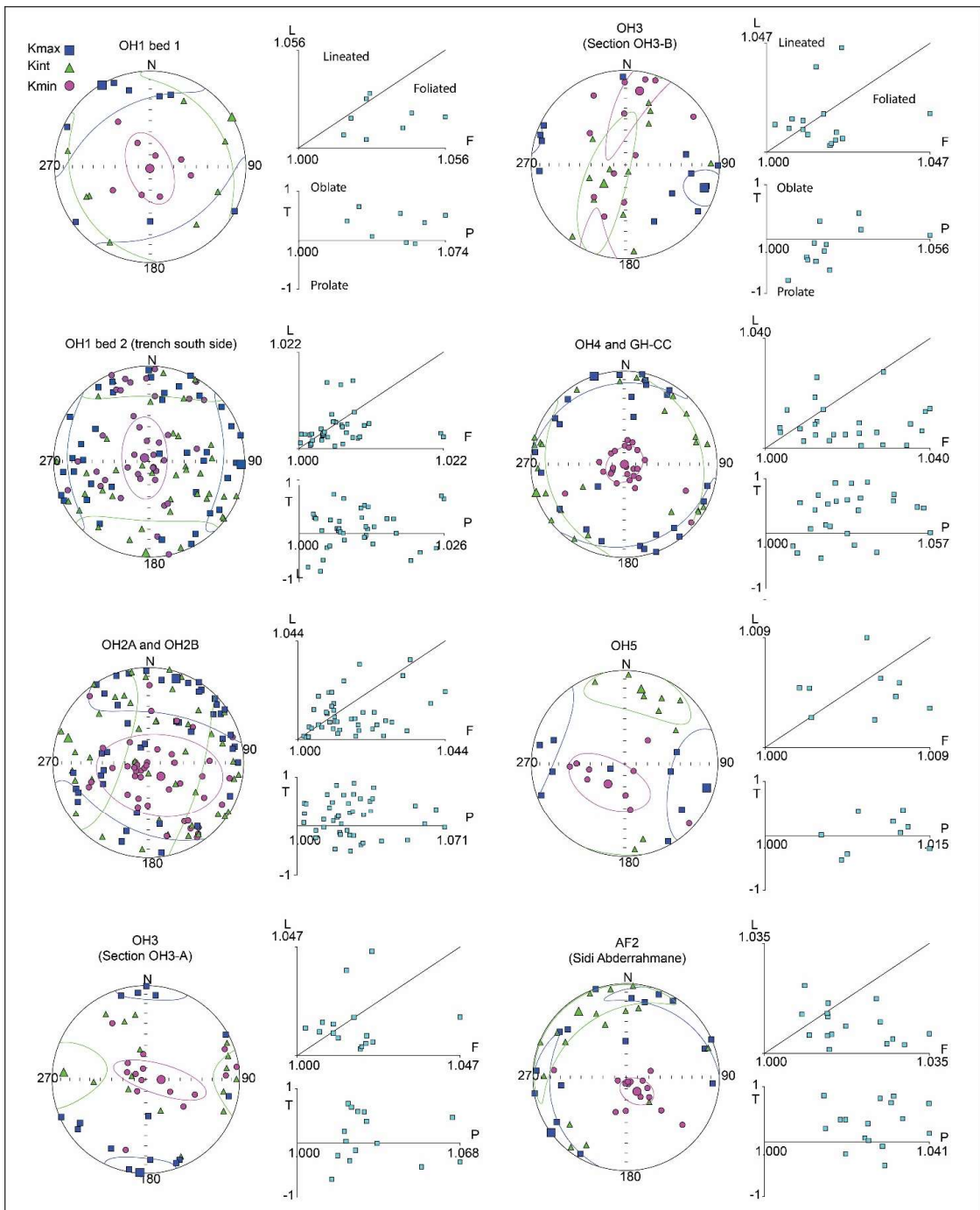
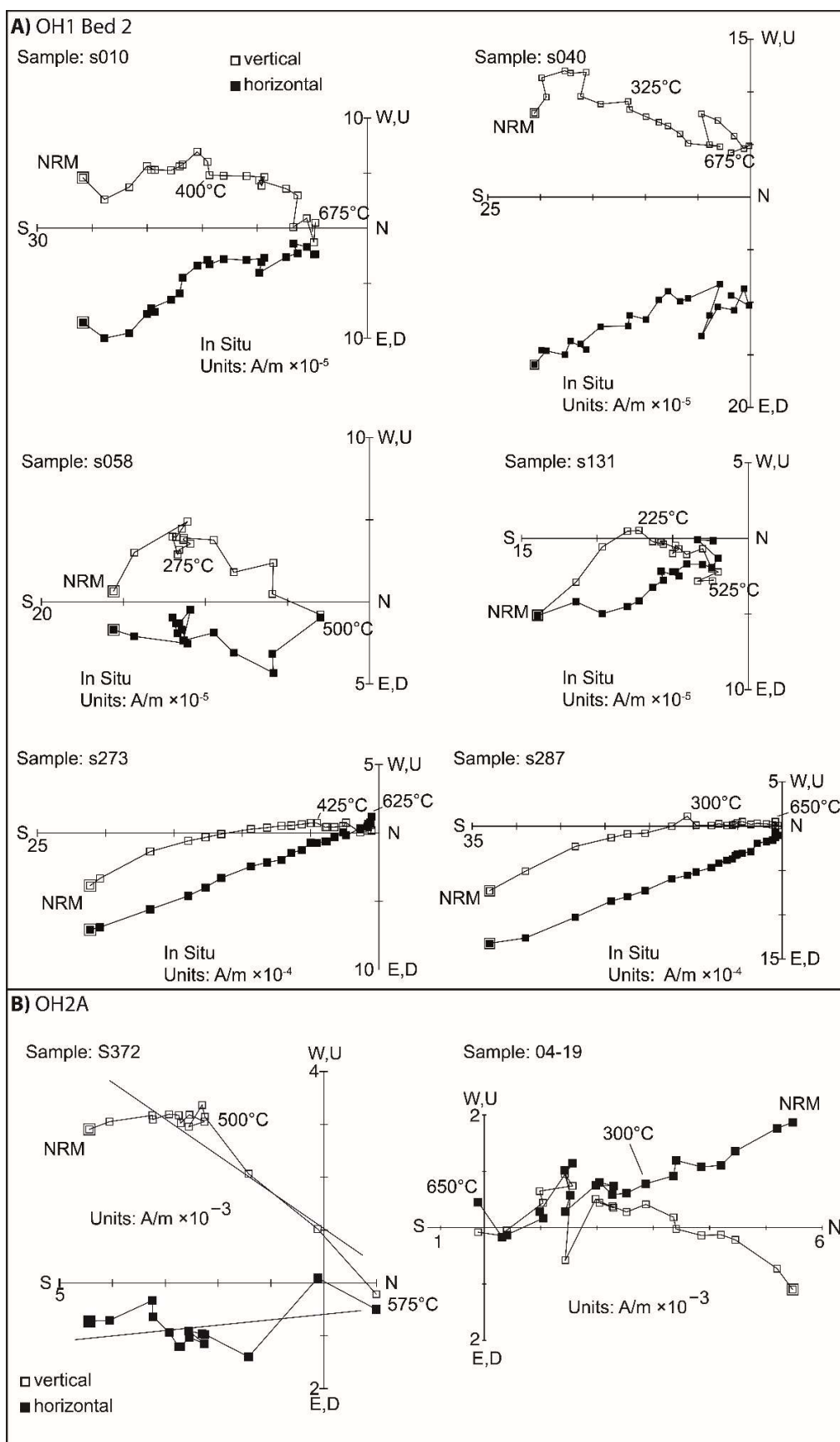


Fig. S12. Anisotropy of magnetic susceptibility data. See Material and Methods for anisotropy parameters definition and text for discussion.



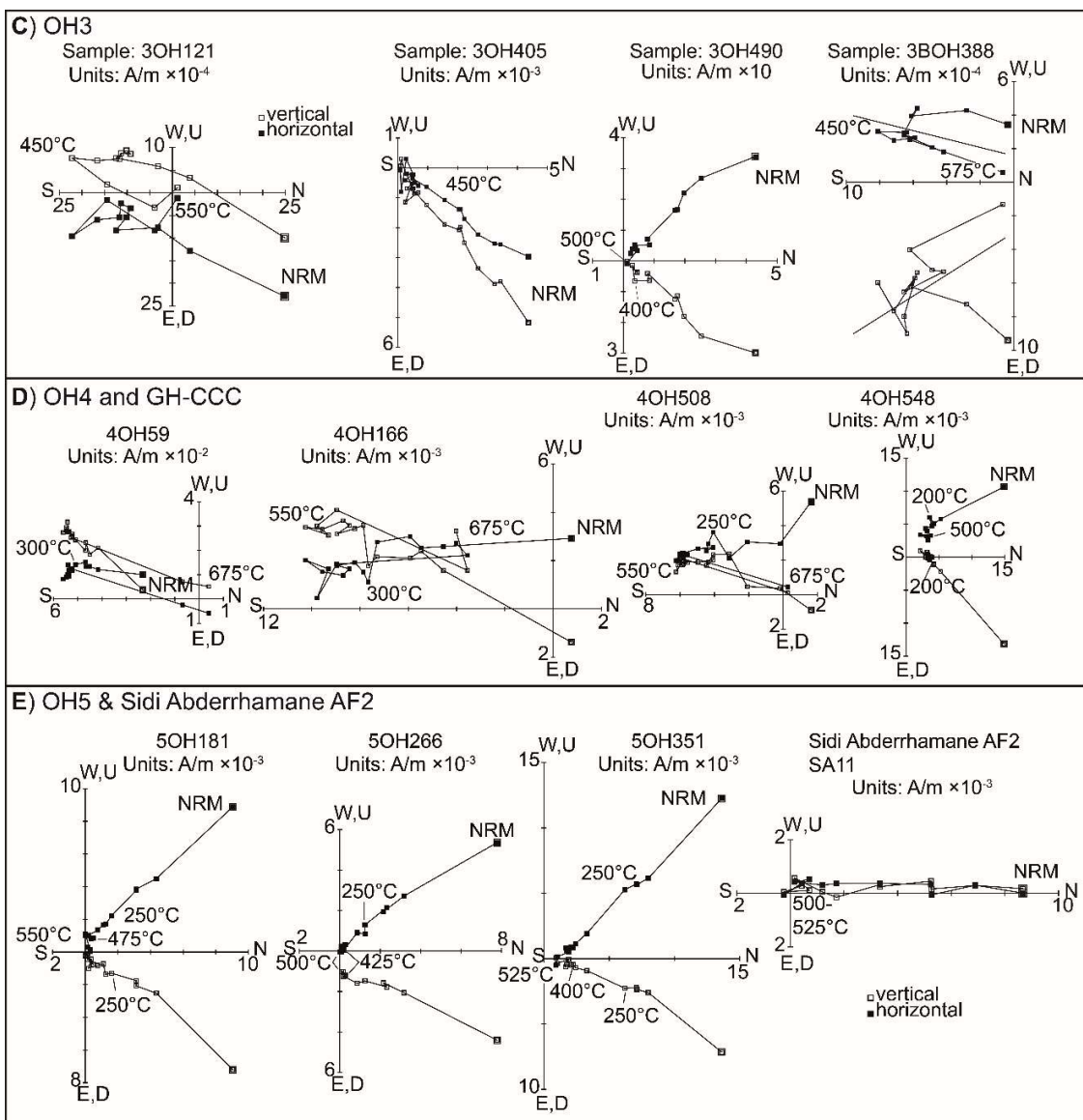


Fig. S13. Vector end-point demagnetization diagrams of representative samples from the main units investigated. (A) OH1 Bed 2, (B) OH2A, (C) OH3 (samples 3OH121, 3OH405, 3OH490 from section OH3-A, and sample 3BOH388 from section OH3-B), (D) OH4 and GH-CCC, (E) OH5, and AF2 at Sidi Abderrahmane Quarry. Filled/open symbols are projections onto the horizontal/vertical plane.

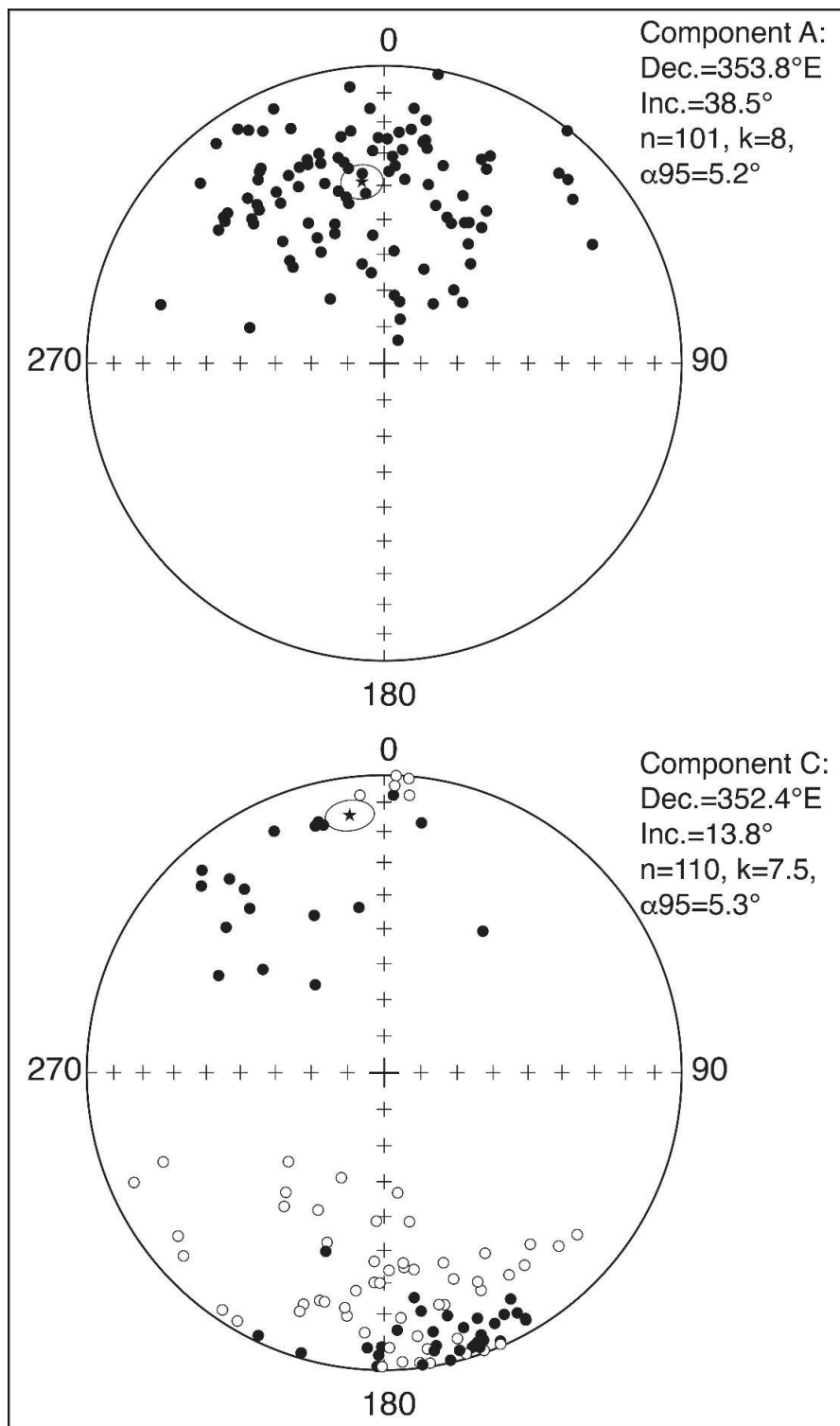


Fig. S14. Equal area plots and standard Fisher statistics of the A and C component directions from the studied sections. Filled/open symbols are projections on lower/upper hemisphere.

| | | | | | | | | | | |
|-------|--------------------|-------------------|-----------|---------------------|---------|-------------------|--------|------------|---------|---------|
| 32.35 | 61010.44 ± 3800.47 | 14798.13 ± 438.78 | 1660 ± 49 | 246037.87 ± 4042.97 | 268 ± 6 | 13639.01 ± 370.25 | 29 ± 2 | 25.9 ± 1 | 361 ± 5 | 186 ± 3 |
| 32.31 | 56394.36 ± 3680.83 | 14483.62 ± 417.91 | 1836 ± 49 | 246038.46 ± 3886.15 | 266 ± 6 | 12675.35 ± 336.91 | 31 ± 2 | 27.4 ± 1 | 365 ± 5 | 187 ± 3 |
| 32.27 | 52203.14 ± 3636.66 | 12280.72 ± 389.78 | 1677 ± 49 | 260887.9 ± 4217.13 | 189 ± 5 | 10687.31 ± 313.18 | 23 ± 2 | 22.7 ± 0.9 | 344 ± 4 | 163 ± 3 |
| 32.23 | 52163.37 ± 3665.88 | 12892.18 ± 400.77 | 1868 ± 49 | 251822.6 ± 4108.25 | 226 ± 5 | 11758.74 ± 331.48 | 26 ± 2 | 26.8 ± 1 | 341 ± 4 | 152 ± 3 |
| 32.19 | 54322.8 ± 3674.52 | 12487.89 ± 384.14 | 2781 ± 57 | 258227.44 ± 4169.5 | 247 ± 6 | 11297.98 ± 320.06 | 28 ± 2 | 21.9 ± 0.9 | 416 ± 5 | 201 ± 3 |
| 32.15 | 67671.32 ± 3657.86 | 11828.21 ± 365.69 | 3075 ± 57 | 244089.75 ± 3780.51 | 257 ± 6 | 11665.06 ± 316.19 | 27 ± 2 | 21.9 ± 0.9 | 285 ± 4 | 209 ± 3 |
| 32.11 | 45066.72 ± 3490.59 | 10334.55 ± 345.22 | 1651 ± 48 | 263743.81 ± 4132.33 | 198 ± 5 | 12401.92 ± 330.32 | 26 ± 2 | 20.8 ± 0.9 | 300 ± 4 | 151 ± 3 |

Table S5. Parameters of coastal deposits related to sea-level high-stands used to estimate uplift in the area of Casablanca from ca. 2.5 to 1 Ma. Coastal deposits identified from Lefèvre and Raynal¹. Chronological data from this study for OH3 and from Geraads¹⁴ for AAO. Minimum and maximum sea-level high-stand estimated from minimum and maximum relative sea level in Supplementary Fig. S17A, respectively. Uplift of coastal deposits related to sea-level high-stand is calculated by subtracting the mean relative sea level from the mean elevation of intertidal deposits. Uncertainties of uplift for a sea-level high-stand = [(Maximum relative sea level – Minimum relative sea level)² + (Maximum elevation of intertidal deposits – Minimum elevation of intertidal deposits)²]^{0.5}.

| Coastal deposits related to sea-level high-stand | Chronological data of intertidal deposits | Minimum / maximum elevation of intertidal deposits (m asl) | Minimum / maximum sea-level high-stand (m) | Estimated uplift (m) |
|--------------------------------------------------|--------------------------------------------------------------------|------------------------------------------------------------|--------------------------------------------|----------------------|
| OH3 (Oulad Hamida Formation) | 1075-1070 ka (Slightly earlier than Matuyama-Jaramillo transition) | 34 / 37 | -15 / 0 | 43.0 ± 7.6 |
| AAO (Ahl al Oughlam Formation) | 2500-2400 ka (biostratigraphy) | 100 / 105 | -35 / 15 | 112.5 ± 25.1 |

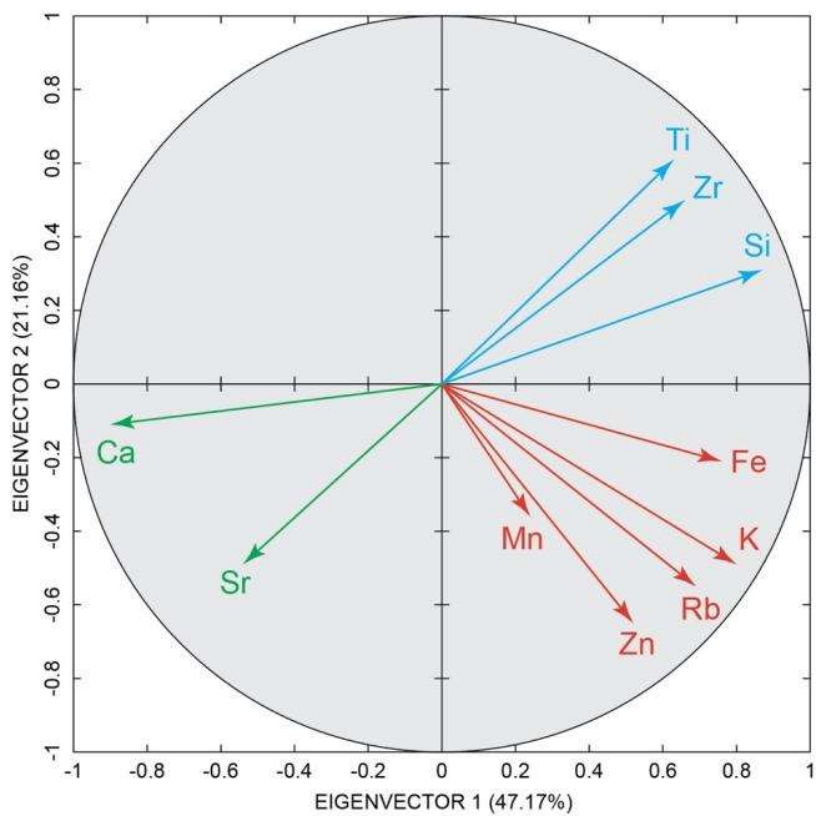


Fig. S15. Correlations between the initial variables (element concentrations) and the two first eigenvectors of the principal component analysis of geochemical data from the sediments of THI-L. The principal component analysis shows three groups of elements. The first group (Ca, Sr) can be related to detrital sediments eroded from local carbonate rocks (calcareous). The second group (K, Mn, Fe, Zn, Rb) is representative of chemically weathered sediments, with carbonate dissolution leading to an enrichment in K and Rb relatively to Ca and Sr⁶⁶⁻⁶⁸, while Mn, Fe and Zn are typically associated with redox processes⁶⁹⁻⁷³. The third group (Si, Ti, Zr) is supposed to be representative of Saharan dust input in the sediments of unit L, given that these three elements are typical of aeolian dust transported from the Sahara Desert⁶⁹⁻⁷⁰.

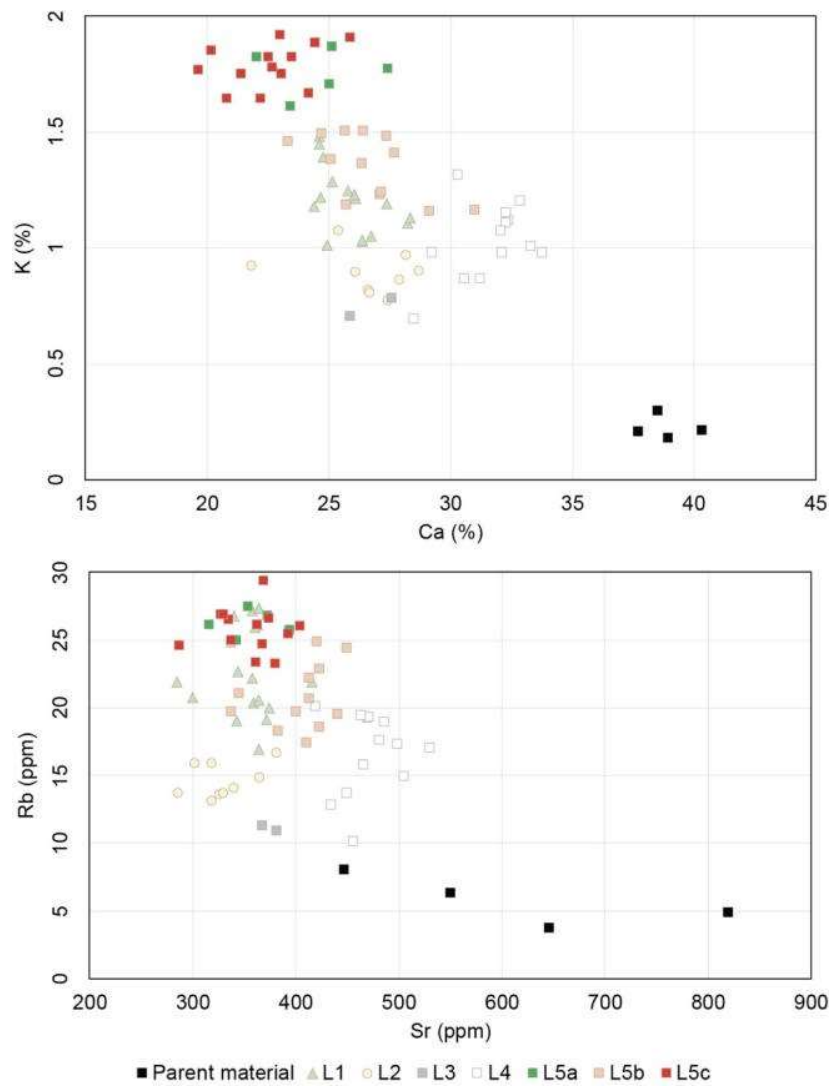


Fig. S16. Plots of K vs. Ca and Rb vs. Sr for the sediments of unit L. The samples of parent material were collected in calcarenite underlying unit L. Elements representative of parent rocks (Ca, Sr) are depleted in weathered subunits. K and Rb are increasingly enriched relatively to Ca and Sr, respectively, with an increasing degree of weathering.

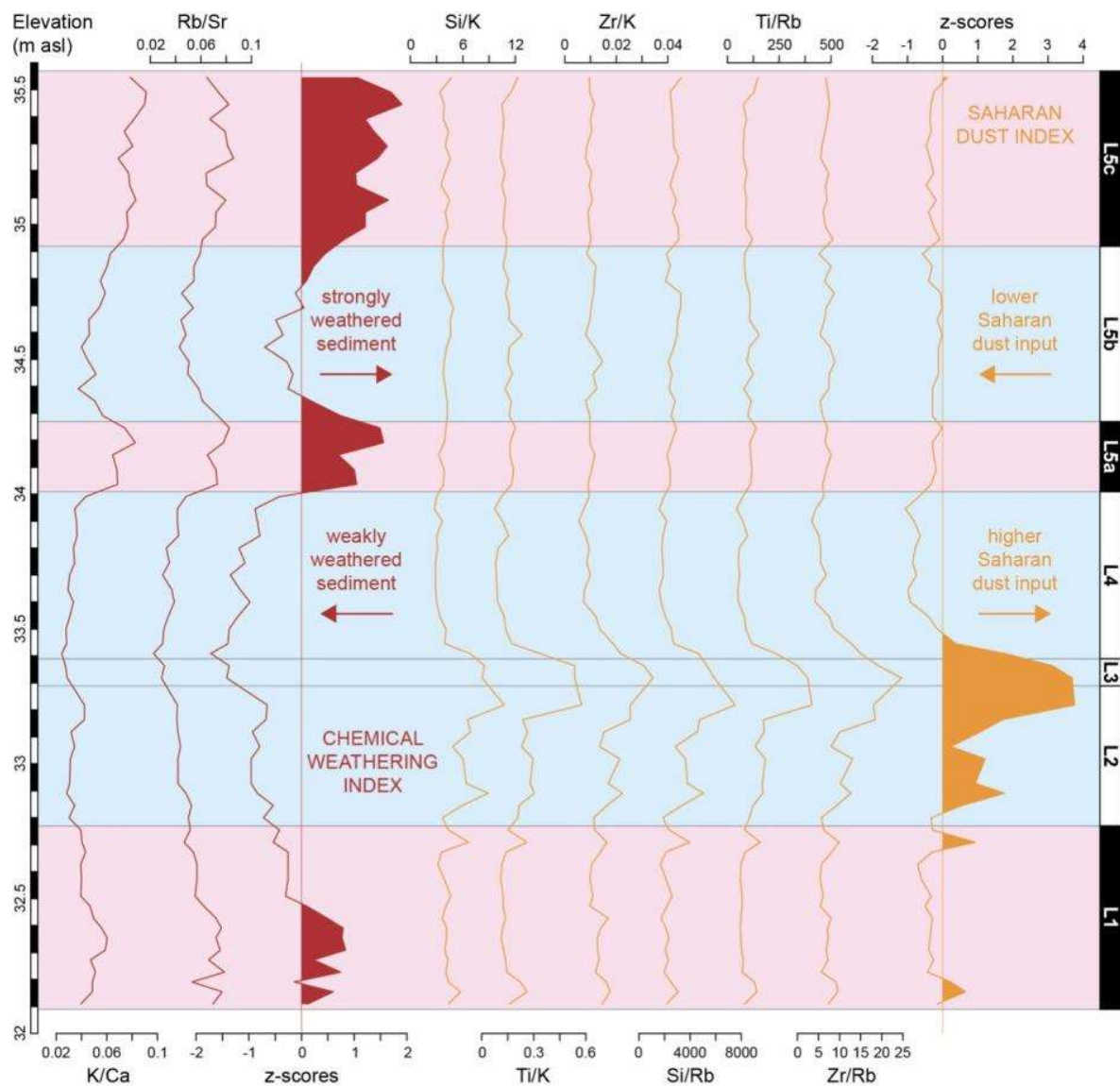


Fig. S17. Elemental ratios for the sediments of ThI-L. Rb/Sr and K/Ca ratios are useful for estimating the degree of chemical weathering of Pleistocene sediments^{66,67,74,75}. A chemical weathering index was calculated from the average of z-scores of Rb/Sr and K/Ca ratios. The elements representative of eolian input from the Sahara (Si, Ti, Zr) were normalized to K and Rb, which can be associated with fluvial input^{69,70,76,77}. An index of Saharan dust input was calculated from the average of z-scores of Si/K, Ti/K, Zr/K, Si/Rb, Ti/Rb and Zr/Rb ratios.

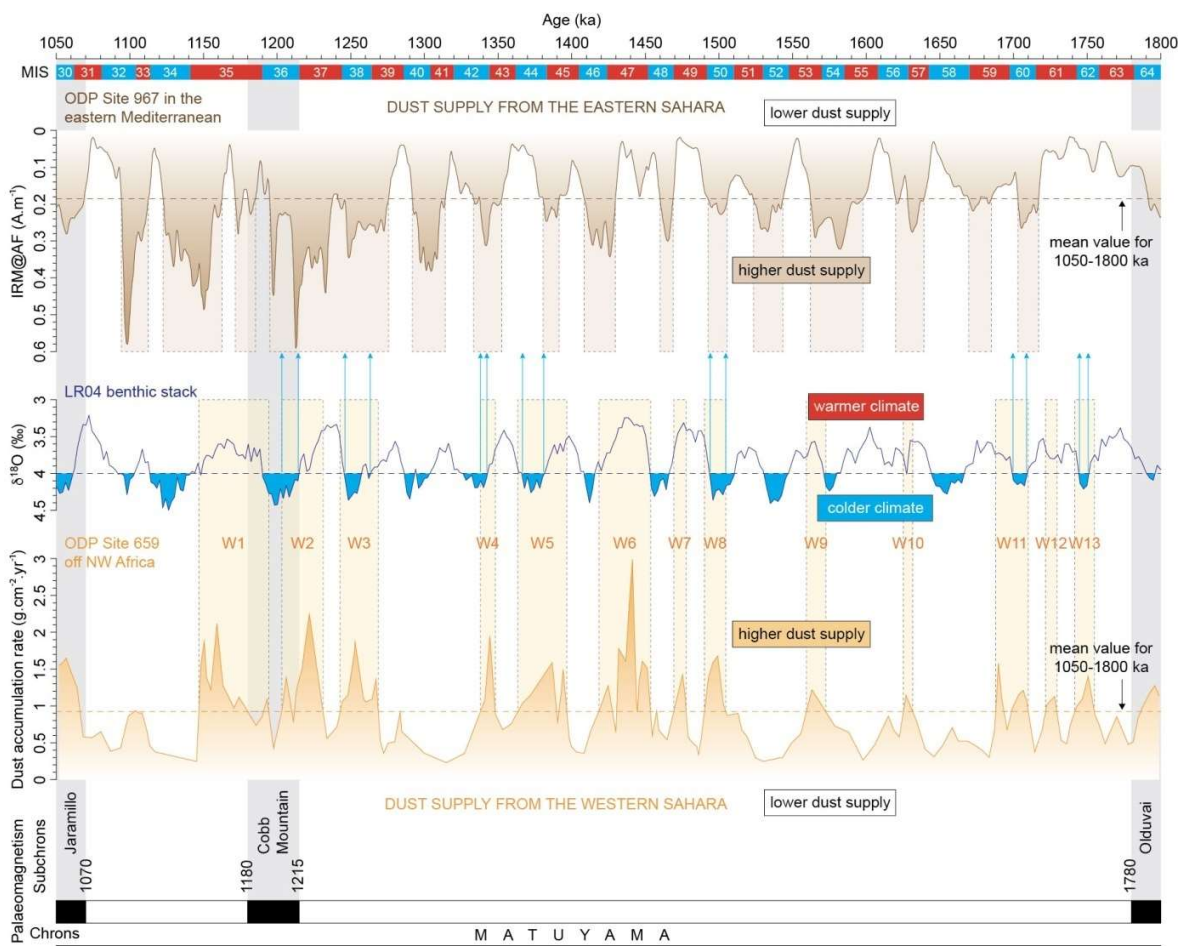


Fig. S18. Dust supply from the western and eastern Sahara between the Jaramillo and Olduvai subchrons. The most proximal marine records of Saharan dust supply around Morocco are located off northwestern Africa (ODP Site 659) and in the eastern Mediterranean (ODP Site 967), and are representative of dust flux from the western Sahara in northwestern Africa and from the eastern Sahara in northeastern Africa, respectively⁷⁸. Hence, the dust record from ODP Site 659 should be preferentially used for comparison of Saharan dust input in unit L with Saharan dust supply recorded in marine sediments, which allows to distinguish thirteen periods of higher than average dust supply from the western Sahara between the Jaramillo and Olduvai subchrons (W1-W13, pale yellow vertical bands). However, dust supply from this CaCO₃-based proxy record is potentially biased and overestimated during glacial maximum characterized by values of the LR04 $\delta^{18}\text{O}$ benthic stack higher than 4 ‰. The reliability of these periods was controlled and validated by a comparison with the periods of higher than average dust supply highlighted by the dust record from ODP Site 967 (light brown vertical bands). Amongst the seven above-mentioned periods, only W13 and the later half of W5 were not associated with periods of high Saharan dust supply at ODP Site 967 and could thus be artifacts. Saharan dust proxy record from ODP Site 659 (dust accumulation rate) from Tiedemann et al.⁸⁰. Saharan dust proxy record from ODP Site 967 (IRM@AF) from Larrasoña et al.⁸¹ with age model from Grant et al.⁸². Marine Isotopic Stages (MIS) and LR04 benthic stack from Lisiecki and Raymo⁸³. Palaeomagnetic record from Channell et al.⁸⁴.

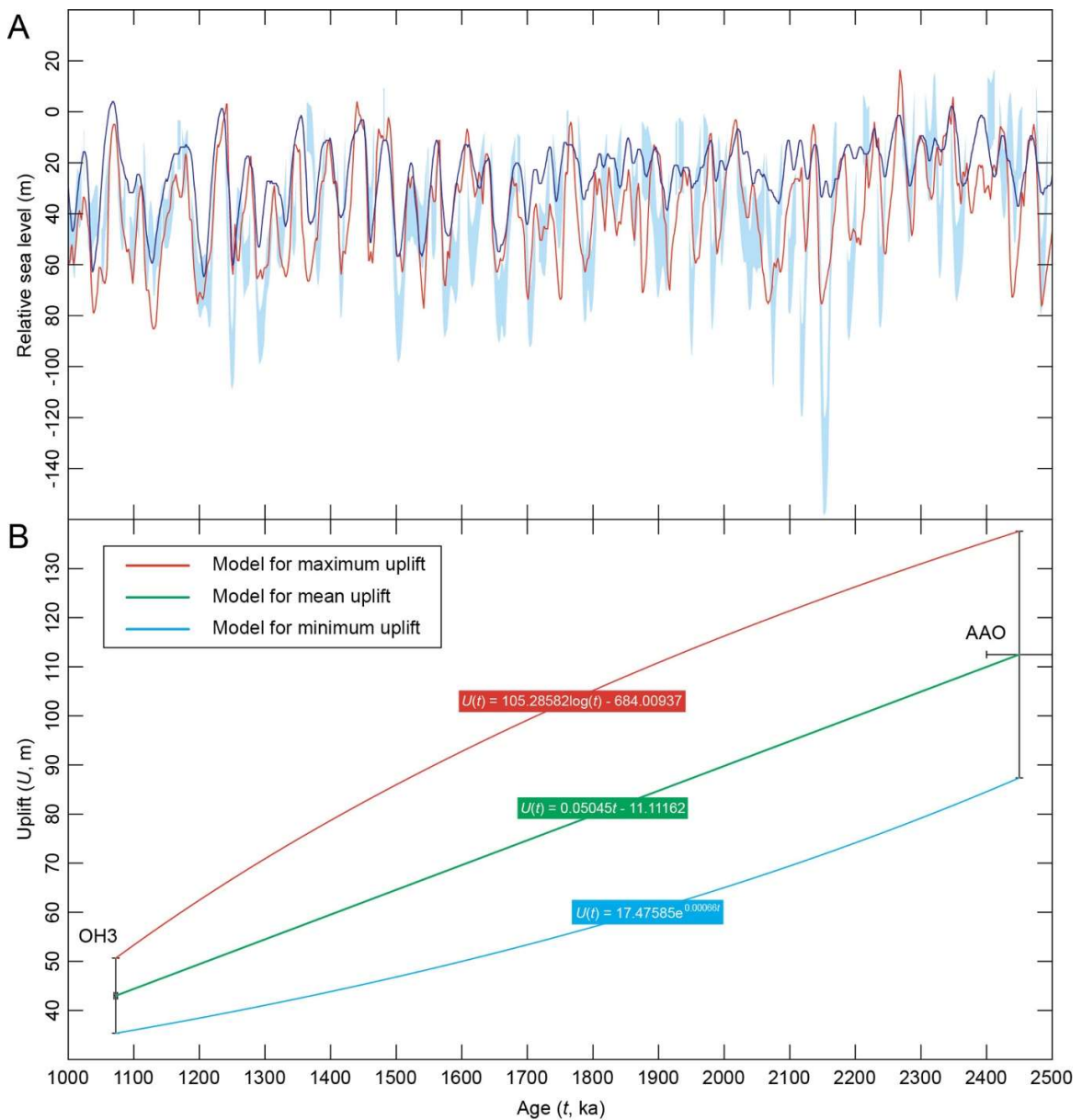


Fig. S19. Estimates of relative sea-level (RSL) changes (A) and uplift in the area of Casablanca from ca. 2.5 to 1 Ma (B). A: blue shaded area: RSL from Rohling et al.⁸⁵ corrected by Amies⁸⁶; dark blue line: RSL from de Boer et al.⁸⁷; red line: RSL from SPECMAP data⁸⁸ rescaled with 121 m sea level fall at 17 ka⁸⁹ corresponding to a $\delta^{18}\text{O}$ value of ca. 1.78. All RSL data were resampled at 1 ka interval. B: Maximum, mean and minimum uplift estimated for sea-level high-stands OH3 and AAO were used in order to test three uplift models based on logarithmic, linear and exponential regressions, respectively, assuming no subsidence during the Quaternary^{4,90}. OH3: sea-level high-stand of the Oulad Hamida formation; AAO: sea-level high-stand of the Ahl al Oughlam Formation. The parameters of sea-level high-stands are listed in Supplementary Table S5.

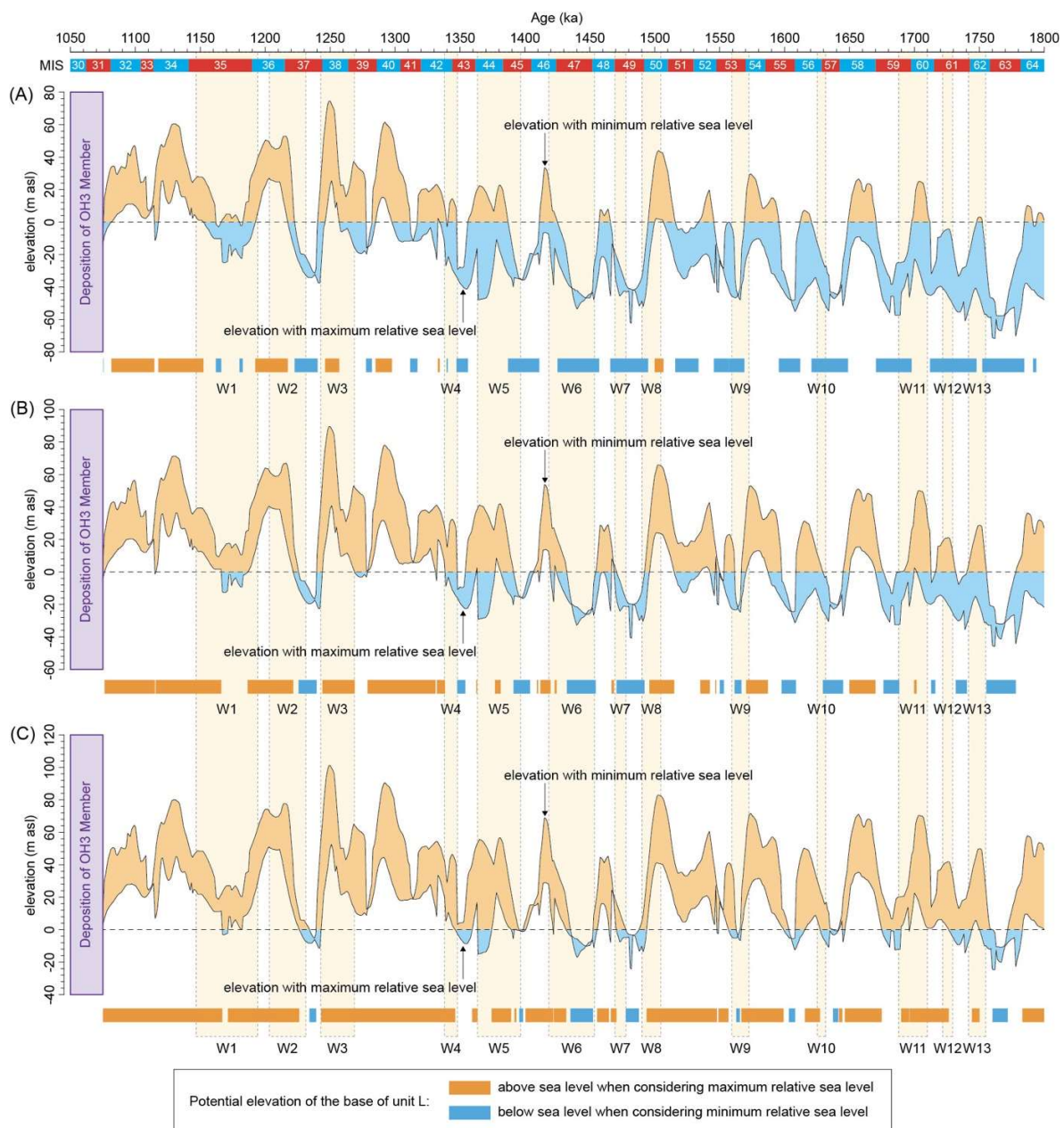


Fig. S20. Potential elevation of the base of unit L during the periods of higher than average dust supply from the western Sahara (W1-W13, pale yellow vertical bands) for different uplift models. A: Logarithmic model for maximum uplift. B: Linear model for mean uplift. C: Exponential model for minimum uplift. Elevation was calculated by subtracting relative sea level and uplift from the present elevation of the base of unit L (ca. 32 m above sea level). Maximum and minimum relative sea level were determined from Supplementary Fig. S19A. Uplift was estimated from models in Supplementary Fig. S19B. Palaeo-elevation reconstruction is supposed to give potential elevations because it does not take into account potential periods of sedimentation and erosion at the site of Thomas Quarry I before the deposition of unit L. Marine Isotopic Stages (MIS) from Lisiecki and Raymo⁸³.

6. Palynology

Fossil pollen data from Th-L1 (Supplementary Table S6) show that the vegetal landscape was dominated by a steppe (66.8%) with Compositae (42.5 %), Poaceae (4 %) Chenopodiaceae (3.7 %) and varied plants: *Convolvulus*, *Helianthemum*, and *Reseda*. Regionally, an open Mediterranean forest (Arboreal Pollen: 26.7 %) was present. It consists mainly of deciduous *Quercus* (9.9 %), *Pinus* (1.2 %) and *Olea* (0.3 %). *Myrtus* (11.2%) could develop either in the oak wood undergrowth or in wet depressions⁹¹. Edible plants were identified in the pollen assemblage (Supplementary Table S6). They correspond to 76% of all the identified phanerogams. They could constitute a significant part of the potential diet of the hominins.

6.1 Methods. The Casablanca region is located in the sclerophyllous forest ecoregion⁹² which is nowadays degraded by human activities.

Of the seven samples taken from profile 19 of the ThI-L, only sample CT 19-01 was polliniferous. The sporo-pollinic material was extracted from the sediment using chemical treatment (HCl acid, NaOH 10% and acetolysis), a flotation in heavy liquid ($d = 2$) and $160 + 10 \mu\text{m}$ sieving. The identification was carried out with a photonic microscope (x500 magnification). The palynological identifications were based on the pollen reference collection of IMBE (CNRS, Aix-en-Provence, France) and the bibliography⁹³⁻⁹⁶. The pollen percentages were calculated on a Pollen Sum (PS: 322) including only the phanerogams. The weight of the pollen sample is: 15.6 g. The analysed volume is 45 μl . The Absolute pollen Frequency is of 20.6 pollen grain/gram. The biodiversity is high: in total, 42 taxa were identified, among them 38 phanerogams et 4 non pollen palynomorphs (charcoal (very few) and unidentifiable insect, chironomid and fungi).

Table S6. Phanerogams and edible plants (in bold) of the pollen sample CT 19-1. Values are in counting values and in percentages (calculated on a pollen sum including all the phanerogams). The systematic is from Cronquist⁹⁷.

| Sample | Counting value | % | Edible organ | Sample | Counting value | % | Edible organ |
|-------------------------|----------------|-------|--------------------|--------------------------------|----------------|-------|----------------------------|
| Acer sp | 2 | 0.62 | | Hippophae rhamnoides | 4 | 1.24 | Fruit |
| Ammi t. | 14 | 4.35 | Seed | Hypericum sp. | 1 | 0.31 | Leaf |
| Apiaceae | 7 | 2.17 | Leaf, stem, root | Linum usitatissimum | 2 | 0.62 | Seed |
| Artemisia sp. | 31 | 9.63 | Leaf, shoot | Myrtus sp. | 36 | 11.18 | Fruit, bud |
| Aster t. | 2 | 0.62 | Leaf, stem | Odontites sp. | 3 | 0.93 | |
| Atriplex t. | 7 | 2.17 | All | Olea sp | 1 | 0.31 | Fruit |
| Blackstonia t. | 3 | 0.93 | | Pimpinella sp. | 1 | 0.31 | Seed |
| Bupleurum sp. | 1 | 0.31 | | Pinus sylvestris t. | 2 | 0.62 | Seed, young shoot |
| Calendula t. | 1 | 0.31 | Leaf, flower | Pinus (mediterranean) | 2 | 0.62 | Seed, young shoot |
| Carduus t. | 2 | 0.62 | Leaf | Poaceae | 13 | 4.04 | Young shoot, leaf |
| Chenopodiaceae | 5 | 1.55 | Leaf | Polygonum aviculare sp. | 2 | 0.62 | Seed, young leaf and plant |
| Cichorioideae | 100 | 31.06 | Leaf, flower, stem | Prunus sp. | 4 | 1.24 | Fruit |
| Cirsium t. | 1 | 0.31 | Leaf, flower, stem | Quercus sp. (deciduous) | 32 | 9.94 | Fruit |
| Convolvulus sp | 1 | 0.31 | Leaf, young shoot | Ranunculus sp. | 2 | 0.62 | |
| Cyperaceae | 3 | 0.93 | Root | Reseda sp. | 5 | 1.55 | Young shoot, leaf |
| Euphorbia sp. | 7 | 2.17 | | Scutellaria t. | 12 | 3.73 | |
| Galium sp | 1 | 0.31 | Leaf | Sinapis t. | 3 | 0.93 | Seed, leaf |
| Gentiana sp. | 3 | 0.93 | | Urtica sp. | 1 | 0.31 | Leaf |
| Helianthemum sp. | 2 | 0.62 | | Vitis sp. | 3 | 0.93 | Fruit |

References

1. Lefèvre, D. & Raynal, J.-P. Les formations plio-pléistocènes de Casablanca et la chronostratigraphie du Quaternaire marin du Maroc revisitées, *Quaternaire* **13**, 9-21 (2002).
2. Lecointre, G. *Recherches sur le Néogène et le Quaternaire marins de la côte atlantique du Maroc* (Mémoires du Service Géologique du Maroc, 99, t.1 : Stratigraphie, 1952).
3. Biberson, P. *Le Paléolithique inférieur du Maroc atlantique* (Publications du Service des Antiquités du Maroc 17, 1961).
4. Stearns, C. E. Pliocene-Pleistocene emergence of the Moroccan Meseta. *Geol. Soc. Am. Bull.* **89**, 1630-1644 (1978).
5. Texier, J.-P., Lefèvre, D., Raynal, J.-P. & El Graoui, M. Lithostratigraphy of the littoral deposits of the last one million years in the Casablanca region (Maroc). *Quaternaire* **13**, 23-41 (2002).
6. Texier, J.-P. *et al.* Contribution pour un nouveau cadre stratigraphique des formations littorales Quaternaires de la région de Casablanca (Maroc). *Cr. Acad. Sci. Paris* **318**, séries II, 1247-1253 (1994).
7. Biberson, P. *Le cadre paléogéographique de la Préhistoire du Maroc atlantique* (Publications du Service des Antiquités du Maroc 16, 1961).
8. Lefèvre, D., Raynal, J.-P. & El Graoui, M. Le Quaternaire d'Oulad Hamida in *Préhistoire de Casablanca. I - La grotte des Rhinocéros (fouilles 1991 et 1996)* (eds. Raynal, J.-P. & Mohib, A.) 45-59 (Institut National des Sciences de l'Archéologie et du Patrimoine, VESAM volume VI, 2016).
9. Raynal, J.-P. & Texier, J.-P. Découverte d'Acheuléen ancien dans la carrière Thomas 1 à Casablanca et problème de l'ancienneté de la présence humaine au Maroc, *C. R. Acad. Sci. II* **308**, 1743-1749 (1989).
10. Raynal, J.-P., Sbihi-Alaoui, F.Z., Geraads, D., Magoga, L. & Mohib, A. The earliest occupation of North-Africa: the Moroccan perspective. *Quat. Int.* **75**, 65-75 (2001).
11. Raynal, J.-P., Sbihi-Alaoui, F.Z., Magoga, L., Mohib, A. & Zouak, M. The Lower Palaeolithic Sequence of Atlantic Morocco Revisited After Recent Excavations at Casablanca. *Bulletin d'archéologie marocaine* **20**, 44-76, (2004).
12. Raynal, J.-P. *et al.* Contextes et âge des nouveaux restes dentaires humains du Pléistocène moyen de la carrière Thomas I à Casablanca (Maroc). *Bull. Soc. Prehist. Fr.* **108**, 645-669 (2011).
13. Raynal, J.-P. *et al.* Hominid Cave at Thomas Quarry I (Casablanca, Morocco): recent findings and their context. *Quat. Int.* **223-224**, 369-382 (2010).
14. Geraads, D. Plio-Pleistocene mammalian biostratigraphy of Atlantic Morocco. *Quaternaire* **13**, 43-53 (2002).

15. Geraads, D. Biochronologie mammalienne du Quaternaire du Maroc atlantique, dans son cadre régional, *L'Anthropologie* **114**, 324–340 (2010).
16. Rhodes, E. J., Singarayer, J., Raynal, J.-P., Westaway, K. & Sbihi-Alaoui, F.-Z. New age estimations for the Palaeolithic assemblages and Pleistocene succession of Casablanca, Morocco. *Quat. Sci. Rev.* **25**, 2569–2585 (2006).
17. Guilloré, P. *Méthode de fabrication mécanique et en série des lames minces* (Document du département des sols de l'I.N.A. Paris-Grignon, 1980).
18. El Graoui, M. PhD dissertation (Université de Bordeaux 1, 1994).
19. Cremaschi, M., Trombino, L. & Zerboni, A. Palaeosoils and relict soils, a systematic review in *Interpretation of micromorphological features of soils and regoliths – Revised Edition* (eds. Stoops, G., Marcelino, V. & Mees, F.) 863–894 (Elsevier, 2018).
20. Courty, M.-A. Microfacies analysis assisting archaeological stratigraphy in *Earth sciences and archaeology* (eds. Goldberg, P., Holliday, V. T. & Ferring C.R.) 205–239 (Kluwer Academic/Plenum Publishers, 2001).
21. Goldberg, P. & Macphail, R. I. *Practical and theoretical geoarchaeology* (Blackwell Publishing, 2006).
22. Goldberg, P., Berna, F. Micromorphology and context. *Quat. Int.* **214**, 56–62 (2010).
23. Stoops, G. Fluorescence microscopy in *Archaeological Soil and Sediment Micromorphology* (eds. Nicosia, C. & Stoops G.) 393–397 (John Wiley & Sons, 2017).
24. Stoops, G. *Guidelines for Analysis and Description of Soil and Regolith Thin Sections* (Soil Science Society of America Inc., 2003).
25. Courty, M. A., Goldberg, P. & Macphail, R. I. *Soils and Micromorphology in Archaeology* (University Press, 1989).
26. Nicosia, C. & Stoops, G. *Archaeological Soil and Sediment Micromorphology* (John Wiley & Sons, 2017).
27. Stoops, G., Marcelino, V. & Mees, F. *Interpretation of Micromorphological Features of Soils and Regoliths*, (Elsevier, 2nd ed, 2018).
28. Ward, W. C. Petrology and diagenesis of carbonate eolianites on northwestern Yucatan Peninsula, Mexico in *Belize Shelf--Carbonate Sediments, Clastic Sediments, and Ecology* (eds. Pusey, W. C. & Wantland K. F.) 500–571 (AAPG Special Volumes, 1975).
29. Wieder, M. & Yaalon, D. H. Effect of matrix composition of carbonate nodule crystallisation. *Geoderma* **11**, 95–121 (1974).
30. Monger, H. C., Daugherty, L. A. & Gile, L. H. A microscopic examination of pedogenic calcite in an Aridisol of southern New Mexico in *Occurrence, Characteristics, and Genesis of Carbonate, Gypsum, and Silica Accumulations in Soils* (ed. Nettleton, W. D.) 37–60 (Soil Science Society of America Journal Special Publication 26, 1991).

31. Verrecchia, E. P. Lacustrine and palustrine geochemical sediments, in *Geochemical Sediments and Landscapes* (eds. Nash, D. J. & McLaren, S. J.) 298–329 (Blackwell, 2007).
32. Durand, N., Monger, H. C., Canti, M. G. & Verrecchia, E. P. Calcium carbonate features in *Interpretation of micromorphological features of soils and regoliths – Revised Edition* (eds. Stoops, G., Marcelino, V. & Mees, F.) 205–258 (Elsevier, 2018).
33. Tsatskin, A. & Ronen, A. Micromorphology of a Mousterian paleosol in aeolianites at the site Habonim, Israel. *Catena* **34**, 365–384 (1999).
34. Zhao, Q. *et al.* Sedimentary facies and evolution of aeolianites on Shidao Island, Xisha Islands. *Chin. J. Oceanol. Limn.* **29**, 398–413 (2011).
35. Li, R. *et al.* Composition and diagenesis of Pleistocene aeolianites at Shidao, Xisha Islands: Implications for palaeoceanography and palaeoclimate during the last glacial period. *Palaeogeogr. Palaeocl. Palaeoecol.* **490**, 604–616 (2018).
36. Shtienberg, G. *et al.*, New perspectives on coastal landscape reconstruction during the Late Quaternary: A test case from central Israel. *Palaeogeogr. Palaeocl. Palaeoecol.* **468**, 503–519 (2017).
37. Brooke, B. The distribution of carbonate eolianite. *Earth Sci. Rev.* **55**, 135–164 (2001).
38. Simpson, E. L. & Eriksson, K. A. Thin eolianites interbedded within a fluvial and marine succession: early Proterozoic Whitworth Formation, Mount Isa Inlier, Australia. *Sediment. Geol.* **87**, 39–62 (1993).
39. Hearty, P. J. Stratigraphy and timing of eolianite deposition on Rottnest Island, Western Australia. *Quat. Res.* **60**, 211–222 (2003).
40. Assal, E. M., Adbel-Fattah, Z. A. & El-Asmar, H. M. Facies architecture and controlling factors induced depositional model of the Quaternary carbonate eolianites in the northwestern Mediterranean coast of Egypt. *Int. J. Earth Sci.* **109**, 1659–1682 (2020).
41. Zerboni, A. Micromorphology reveals in situ Mesolithic living floors and archaeological features in multiphase sites in central Sudan. *Geoarchaeology* **26**, 365–391 (2011).
42. Miller, C. E. Trampling in *Encyclopedia of Geoarchaeology* (ed. Gilbert, A.S.) 981–982 (Springer, 2017).
43. Villagran, X. S., Huisman, D. J., Mentzer, S. M., Miller, C. E. & Jans, M. M. Bone and Other Skeletal Tissues in *Archaeological Soil and Sediment Micromorphology* (eds. Nicosia, C. & Stoops, G.) 11–38 (John Wiley & Sons, 2017).
44. Karkanas, P. & Goldberg, P. Phosphatic features, in *Interpretation of Micromorphological Features of Soils and Regoliths* (eds. Stoops, G., Marcelino, V. & Mees, F.) 323–346 (Elsevier, 2nd ed, 2018).
45. Angelucci, D. E. The recognition and description of knapped lithic artifacts in thin section. *Geoarchaeology* **25**, 220–232 (2010).

46. Angelucci, D. E. Lithic artefacts in *Archaeological Soil and Sediment Micromorphology* (Nicosia, C. & Stoops, G.) 223–230 (John Wiley & Sons, 2017).
47. Macphail, R. I., & Goldberg, P. Archaeological materials in *Interpretation of Micromorphological Features of Soils and Regolith* (eds. Stoops, G., Marcelino, V. & Mees, F.) 779–819 (Elsevier, 2nd ed, 2018).
48. Souron, A. PhD dissertation (Université de Poitiers, 2012).
49. Suwa, G., Souron, A. & Asfaw, B. Fossil Suidae of the Konso Formation in *Konso-Gardula Research Project, Vol. 1: Paleontological Collections: Background and Fossil Aves, Cercopithecidae, and Suidae* (Suwa, G., Beyene, Y. & Asfaw, B.) 73-88 (The University Museum, The University of Tokyo, Bulletin N. 47, 2014).
50. Geraads, D., Alemseged, Z., Reed, D., Wynn, J. & Roman, D. C. The Pleistocene fauna (other than Primates) from Asbole, lower Awash Valley, Ethiopia, and its environmental and biochronological implications. *Geobios* **37**, 697-718 (2004).
51. Gilbert, H. 11 – Suidae in *Homo erectus - Pleistocene Evidence from the Middle Awash, Ethiopia* (Gilbert, H. & Asfaw, B.) 231-260 (University of California Press, 2008).
52. Ameur, R. PhD Dissertation (Université d'Oran, 1988).
53. Geraads, D. Biogeography of Miocene-Pliocene circum-mediterranean rodents: a revision based upon factor analysis and parsimony analysis of endemicity. *Palaeogeogr. Palaeocl. Palaeoecol.* **137**, 273-288 (1998).
54. Geraads, D. Biogeographic relationships of Pliocene and Pleistocene North-western African Mammals. *Quat. Int.* **212**, 159-168 (2010).
55. Chaid-Saoudi, Y., Geraads, D. & Raynal, J.-P. The fauna and associated artefacts from the Lower Pleistocene site of Mansourah (Constantine, Algeria). *C. R. Palevol* **5**, 963-971 (2006).
56. Sahnouni, M. *et al.* Further research at the Oldowan site of Aïn Hanech, north-eastern Algeria. *J. Hum. Evol.* **43**, 925–937 (2002).
57. Geraads, D. *et al.* The Pleistocene Hominid site of Ternifine, Algeria: new results on the environment, age and human industries. *Quat. Res.* **25**, 380-386 (1986).
58. Geraads, D. Pleistocene Carnivora (Mammalia) from Tighennif (Ternifine), Algeria. *Geobios* **49**, 445–458 (2016).
59. Pickford, M. The fossil Suidae (Mammalia, Artiodactyla) from Ternifine (Tighenif) Algeria. *Münchner Geowissenschaftliche Abhandlungen* **50**, 1–67 (2020).
60. Gilbert, W. H., Asfaw, B. *Homo erectus - Pleistocene evidence from the Middle Awash* (University of California Press, 2009).
61. Geraads, D. Bovidae et Giraffidae (Artiodactyla, Mammalia) du Pléistocène de Ternifine (Algérie). *B. Mus. Natl. His. Nat. 4^{eme}sér. C* **3**, 47–86 (1981).

62. Domínguez-Rodrigo, M. & Baquedano, E. Distinguishing Butchery Cut Marks from Crocodile Bite Marks through Machine Learning Methods. *Sci. Rep.* **8**, 1–8 (2018).
63. Njau, J. K. & Blumenschine, R. J. A Diagnosis of Crocodile Feeding Traces on Larger Mammal Bone, with Fossil Examples from the Plio-Pleistocene Olduvai Basin, Tanzania. *J. Hum. Evol.* **50**, 142–62 (2006).
64. Njau, J. K. & Blumenschine, R. J. Crocodylian and Mammalian Carnivore Feeding Traces on Hominid Fossils from FLK 22 and FLK NN 3, Plio-Pleistocene, Olduvai Gorge, Tanzania. *J. Hum. Evol.* **63**, 408–17 (2012).
65. Sahle, Y., El Zaatar, S. & White, T. D. Hominid Butchers and Biting Crocodiles in the African Plio–Pleistocene. *Proc Natl Acad Sci* **114**, 13164–13169 (2017).
66. Yang, S. Y., Li, C. X., Yang, D. Y. & Li, X. S. Chemical weathering of the loess deposits in the lower Changjiang Valley, China, and paleoclimatic implications. *Quat. Int.* **117**, 27-34 (2004).
67. Profe, J., Zolitschka, B., Schirmer, W., Frechen, M. & Ohlendorf, C. Geochemistry unravels MIS 3/2 paleoenvironmental dynamics at the loess–paleosol sequence Schwalbenberg II, Germany. *Palaeogeogr. Palaeoclimatol. Palaeoecol.* **459**, 537-551 (2016).
68. Hosek, J. *et al.* An integrated rock-magnetic and geochemical approach to loess/paleosol sequences from Bohemia and Moravia (Czech Republic): Implications for the Upper Pleistocene paleoenvironment in central Europe. *Palaeogeogr. Palaeocl. Palaeoecol.* **418**, 344-358 (2015).
69. Rodrigo-Gamiz, M., Martínez-Ruiz, F., Rodríguez-Tovar, F. J., Jiménez-Espejo, F.J. & Pardo-Igúzquiza, E. Millennial-to centennial-scale climate periodicities and forcing mechanisms in the westernmost Mediterranean for the past 20,000 yr. *Quat. Res.* **81**, 78-93 (2014).
70. Martinez-Ruiz, F. *et al.* Paleoclimate and paleoceanography over the past 20,000 yr in the Mediterranean Sea Basins as indicated by sediment elemental proxies. *Quat. Sci. Rev.* **107**, 25-46 (2015).
71. Scarciglia, F., Pelle, T., Pulice, I. & Robustelli, G. A comparison of Quaternary soil chronosequences from the Ionian and Tyrrhenian coasts of Calabria, southern Italy: Rates of soil development and geomorphic dynamics. *Quat. Int.* **376**, 146-162 (2015).
72. Scarciglia, F. *et al.*, Weathering profiles in granitoid rocks of the Sila Massif uplands, Calabria, southern Italy: New insights into their formation processes and rates. *Sedim. Geol.* **336**, 46-67 (2016).
73. Krauss, L. *et al.* A Multi-Proxy Analysis of two Loess-Paleosol Sequences in the Northern Harz Foreland, Germany. *Palaeogeogr. Palaeocl.* **461**, 401-417 (2016).
74. Buggle, B., Glaser, B., Hambach, U., Gerasimenko, N. & Markovic, S. An evaluation of geochemical weathering indices in loess-paleosol studies. *Quat. Int.* **240**, 12-21 (2011).
75. Degeai, J.-P. *et al.*, Chemical weathering of palaeosols from the Lower Palaeolithic site of Valle Giumentina, central Italy. *Quat. Sci. Rev.* **183**, 88-109 (2018).
76. Degeai, J.-P. *et al.* Fluvial response to the last Holocene rapid climate change in the Northwestern Mediterranean coastlands. *Glob. Planet. Chang.* **152**, 176-186 (2017).

77. Degeai, J.-P. *et al.* A new interpolation method to measure delta evolution and sediment flux: Application to the late Holocene coastal plain of the Argens River in the western Mediterranean. *Mar. Geol.* **424**, 106159 (2020).
78. Trauth, M. H., Larrasoña, J. C. & Mudelsee, M. Trends, rhythms and events in Plio-Pleistocene African climate. *Quat. Sci. Rev.* **28**, 399-411 (2009).
79. Skonieczny, C. *et al.* Monsoon-driven Saharan dust variability over the past 240,000 years. *Sci. Adv.* **5**, eaav1887 (2019).
80. Tiedemann, R., Sarnthein, M., Shackleton, N. J. Astronomic timescale for the Pliocene Atlantic $\delta^{18}\text{O}$ and dust flux records of Ocean Drilling Program Site 659. *Paleoceanography* **9**, 619-638 (1994).
81. Larrasoana, J. C., Roberts, A. P., Rohling, E. J., Winklhofer, M. & Wehausen, R. Three million years of monsoon variability over the northern Sahara. *Clim. Dyn.* **21**, 689-698 (2003).
82. Grant, K. M. *et al.*, A 3 million year index for North African humidity/aridity and the implication of potential pan-African Humid periods. *Quat. Sci. Rev.* **171**, 100-118 (2017).
83. Lisiecki, L. E. & Raymo, M. E. A Pliocene-Pleistocene stack of 57 globally distributed benthic D18O records. *Paleoceanography* **20**, PA1003 (2005) doi:10.1029/2004PA001071.
84. Channell, J. E. T., Singer, B. S., Jicha, B. R. Timing of Quaternary geomagnetic reversals and excursions in volcanic and sedimentary archives. *Quat. Sci. Rev.* **228**, 106114 (2020).
85. Rohling, E. J. *et al.* Sea-level and deep-sea-temperature variability over the past 5.3 million years. *Nature* **508**, 477-482 (2014).
86. Amies, J. D. PhD Dissertation (The Australian National University, Research School of Earth Sciences, 2018).
87. De Boer, B., van de Wal, R. S. W., Bintanja, R., Lourens, L. J. & Tuenter, E. Cenozoic global ice-volume and temperature simulations with 1-D ice-sheet models forced by benthic $\delta^{18}\text{O}$ records. *Ann. Glaciol.* **51**, 23-33 (2010).
88. Shackleton, N. J. New data on the evolution of Pliocene climate variability in *Palaeoclimate and evolution, with emphasis on human origins* (eds. Denton, G. H., Vrba, E., Partridge, T. C. & Burckle, L. H.) 242-248 (Yale University Press, 1995).
89. Fairbanks, R. G. A 17,000-year glacio-eustatic sea level record: influence of glacial melting rates on the Younger Dryas event and deep-ocean circulation, *Nature* **342**, 637-642 (1989).
90. El Kadiri, K. *et al.* Eustatic and tectonic controls on Quaternary Ras Leona marine terraces (Strait of Gibraltar, northern Morocco). *Quat. Res.* **74**, 277-288 (2010).
91. Emberger, L. *Les arbres du Maroc et comment les reconnaître* (Larose, 1938).
92. Benabid, A. *Flore et écosystèmes du Maroc, évaluation et préservation de la biodiversité* (Ibis Press, 2000).

93. Reille, M. *Pollen et spores d'Europe et d'Afrique du Nord* (Laboratoire de Botanique historique et de Palynologie, 1992).
94. M. Reille, *Pollen et spores d'Europe et d'Afrique du Nord, supplément 1* (Laboratoire de Botanique historique et de Palynologie, 1995).
95. Reille, M. *Pollen et spores d'Europe et d'Afrique du Nord, supplément 2* (Laboratoire de Botanique historique et de Palynologie, 1998).
96. Cugny, C., Mazier, F., Galop, D. Modern and fossil non-pollen palynomorphs from the Basque mountains (western Pyrenees, France): the use of coprophilous fungi to reconstruct pastoral activity. *Hist. Archaeobot.* **19**, 391-408 (2010).
97. Cronquist, A. *An integrated system of classification of flowering plants* (Columbia University Press, 1981).